REPORT NO.
UCB/EERC-77/07
MARCH 1977

EARTHQUAKE ENGINEERING RESEARCH CENTER

A LITERATURE SURVEY–TRANSVERSE STRENGTH OF MASONRY WALLS

by

YUTARO OMOTE
RONALD L. MAYES
SHY-WEN J. CHEN
RAY W. CLOUGH

Report to the Department of Housing and Urban Development

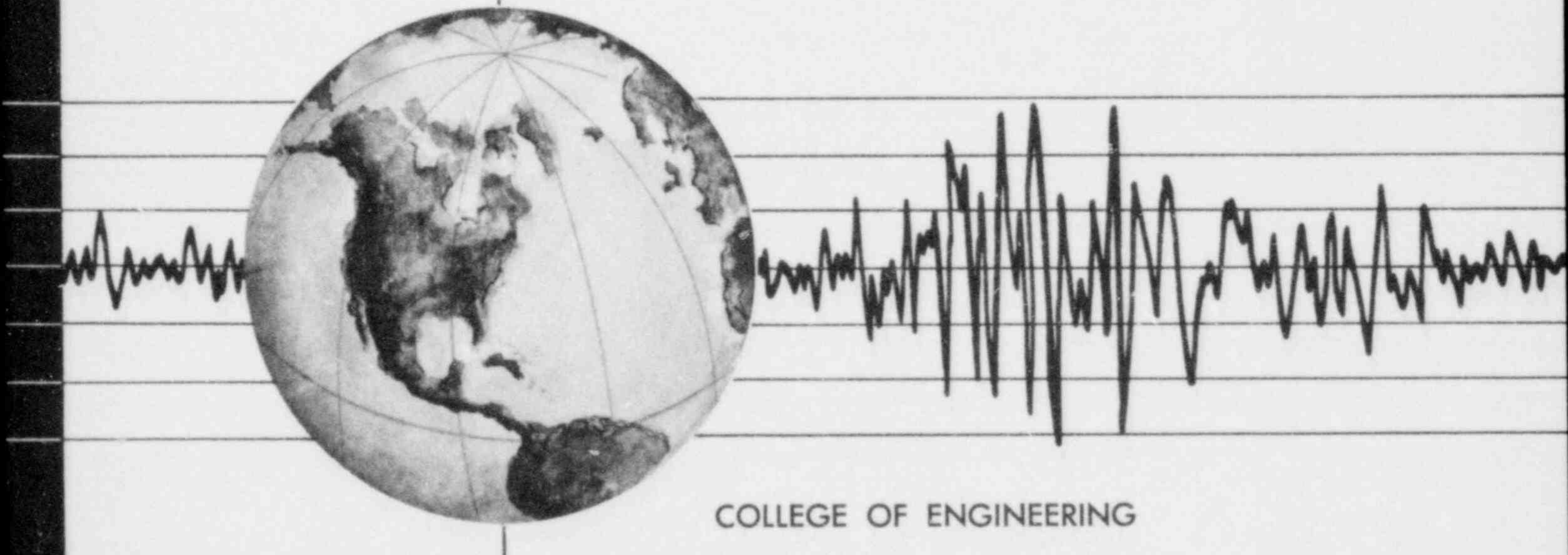

COLLEGE OF ENGINEERING

UNIVERSITY OF CALIFORNIA · Berkeley, California

For sale by the National Technical Information Service, U. S. Department of Commerce, Springfield, Virginia 22161.

THIS TEST REPORT IS MAILED TO YOU

THROUGH THE COURTESY OF

WESTERN STATES CLAY PRODUCTS ASSOCIATION

A LITERATURE SURVEY
TRANSVERSE STRENGTH OF MASONRY WALLS

by

Yutaro Omote

Ronald L. Mayes

Shy-wen J. Chen

and

Ray W. Clough

Prepared under the sponsorship of the
Department of Housing and Urban Development,
Washington, D.C. 20410 Under Contract No. H2387

Report No. UCB/EERC-77/07
Earthquake Engineering Research Center
College of Engineering
University of California
Berkeley, California

March 1977

ABSTRACT

The literature survey presented collates most of the available relevant information on the transverse or out-of-plane strength of masonry walls. The report discusses several of the test techniques used and summarizes the most significant available test results. Formulations for predicting the capacity of walls subjected to transverse loads are presented together with their correlation with experimental results. Also included is a section relating test results to present design practices and code requirements.

ACKNOWLEDGEMENT

This investigation was sponsored by the Department of Housing and Urban Development as part of a broad research program, "Laboratory Studies of the Seismic Behavior of Single Story Residential Masonry Buildings in Seismic Zone 2 of the U.S.A". The authors acknowledge the research performed by all investigators, which made this survey possible.

The authors thank Dr. B. Bolt for editing the manuscript, Shirley Edwards for typing it and Ms. Gale Feazell for the draft.

TABLE OF CONTENTS

TABLE OF CONTENTS (cont.)

LIST OF TABLES

LIST OF FIGURES

LIST OF FIGURES (cont.)

LIST OF FIGURES (cont.)

LIST OF FIGURES (cont.)

1. INTRODUCTION

An important consideration in the analysis and design of a masonry building is its ability to withstand lateral loads. Figure 1.1 shows a schematic drawing of the load transfer mechanism of a wall subjected to lateral forces - either wind or earthquake. The lateral loads act on Wall A and are transferred to Wall B by horizontal diaphragms which may include the floors and/or roof of the structure. Consequently, in the design of a masonry building there are three important factors to consider: (1) the ultimate in-plane shear capacity of Wall B; (2) the shear transfer capacity between the diaphragm and Wall B, and (3), the out-of-plane flexural capacity of the transverse Wall A.

The in-plane shear strength of masonry walls has been the subject of three recent reports by Mayes and Clough[1,2,3], and the objective of this literature survey is to summarize most of the available information on the out-of-plane flexural capacity of masonry walls subjected to transverse loads. Chapter 2 describes most of the test techniques that have been used to simulate transverse loads on masonry walls. In Chapter 3, test results on the transverse strength of masonry walls are summarized. In Chapter 4 formulations to predict the transverse flexural capacity of masonry walls are discussed. In Chapter 5 present design practices are considered with regard to transverse load test results.

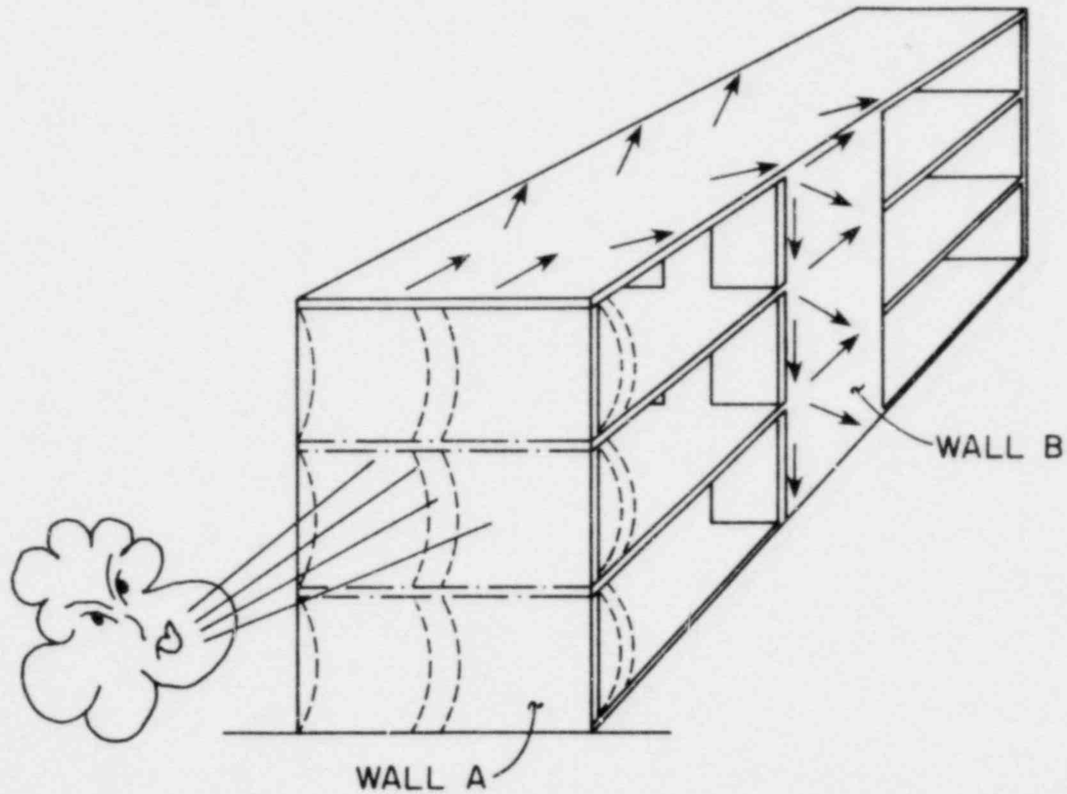

FIG. 1.1 LATERAL FORCE ON WALLS

2. TEST TECHNIQUES

2.1 Introduction

In order to determine the flexural capacity of a masonry wall subjected to transverse loading, several kinds of test techniques have been used in laboratory test programs. One of the most common and frequently used methods is the air-bag test described in Section 2.2, which usually uses a large wall panel as the test specimen. Small specimens are used in the wallette test discussed in Section 2.3. Other methods used by investigators include the use of hydraulic jacks to apply line loads to the wall. Dynamic tests have been performed with explosive or pulse loadings to simulate gas explosions on a wall.

2.2 Air-bag Tests

Typical transverse air-bag test equipment for full-size walls is shown in Figs. 2.1 and 2.2. It consists of a movable restraining steel frame with a plywood backboard stiffened with steel channels. Seamless steel pipes welded to steel channels provide support behind the test specimen. These support members are firmly attached to the retaining framework in positions that provide the required vertical span for the specimen, which is usually 7.5 ft. An air-bag (nylon reinforced neoprene or polyvinyl sheeting, etc.) is hung between the backboard and the face or compressive side of the test wall. The air-bag is inflated with air from a compressor to produce a uniformly distributed transverse load over the face of the wall. Pressure in the system is measured by means of a manometer or pressure transducer.

The transverse load is applied in increments (usually four psi) and deflections at every one-third point along the height are measured

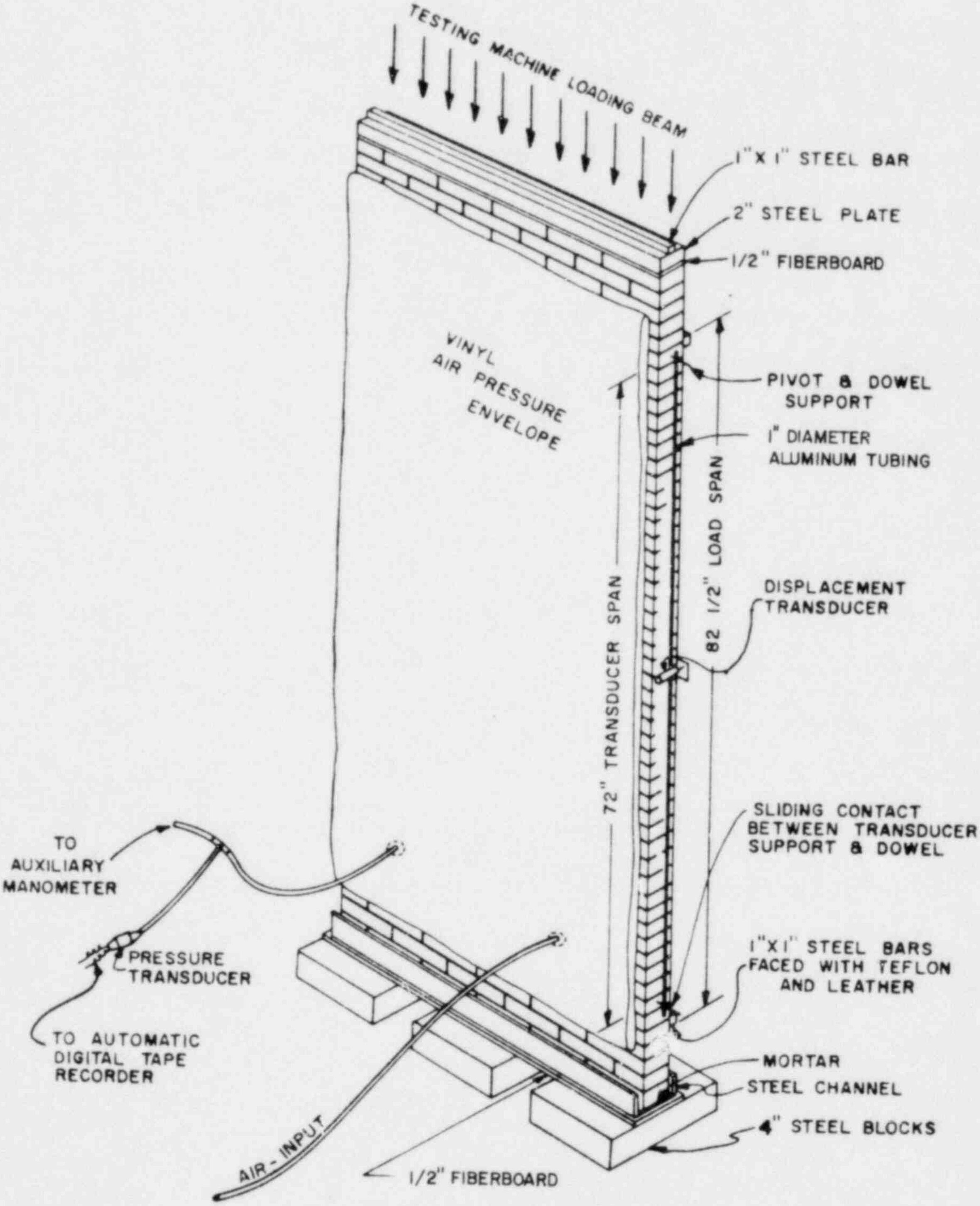

FIG. 2.1 AIR-BAG EXPERIMENTAL SET-UP FOR FLEXURAL TEST

From Reference (6)

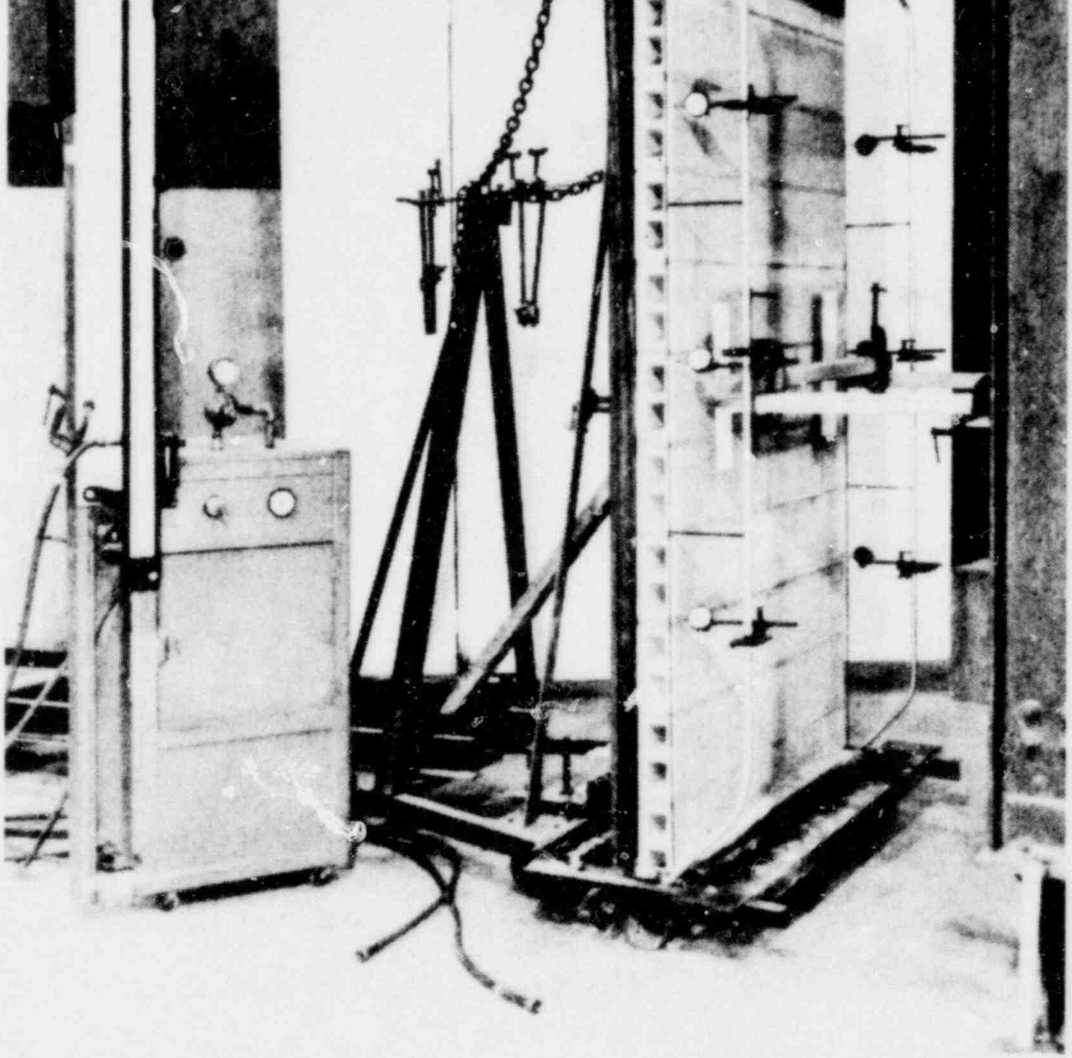

FIG. 2.2 AIR-BAG TRANSVERSE WALL TEST EQUIPMENT AND SPECIMEN

From Reference (26)

by dial gages or transducers and recorded at each increment. To prevent complete collapse of the wall at failure and resulting damage to the displacement equipment, wood restraining members are generally clamped to an adjacent steel frame. As shown in Fig. 2.2 these wood restraining members are far enough away from the tensile side of the wall to permit maximum deflections of the wall.

The test procedure described above is in accordance with ASTM E 72-61[4] which specifies (paragraph 20(6)) that the load shall be applied to the outside face of three test specimens and to the inside face of another three. Most investigators, however, tested with the load applied to what would be considered the "outside" face only. In the case of brick-block composite walls, a load is applied from each side[5].

The walls are considered non-load-bearing walls when only a horizontal transverse load is applied. When both a transverse load and a vertical compressive load are applied[5,6], the walls are considered load bearing walls. When there is both vertical and horizontal loading, the vertical compressive load is applied first and after the desired stress level is reached, the transverse load is applied and gradually increased until the specimen fails.

2.3 Wallette Tests

A second test, frequently used to determine the flexural strength of masonry walls, is the wallette test as shown in Fig. 2.3. A 2-block high prism (described in ASTM Standard E149-66[7]) is usually used in this test, although sometimes 3-block or 4-block high prisms are used.

A comparison of results from the air-bag system and from the wallette test is given in Section 3.6.

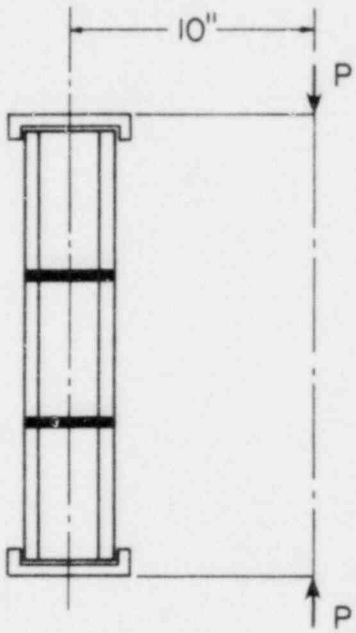

FIG. 2.3 WALLETTE TEST EQUIPMENT
From Reference (24)

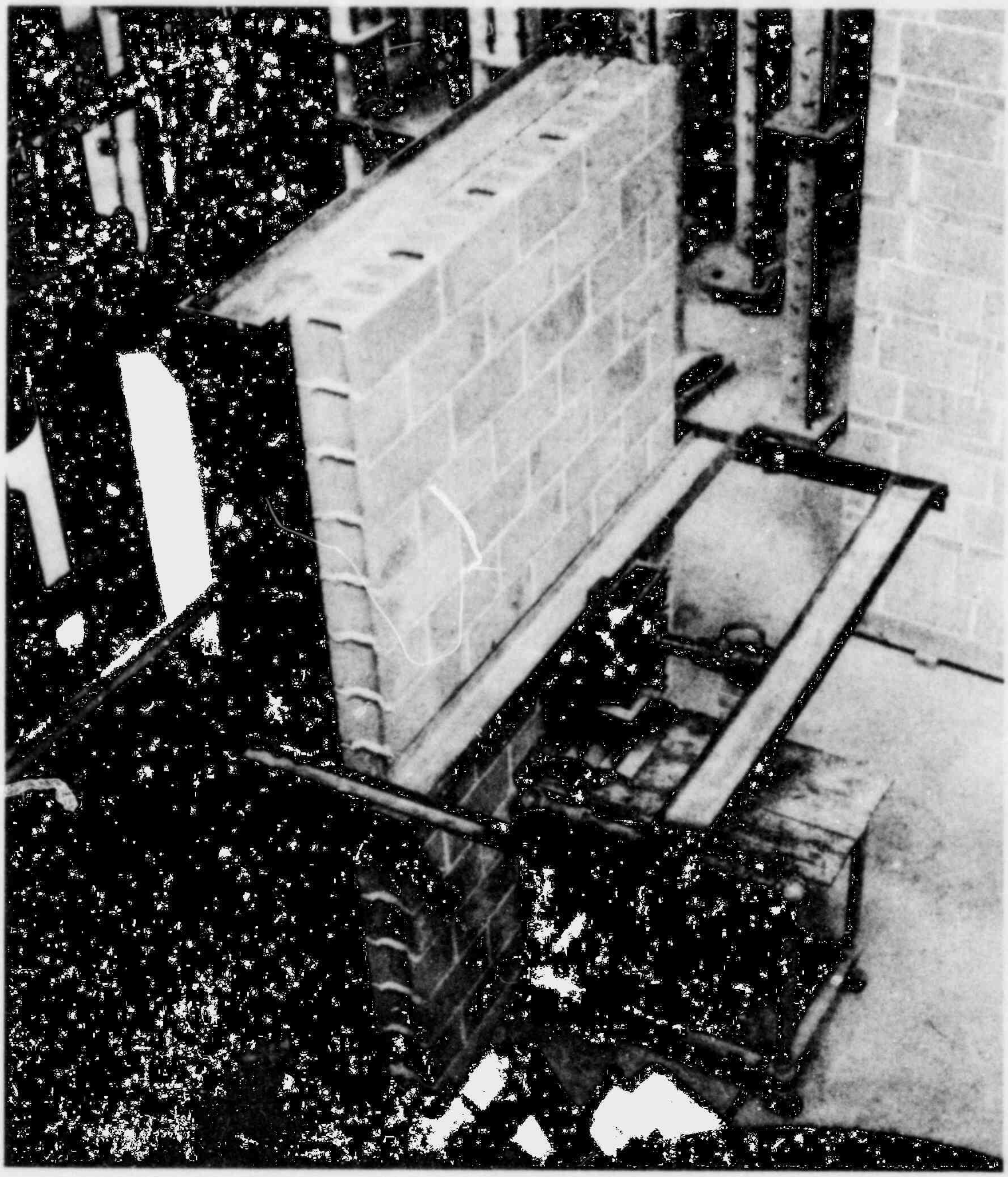

FIG. 2.4 TRANSVERSE TEST BY SINGLE-LINE LOAD

From Reference (10)

2.4 Other Static Tests

Some transverse load tests have been conducted with the use of hydraulic jacks[8,9,10,40]. An example is shown in Fig. 2.4[10]. A line load is applied at the mid-height of the test specimen by an hydraulic jack. Figure 2.5 shows another example where two line loads are applied (through rollers) at the outer quarter points of the height of the wall[40]. In this case, the total load theoretically produces the same maximum bending moment as that induced by an equal total wind pressure uniformly distributed over the wall. Actually the load is applied to the face of the wall by rollers or similar devices, and care must be taken to avoid a local failure at the loading point.

2.5 Dynamic Tests

Some transverse dynamic load tests have been conducted in order to test the resistance of a masonry wall to a blast load such as a gas explosion. An example of the blast loading technique is a recent series conducted by the UAS Research Company[11 to 16]. The test setup for this program is shown in Figs. 2.6 and 2.7. Tests of masonry walls under blast loading were also carried out by McKee and Sevin[17].

Another dynamic loading test was conducted b Morton and Hendry[18]. The walls used in this program were one-third scale brick subjected to precompression. Twenty-three walls were tested to failure using a la al dynamic pulse applied as a line load to the wall at mid-height. The lateral strengths of the walls for both dynamic and static loading were compared, and it was concluded that the different rates of loading have little effect on the ultimate strength of masonry panels.

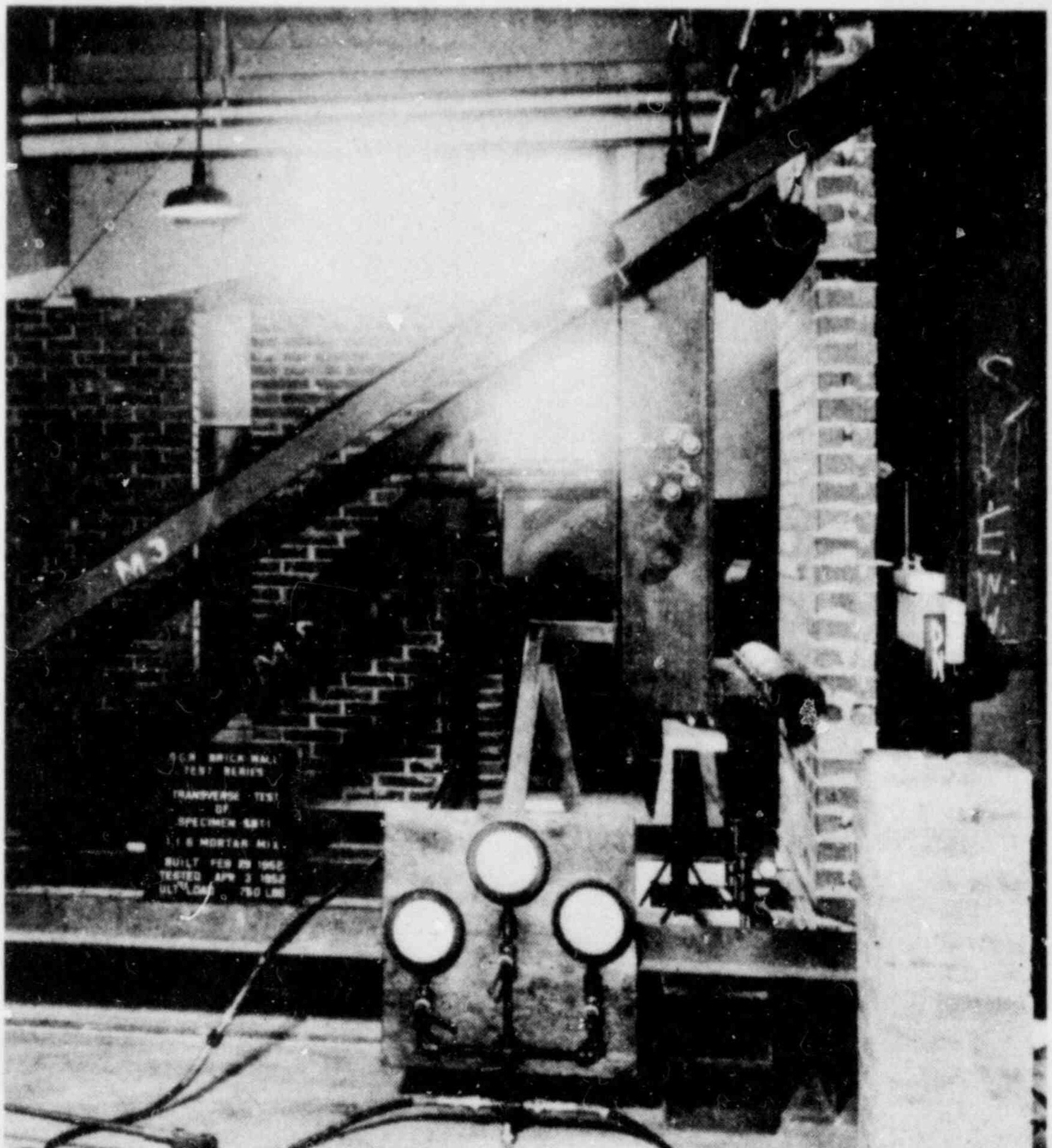

FIG. 2.5 TRANSVERSE TEST BY TWO-LINE LOAD
From Reference (40)

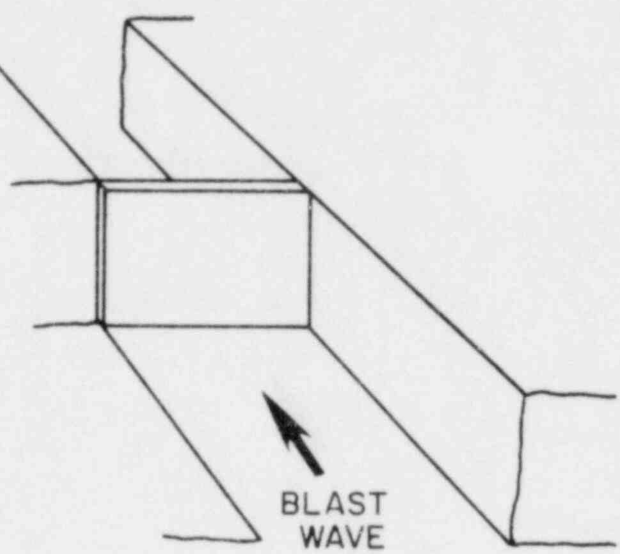

FIG. 2.6 DYNAMIC LOADING

From Reference (12)

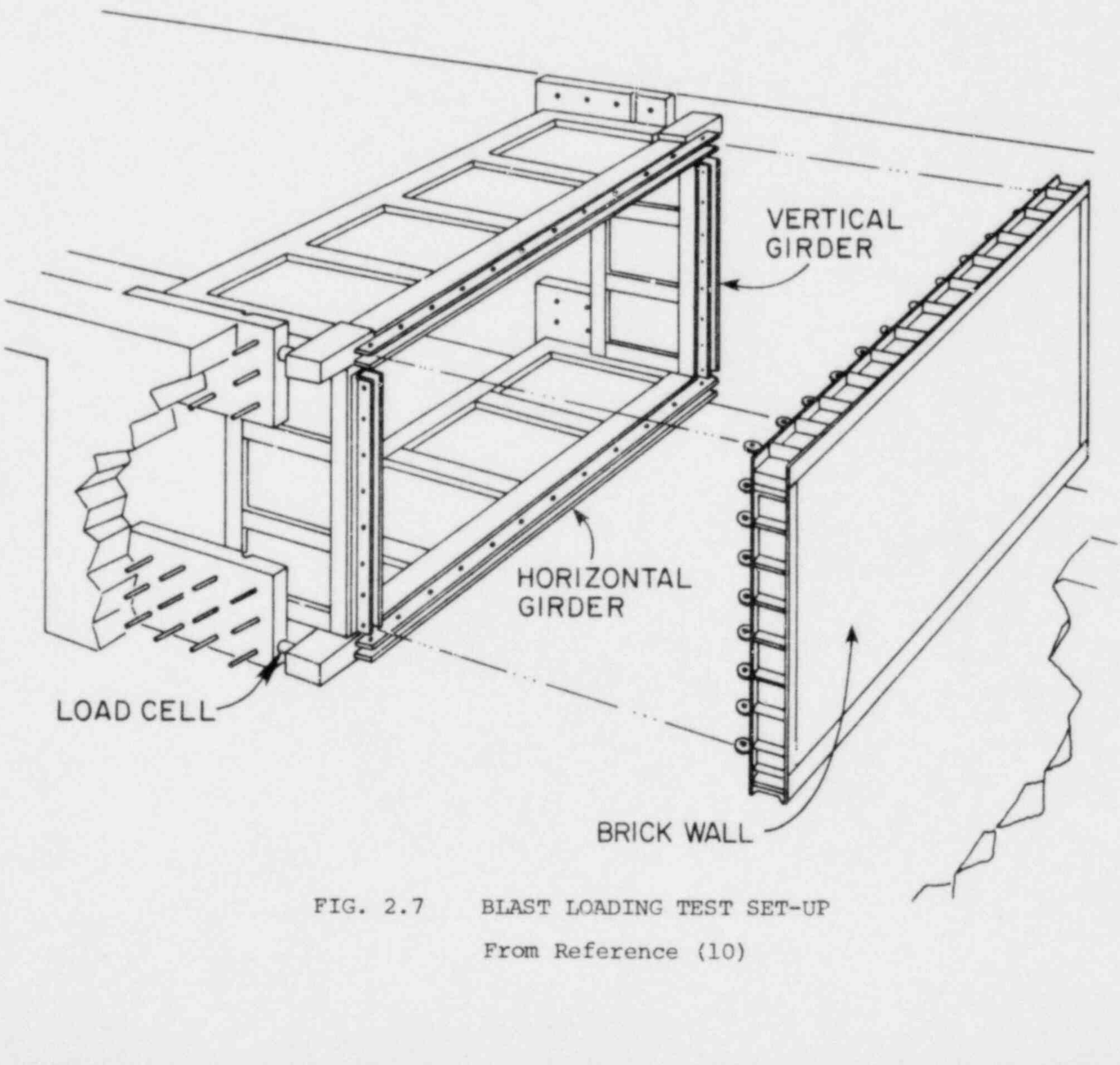

FIG. 2.7 BLAST LOADING TEST SET-UP

From Reference (10)

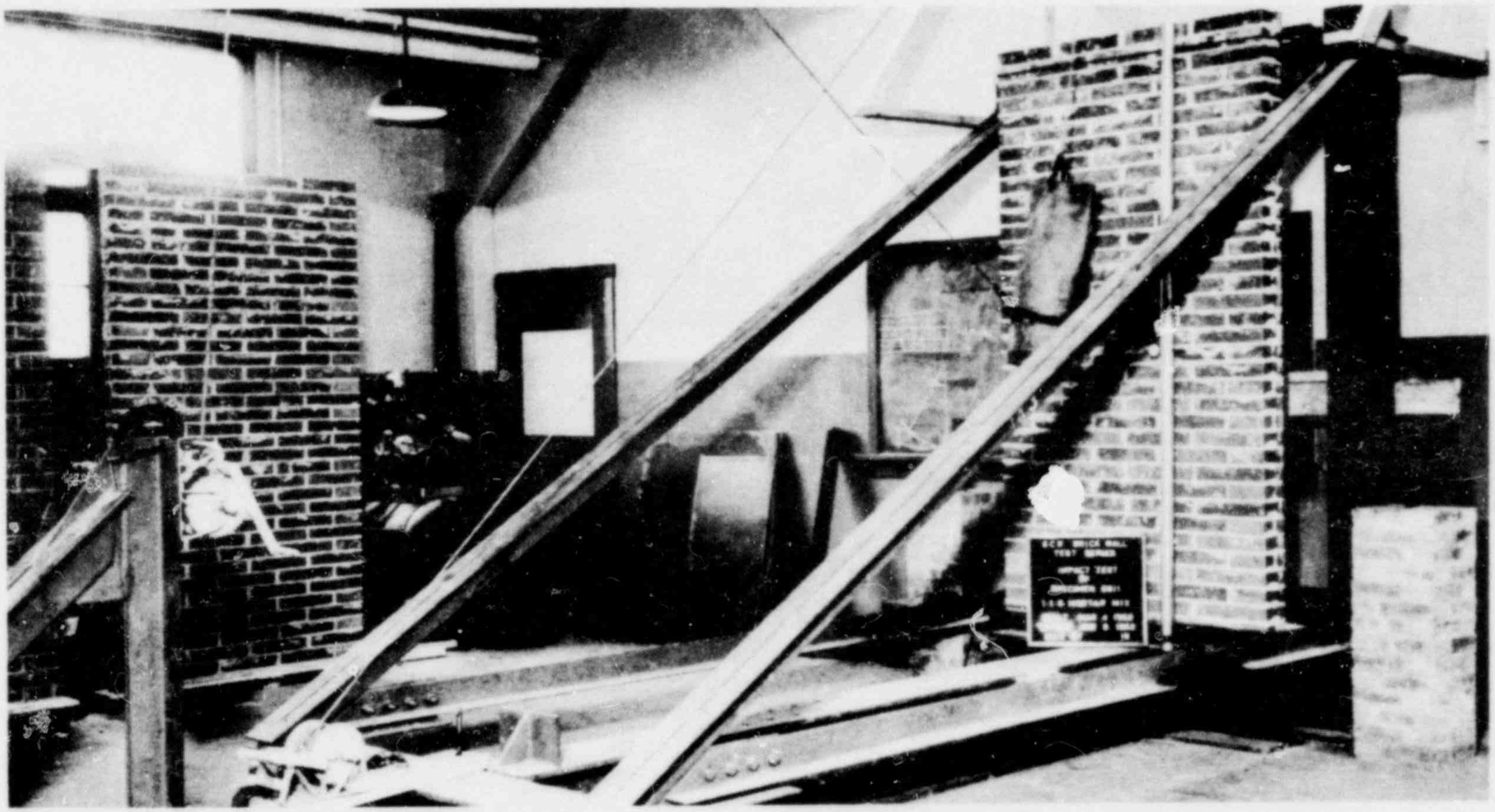

FIG. 2.8 IMPACT LOAD TEST

From Reference (40)

Monk[40] conducted impact loading tests for full size SCR masonry wall panels (4 ft. x 8 ft.), using a sandbag as shown in Fig. 2.8. The bag is raised and then released producing an instantaneous load on the wall at impact. The walls are tied to the support rollers to hold them in place when complete failure takes place; tying does not restrict the walls from rotating around the supports. The bottom of the specimen rests on rollers.

3. FACTORS AFFECTING THE TRANSVERSE STRENGTH OF MASONRY WALLS

3.1 Introduction

Factors generally included in formulations to predict the transverse strength of a masonry wall include the tensile and compressive strength of the masonry, the vertical load and the amount of reinforcement. Variables that affect the transverse strength but which are not directly included in the formulations are the strength of the masonry units, the strength of the mortar, the initial rate of absorption of the masonry unit, the thickness and width of the mortar joint, the pattern in which the units are laid and the workmanship.

A substantial number of research programs have been conducted in an attempt to determine the effect of the above variables on the transverse strength of masonry walls. A summary of most of the test programs that have been performed is given in Table 3.1 together with the appropriate reference. The tests on solid brick walls, hollow clay brick walls and concrete block walls are listed separately. Although the influence of the variables mentioned above are interrelated, they are discussed here separately. Formulations to predict the transverse strength of masonry walls are discussed in the following chapter.

3.2 Effect of Masonry Unit Strength and Initial Rate of Absorption

The two major properties of a masonry unit that affect the bond strength between the masonry unit and the mortar are the strength and initial rate of absorption (IRA) of the unit. The Structural Clay Products Research Foundation[(19)] investigated the influence of these two variables and found conflicting results.

Table 3.1
List of Transverse Load Tests

Materials			Wall			Load		No. of Tests	Others	Ref. No.
Classification	Size (in) H X W X L	Mortar (C:L:S)	Classification	Size (ft) W X H	Reinforcement	Transverse Load	Compressive Load			
Solid Brick	3 X 4 X 8	S (1:½:4½)	Single Wythe	4 X 8	No	air-bag	No	3		20
	"	"	"	"	"	"	"	15	Changing the brick grade with High, Medium, Low	19
	3 X 5 X 10	"	"	"	"	"	"	5		45
	3 X 5 X 9	?	"	5 X 10	"	"	"	1		24
	"	?	"	"	Yes	"	"	4		11
	"	(1:0:4)	"	4 X 11	Yes	"	"	4	Two walls are supported by ties off structural bearing walls	27
	3 X 4 X 8	(1:1:4)	"	4 X 8	No	"	"	2	Cored brick unit	6
	"	"	"	"	"	"	Yes	5	"	"
	"	high-bond	"	"	"	"	No	2	"	"
	"	"	"	"	"	"	Yes	6	"	"
	"	"	"	"	"	"	No	2	Solid unit	"
	"	"	"	"	"	"	Yes	5	"	"
	"	"	"	"	"	"	No	2	Wire-cut unit	"
	"	"	"	"	"	"	Yes	4	"	"
	2-1/6 X 5½ X 11½	(1:¼:3)	"	"	"	hydraulic jack	No	3		40
	"	(1:½:4½)	"	"	"	"	"	3		"
	"	(1:1:6)	"	"	"	"	"	3		"
	?	(1:¼:3)	"	?	No	?	"	3	High-strength unit	22
	?	(1:1:6)	"	?	"	?	"	6	Medium-strength unit	"
	3 X 4 X 8	S (1:½:4½)	"	2.7 X 8	"	air bag	No	2		5

Table 3.1
List of Transverse Load Tests (cont.)

Materials			Wall			Load		No. of Tests	Others	Ref. No.
Classification	Size (in) H X W X L	Mortar (C:L:S)	Classification	Size (ft) W X H	Reinforcement	Transverse Load	Compressive Load			
Solid Brick	3 X 4 X 8	S (1:½:4½)	Single Wythe	2.7 X 8	No	air bag	Yes	2		5
	one-third scale t = 1.5	(1:0:3)	"	? X 2.6	"	hydraulic jack	"	3		18
	"	"	"	"	"	dynamic pulse	"	13		"
	t = 3.0	(1:0:3)	Double Wythe	"	"	"	"	8		"
	"	(1:0:6)	"	"	"	"	"	2		"
	3 X 4 X 8	S	Single Wythe	8 X 8	"	blast	Yes	11	Two of them have 20% openings	16
	"	"	"	"	"	"	"	6		13
	2-1/6 X 5½ X 11½	B (1:1:6)	"	4 X 8	"	hydraulic jack	No	3	SCR brick	40
	"	"	"	"	"	dynamic impact	"	3	"	"
	"	(1:¼:3)	"	"	"	hydraulic jack	"	3	"	"
	"	(1:½:4½)	"	"	"	"	"	3	"	"

Table 3.1
List of Transverse Load Tests (cont.)

Materials			Wall			Load		No. of Tests	Others	Ref. No.
Classi-fication	Size (in) H x W x L	Mortar (C:L:S)	Classi-fication	Size (ft) W x H	Reinforce-ment	Transverse Load	Compressive Load			
Hollow Clay	4 x 6 x 12	S (1:½:4½)	Single Wythe	3 x 8	No	air-bag	No	6		20
	"	"	"	4 x 8	"	"	"	3		"
	4 x 8 x 12	"	"	3 x 8	"	"	"	6		"
	"	"	"	4 x 8	"	"	"	3		"
	6 x 4 x 12	"	"	"	"	"	"	6	Compare the effect of vertical core and horizontal core of clay	28
	8 x 4 x 16	"	"	"	"	"	"	3		"
	6 x 2 x 12 & 6 x 4 x 12	N (1:1:6)	Com-posite	"	"	"	"	12	Compare the effect of vertical & horizontal core, or masonry bond & metal tie	46
	12x8x12	(0:1¼:3)	Single Wythe	6 x 9	"	hydraulic jack	Yes	2		9
	"	(1:0:3)	"	"	"	"	"	2		"
	"	(1:1¼:4)	"	"	"	"	"	9		"
	"	(1:1¼:6)	"	"	"	"	"	3		"
	10¼x8x12	"	"	"	"	"	"	1		"
	12 x 8 x 5	(1:1¼:4)	"	"	"	"	"	1		"
	5 x 8 x 12	"	"	"	"	"	"	2		"
	6¼x8x12	"	"	"	"	"	"	3		"
	12x12x12	(1:1¼:6)	"	"	"	"	"	2		"
	12x8x12 & 12x4x12	"	Com-posite	"	"	"	"	1		"
	5 x 8 x 12 5 x 4 x 12 4 x 2 x 8	(1:1¼:4)	"	"	"	"	"	1		"

Table 3.1
List of Transverse Load Tests (cont.)

Materials			Wall			Load		No. of Tests	Others	Ref. No.
Classi-fication	Size (in) H x W x L	Mortar (C:L:S)	Classi-fication	Size (ft) W x H	Reinforce-ment	Transverse Load	Compressive Load			
Hollow Clay	5 x 4 x 12	S (1:½:4½)	Single Wythe	8 x 4	No	air-bag	No	6	Wall span normal to bed joint	29
	12x6x12	"	"	"	"	"	"	3	"	"
	5 x 6 x 12	"	"	"	"	"	"	3	"	"
	12x8x12	"	"	"	"	"	"	6	"	"
	5 x 4 x 12	"	"	4 x 8	"	"	"	6	Wall span parallel to bed joint	"
	12x6x12	"	"	"	"	"	"	3	"	"
	5 x 6 x 12	"	"	"	"	"	"	3	"	"
	12x8x12	"	"	"	"	"	"	6	"	"

Table 3.1
List of Transverse Load Tests (cont.)

Materials			Wall			Load		No. of Tests	Others	Ref. No.
Classi- fication	Size (in) H x W x L	Mortar (C:L:S)	Classi- fication	Size (ft) W x H	Reinforce- ment	Transverse Load	Compressive Load			
Concrete Block	8 x 8 x 16	N (1:0:3)	Single Wythe	4 x 8	No	air-bag	No	1	Hollow unit	6
	"	"	"	"	"	"	Yes	4	"	"
	"	high-bond	"	"	"	"	No	3	"	"
	"	"	"	"	"	"	Yes	5	"	"
	"	N (1:0:3)	"	"	"	"	No	2	Solid unit	"
	"	"	"	"	"	"	Yes	10	"	"
	8 x 4 x 16	"	4-2-4 cavity	"	"	"	No	2		"
	"	"	"	"	"	"	Yes	4		"
	8x4x16 & 8x4x8	"	4-2-4 brick-block cavity	"	"	"	No	1		"
	"	"	"	"	"	"	Yes	6		"
	"	"	composit brick-block	"	"	"	No	1		"
	"	"	"	"	"	"	Yes	6		"
	4 x 8 x 16	(2:1:3)	4-2-4 cavity	8 x 3½	"	hydraulic jack	No	3		8
	"	"	"	"	Yes-joint	"	"	3		"
	8 x 8 x 16	"	Single Wythe	8 x a*	"	"	"	3	*a is changed as 2 , 3½ , 4-7/10	"
	8 x 6 x 16	S (1:½:4½)	"	2.7 x 8	No	air-bag	"	2		5
	"	"	"	"	"	"	Yes	6		"
	3 x 4 x 8 & 8 x 6 x 16	"	composite brick-block	"	Yes-joint	"	No	4		"
	"	"	"	"	"	"	Yes	4		"

In one series of fifteen tests on claybrick panels using the air-bag test setup of Fig. 2.1, the only variable included in the program was the strength of the masonry unit. All fifteen walls were built with the same type "S" mortar and the same joint thickness. The dimensions of the brick units are shown in Fig. 3.1 and the physical properties are listed in Table 3.2. The results of the tests are summarized in Table 3.3 and the load-deflection curves for the three sets of wall specimens are plotted in Figs. 3.2(1) to 3.2(3). The test results indicate that a lower brick strength gives a lower ultimate transverse strength of the wall and a lower modulus of rupture. Furthermore a lower brick strength gives a lower modulus of elasticity resulting in larger lateral deflections. It should be noted that the initial rate of absorption of the high strength units is 4.0 (grams per min. per 30 $in.^2$) while that of the medium and low strength units is 14.8 and 24.1, respectively. Consequently it could also be concluded that higher transverse strengths are associated with the lowest IRA.

In the second series of tests, 135 wallette specimens were tested in the setup shown in Fig. 2.3. The specimens were 4 inches by 4 inches by 16 inches long and were constructed with type "S" mortar and 27 different types of brick units. The investigators concluded that the property that appears to have had the greatest influence on the transverse strength of the wallettes was the initial rate of absorption (IRA) or suction of the unit at the time of laying. The effect of the IRA is shown in Table 3.4 and indicates that lower transverse strengths are associated with IRA's of less than 5 grams per min. per 30 $in.^2$ and greater than 30 grams per min. per 30 $in.^2$.

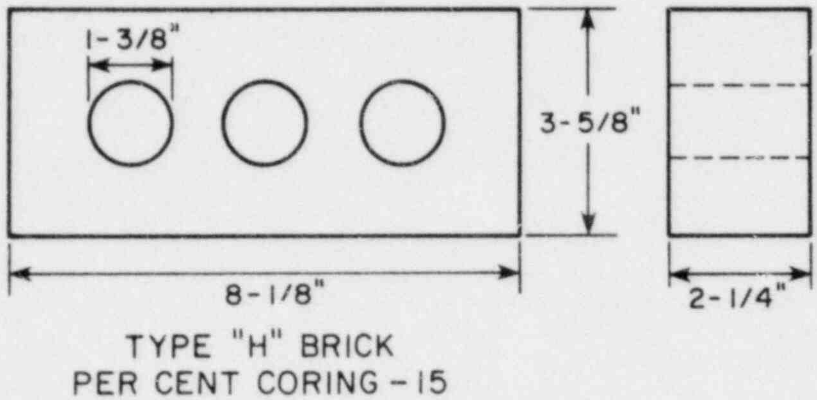

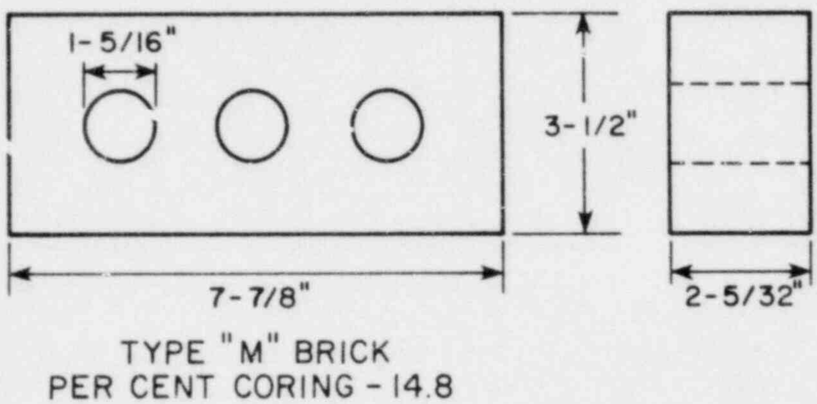

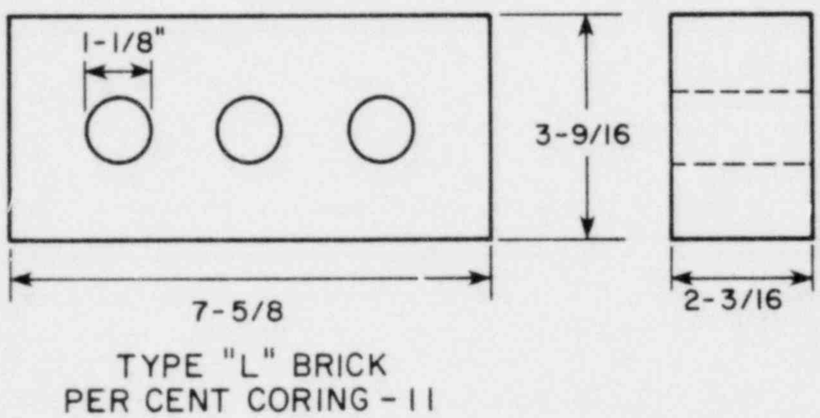

FIG. 3.1 DIMENSIONS OF BRICK UNITS
From Reference (19)

Table 3.2

Physical Properties of Brick

$n = 5$

Physical Property	Type L			Type M			Type H		
	$\bar{X}$	s	v %	$\bar{X}$	s	v %	$\bar{X}$	s	v %
Compressive Strength, psi	6,306	955	15.1	10,711	547	5.1	16,093	2,801	17.4
Modulus of Rupture, psi	686	58.7	8.6	1,105	102	9.2	1,568	116	7.4
Initial Rate of Absorption*	24.1	5.1	21.0	14.8	4.1	27.6	4.0	0.7	17.2
24-hr Cold Absorption(C), %	9.8	1.1	10.8	5.9	0.6	10.8	3.7	0.5	12.5
5-hr Boil Absorption(B), %	11.9	0.9	7.5	8.0	0.6	7.5	4.2	0.5	10.9
Saturation Coefficient, C/B	0.82	0.029	3.6	0.74	0.032	4.3	0.90	0.052	5.8

*grams per min per 30 sq in.

$\bar{X}$ = mean of samples

s = standard deviation of sample, expressed in same units as mean

v = coefficient of variation of samples

n = number of samples

from reference (19)

Table 3.3
Transverse Strength of 4-In. Brick Walls*

Series	Specimen	Transverse Strength of 4-in. Brick Walls							Modulus of Elasticity, E_m**			
		Ultimate Load psf	Modulus of Rupture psi	$\bar{x}$		s		v %	E_m million psi	$\bar{x}$ million psi	s million psi	v %
				Ultimate Load psf	Modulus of Rupture psi	Ultimate Load psf	Modulus of Rupture psi					
	T1	63.8	204.8						6.26			
	T2	57.0	183.0						5.41			
H	T3	55.5	178.2	58.7	188.5	3.42	10.95	5.8	5.53	5.95	0.499	8.4
	T4	60.6	194.5						5.95			
	T5	56.7	182.0						6.61			
	T6	45.9	152.4						3.39			
	T7	59.0	195.9						3.39			
M	T8	47.2	156.7	45.8	152.1	8.85	[illegible]9.41	19.3	3.53	3.50	0.385	11.0
	T9	34.6	114.9						3.06			
	T10	42.3	140.4						4.11			
	T11	26.9	89.3						1.18			
	T12	31.9	105.9						1.13			
L	T13	37.4	124.2	36.0	118.6	6.70	21.71	18.6	1.63	1.41	0.273	19.4
	T14	44.0	146.1						1.75			
	T15	39.7	127.4						1.36			

*4 by 8-ft walls built with type S mortar and 3/8-in. joints

**Secant modulus from origin to 20-psf load and corresponding deflection

from reference (19)

Table 3.4

Effect of Brick Suction on Transverse Strength of 4-In. Brick Masonry Wallettes*

Suction of Brick g per min per 30 sq in.	Wallette Strength		
	n	Modulus of Rupture psi	Strength Ratio
Less than 5	30	113	0.84
5 to 30	80	135	1.00
Over 30	25	98	0.73

*16 by 16-in. wallettes built with type S mortar and 3/8-in. joints

from reference (19)

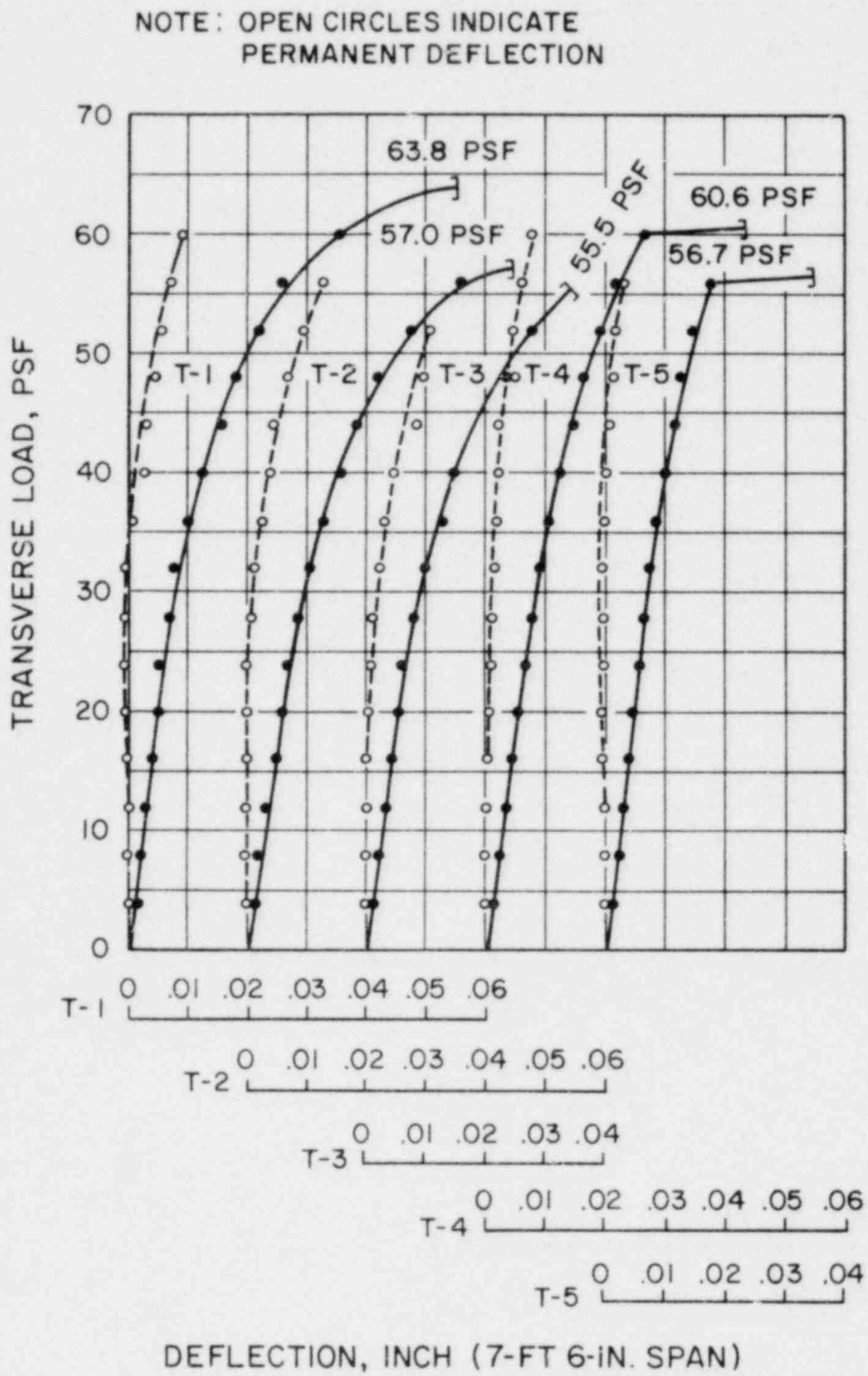

FIG. 3.2(1) TRANSVERSE STRENGTH OF 4-IN. BRICK WALLS (SERIES H)

From Reference (19)

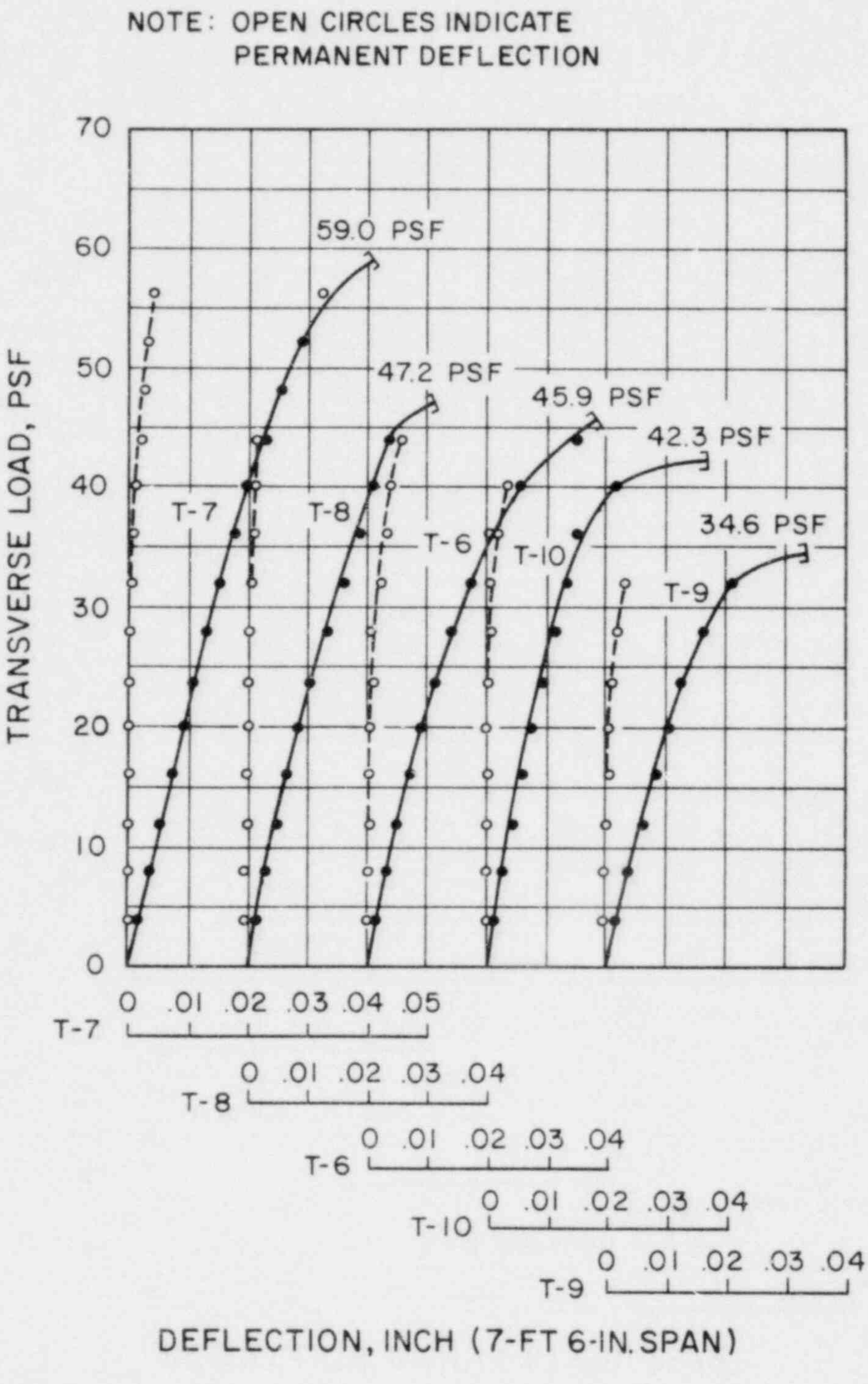

FIG. 3.2(2) TRANSVERSE STRENGTH OF 4-IN. BRICK WALLS (SERIES M)
From Reference (19)

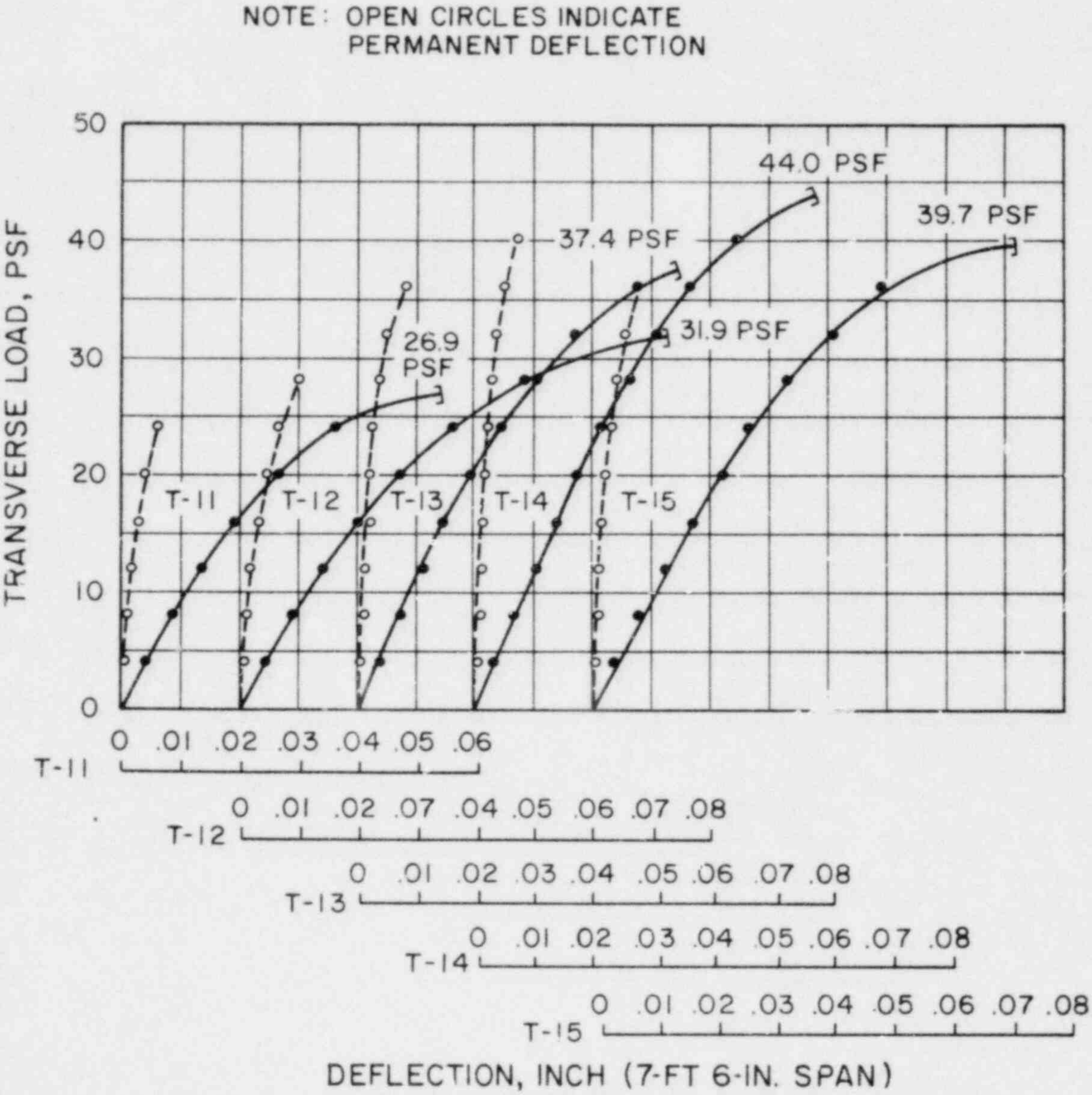

FIG. 3.2(3) TRANSVERSE STRENGTH OF 4-IN. BRICK WALLS (SERIES L)
From Reference (19)

The contradiction in the two sets of results led the investigators to conclude that other variables affect the bond developed at the brick mortar interface; e.g. the character of the bedding surface and the extent to which mechanical interlocking of the mortar with brick is achieved. The investigators suggested the possibility of developing a measure of surface roughness, not only at the surface itself but the size, shape and depth of pores contiguous with the surface of the brick.

3.3 Effect of Mortar

As stated in Section 3.1 the transverse strength of a masonry wall is primarily affected by the bond characteristics between the masonry unit and the mortar. The bond developed at the interface, in addition to being a function of the properties of the masonry unit, is also related to the properties of the mortar. Several investigators have attempted to isolate particular properties of the mortar that affect the bond at the unit-mortar interface. These include the compressive and tensile strength of the mortar, the thickness of the mortar joint, and the width of the mortar joint. Research programs associated with each of these properties are discussed separately in the following sections.

3.3.1 Effect of Mortar Strength

Stang et al.[9] in 1926 conducted a series of twenty-seven transverse wall tests using various types of clay tiles, both wetted and dry at the time of laying, and mortars of various strengths. The walls were 9 ft. long and 6 ft. wide and were loaded with two line loads applied through timber members by hydraulic jacks. The walls

Table 3.5
Results of Transverse Tests of Hollow-Tile Walls

Wall designation [1]	Wall thickness	Description of tiles and size in inches	Maximum load	Distance between restraints	Equivalent uniform load	Modulus of Rupture
	inches		pounds	inches	lbs/ft^2	lbs/in^2
1-E-1	8	6-cell, 8 by 12 by 12	1,080	106	27	18
1-S-1	8	do	1,970	108	49	39
1-E-2	8	do	2,080	107	52	41
4-E-2	8	do	2,390	105	60	47
1-S-2	8	do	2,900	109	71	62
8-S-2	8	H-shaped, 8 by 10¼ by 12	4,350	92	115	73
1-M-2	8	6-cell, 8 by 12 by 12	1,570	107	39	29
1-E-3	8	do	1,670	107	41	32
5-E-3	8	do	[illegible],980	102	50	36
6-E-3	8	XXX, 8 by 12 by 12	[illegible],980	107	49	39
7-E-3	8	do	[illegible],190	104	55	41
9-E-3		Double shell, 8 by 12 by 5	3,320	107	82	70
1-S-3		[illegible]-cell, 8 by 12 by 12	2,700	109	66	57
4-S-3		do	2,080	110	51	44
5-S-3	8	do	1,980	105	50	38
6-S-3	8	XXX, 8 by 12 by 12	2,410	105	60	47
10-S-3	8	2-cell, 8 by 5 by 12	3,010	104	76	60
13-S-3	8	3-cell, 8 by 5 by 12	3,630	103	92	72
14-S-3	8	T-shaped, 8 by 6¼ by 12	1,980	106	49	38
15-S-3	8	do	2,500	108	62	52
1-E-4	8	6-cell, 8 by 12 by 12	2,660	106	66	53
1-S-4	8	do	4,450	109	110	98
2-E-2	12	6-cell, 12 by 12 by 12	5,580	105	14[illegible]	49
(1+3)-E-2	12	6-cell, 8 by 12 by 12 3-cell, 3-3/4 by 12 by 12	5,690	106	142	50
2-S-2	12	6-cell, 12 by 12 by 12	6,100	108	151	57
(10+11+12)-S-3	12	Faced with brick	6,100	106	152	55
14-S-3	12	T-shaped, 8 by 6¼ by 12	4,870	106	121	42

[1] The symbols listed in this column represent, in the order used: Tile lot number, construction, and mortar number.

Table 3.6
Average Strength of Mortar Specimens

Mortar Number	Proportions (by volume)	Specimens tested	Average compressive strength	Average tensile strength
			lbs/in^2	lbs/in^2
1	1¼L:3S	12	85	14
2	1C:1¼L:6S	81	760	80
3	1C:1¼L:4S	105	1,190	135
4	1C:3S	12	1,990	155

from reference (7)

were simply supported at an interval of approximately 9 ft. An equivalent uniform load at failure was calculated that gave the same bending moment as the two line loads at the center of the simply supported panel. The results of the tests are given in Table 3.5 and the mortar strengths in Table 3.6. All walls constructed with mortar types 1, 2 and 4 were laid with dry tiles while those constructed with mortar type 3 were laid with wetted tiles. The failure mode of all walls was a tensile failure between the mortar and the tiles. A comparison of the strengths of equivalent walls constructed with different mortar types indicates that the wall strength increases as the mortar strength increases i.e. Walls 1-E-1, 1-E-2 and 1-E-4 had wall strengths of 18, 41 and 53 $lbs/in.^2$, respectively. Walls 1-S-1, 1-S-2 and 1-S-4 had strengths of 39, 62 and 98 $lbs/in.^2$, respectively. The compressive strengths for mortar types 1, 2 and 4 were 85, 760 and 1990 $lbs/in.^2$, respectively. Similar walls constructed with the wetted tiles, i.e. 1-E-3 and 1-S-3 had wall strengths of 32 and 57 $lbs/in.^2$, respectively. The compressive strength of mortar type 3 was 1190 $lbs/in.^2$. This series of results indicates that an increase in the moisture content of the walls decreases their strength. This is illustrated by the fact that walls 1-E-2 and 1-S-2 constructed with a weaker mortar had greater wall strengths than the corresponding walls 1-E-3 and 1-S-3.

In research performed at the Structural Clay Products Research Foundation (SCPRF) (19) the effect of the tensile strength of mortar on the transverse strength of 4 inch flexural wallette tests was investigated. All 16 inch by 16 inch wallettes were built with the same type of brick (11,771 psi) with a constant 3/8 inch joint thickness. The four types of Uniform Building Code mortars (Type M, S, N and O) were used and the

Table 3.7

Effect of Mortar Tensile Strength on
Transverse Strength of 4-In. Brick Masonry Wallettes*

Mortar			Wallettes		
Type	Proportions by Volume	Tensile Strength** psi	n	Modulus of Rupture psi	Relative Strength
M	1C:¼L:3S	278	5	137	1.10
S	1C:½L:4½S	200	5	125	1.00
N	1C:1L:6S	128	5	96	0.77
O	1C:2L:9S	48	5	85	0.68

*16 by 16-in. wallettes built with same type of brick (11,771 psi) and 3/8-in. joints

**28-day strength of air-cured briquettes

from reference (19)

results are shown in Table 3.7. The modulus of rupture of the wallettes increased with increasing tensile strength of the mortar. Furthermore, the increase in tensile strength of the mortar is also associated with an increase in compressive strength of the mortar and consequently, it could be concluded, that the modulus of rupture of the wallettes increases with increasing compressive strength of the mortar.

The effect of mortar strength on the flexural strength of the walls was included in an extensive research program performed by Yokel, Mathey and Dikkers[6] on walls subjected to compressive and transverse loads. The walls were 8 ft. high and 4 ft. wide and were constructed from both hollow concrete block and clay brick units. The two mortars included in the test program were 1C: 3S and 1C: 1L: 4S, having compressive strengths of 525 psi and 1100 psi, respectively. In addition an 8710 psi (compressive strength) high-bond strength mortar was used with the hollow concrete block units and a 7280 psi high-bond strength mortar was used with the brick units.

The results of both compressive and flexural tests on the wall panels are given in Table 3.8. The results of the hollow concrete block tests indicate that the high strength mortar had a negligible effect on the compressive strength of the walls but increased the flexural strength by a factor of 21 over that with the 1C: 3S mortar. For the 4 in. Brick A walls the high-bond mortar increased the compressive strength by a factor of 1.5 to 4 over that with the 1C: 1L: 4S mortar. The effect of the high-bond mortar on different types of bricks was variable. In comparing Brick A to Brick S the high-bond mortar increased the compressive strength by a factor of 1.25 and decreased the flexural strength by a factor of 0.6, whereas a comparison of

Table 3.8

Summary of Average Compressive and Flexural Strengths of Walls [a]

Wall panel desig.	Type of construction	Average compressive load	Average compressive strength	Average modulus of rupture: Partial fixity assumed	Average modulus of rupture: Pin ended assumed
		kip	psi	psi	psi
1	8-in hollow block, 1 : 3 mortar	141.5	847	6	9
2	8-in hollow block, high-bond mortar	150.0	898	130	191
3	8-in solid block, 1 : 3 mortar	543.5	1500	15	22
4	4-in Brick A, 1 : 1 : 4 mortar	569.0	3187	50	75
5	4-in Brick A, high-bond mortar	858.0	4806	210	310
6	4-in Brick S, high-bond mortar	1069.0	6050	120	180
7	4-in Brick B, high-bond mortar	959.0	5140	300	440
8	4-2-4 in cavity block-brick, 1 : 3 mortar	246.0	1071	23	34
9	4-2-4 in cavity brick-block, 1 : 3 mortar	360.0	1229	(b)	----
10	8-in composite brick-block, 1 : 3 mortar	432.5	1476	30[c]	44[c]

[a] Average stress on net cross section; see figures

[b] No meaningful average stress can be computed.

[c] Based on I of transformed section

from reference (6)

Brick A and Brick B shows the compressive strengths to be comparable and the flexural strength of Brick B to be 1.5 times that of Brick A.

Hence it appears that the higher bond (and compressive) strength mortar has a significant effect in increasing the flexural strength of the walls, by a factor of 4 for the brick walls and a factor of 21 for the concrete block walls.

3.3.2 Effect of Mortar Joint Thickness and Width

The width and thickness of the mortar joint are two factors that were found to affect the transverse strength of masonry walls. These two factors are related to workmanship rather than the quality of mortar and were the subject of three separate investigations[19,20,21]. In the research program performed at the Structural Clay Products Research Foundation[19] the thickness of the mortar joint was varied between 1/4 in. and 3/4 in. by 1/8 in. increments in twenty-five 4 in. x 6 in. x 16 in. clay brick wallette tests. The results are given in Table 3.9 and the strength ratio with respect to the standard 3/8 in. joint is also tabulated. It is clear that the flexural strength varies inversely to the thickness of the mortar joint. This is similar to the effect of mortar joint thickness on compressive strength of prism as shown in Fig. 3.3.

In a test series performed by the Structural Clay Products Institute[20] the effect of the width of the mortar joint was investigated. The test specimens were 8 ft. high and 3 ft. or 4 ft. wide and were tested with the air-bag test setup of Fig. 2.1. The walls were constructed from "solid" clay units with nominal brick thicknesses of 8 in., 6 in., and 4 in. In order to determine the effect of the width of the mortar joint a series of walls were constructed with full bed joints

Table 3.9

Effect of Mortar Bed Joint Thickness

on Transverse Strength of 4-In. Brick Masonry Wallettes*

Bed Joint Thickness in.	Wallettes		
	n	Modulus of Rupture psi	Strength Ratio
1/4	5	154	1.23
3/8	5	125	1.00
1/2	5	104	0.83
5/8	5	83	0.66
3/4	5	64	0.51

*16 by 16-in. wallettes built with same type of brick (11,771 psi) and type S mortar.

from reference (19)

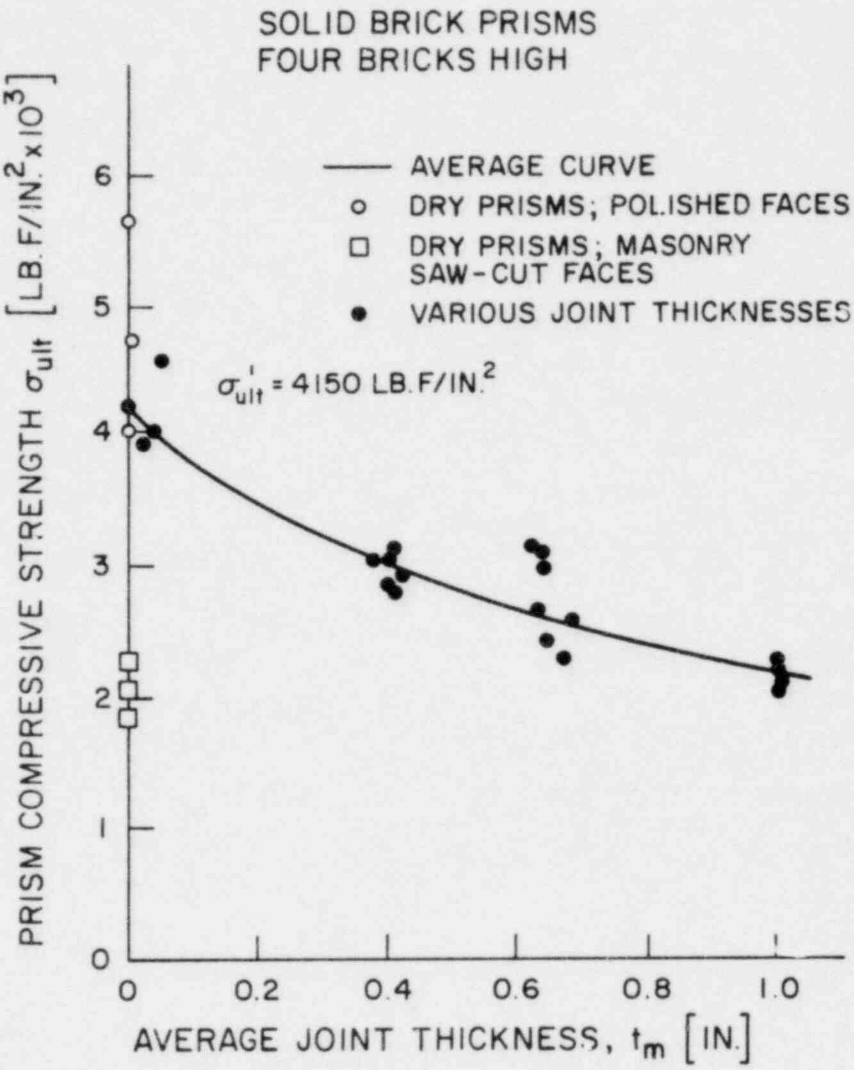

FIG. 3.3 VARIATION OF PRISM COMPRESSIVE STRENGTH WITH MORTAR JOINT THICKNESS--SOLID BRICKS

From Reference (19)

Table 3.10

Influence of Mortar Bed Width on Transverse Strength

Series	Bed Width, in.	Flexural Strength Based on Gross Area, f'_t psi	Design Value, f'_t psi	Ratio Experimental to Design Value, f'_t
8S	7.50	175.0	36	4.9
6S	5.50	141.0	36	3.9
4S	3.63	138.0	36	3.8
6SF	1.88	115.0	24	4.8
6H	1.84	77.0	--	---
8SF	1.63	97.0	24	4.0
8H	1.63	53.0	--	---

from reference (20)

and these were designated 8S, 6S and 4S. A second series of walls were constructed with only face shell bedding and these were designated 8SF and 6SF. In addition to the "solid" clay units with face shell bedding two series of tests were performed on walls with hollow clay units with the same face shell bedding as the solid units and designated 8H and 6H.

The results of the tests are given in Table 3.10. The effect of face shell bedding on the solid units decreases the flexural strength by factors of 0.55 and 0.81 for the 8 inch and 6 inch units, respectively. For hollow units with the same mortar bed width as the solid units (SF and H series), the flexural strength decreases by factors of 0.55 and 0.67 for the 8 inch and 6 inch units, respectively.

The decrease in flexural strength of the solid units due to face shell bedding was attributed to the more rapid drying of the narrower bed. This unfavorable curing condition has an adverse effect on the bond strength between the mortar and masonry unit. The additional decrease in the flexural strength of the hollow units is attributed by the authors to an even worse curing condition than for the face shell bedded solid units. The hollow units apparently provide a great internal "chimney effect" that creates even more rapid drying and consequently decreased bond strength.

3.3.3 Effect of Workmanship

Probably the most difficult parameter to evaluate is the effect of workmanship. The quality of workmanship affects the size, width and thickness of the mortar joint, the quality of the mortar and the IRA of the masonry unit. All these factors affect the transverse strength of a wall, hence attempts to evaluate the overall effect of workmanship

Table 3.11
Transverse Load Tests of Brick Walls

(1) PHYSICAL PROPERTIES OF BRICK

Brick	Compressive Strength psi	Modulus of Rupture psi	Water Absorption					Weight dry lb.
			24-hr. cold, C %	5-hr. boil, B %	Ratio C/B	1-min. Partial immersion[1] Dry	1-min. Partial immersion[1] As laid	
High-strength	17,600	2,275	1.9	3.45	0.53	8	8	5.85
Medium-strength	2,670	550	11.3	15.1	0.74	23	11	4.49

[1]Immersed on flat side in 1/3 in. of water. Absorption in grams per 30 sq. in.

(2) PHYSICAL PROPERTIES OF MORTAR

Kind of Mortar	Proportion, by Volume	Water Content, by Weight of Dry Materials percent	Flow, percent	Compressive Strength	
				Air Storage, psi	Water Storage, psi
Cement	1C:0.25L:3S	19.6	113	1390	3220
Cement-lime	1C:1L:6S	23.3	107	440	640

C = cement, L = lime and S = sand.

(3) TRANSVERSE TESTS OF BRICK WALLS

Wall Type[2]	Equivalent Uniform Load, psf				Modulus of Rupture[1], psi			
	1	2	3	Average	1	2	3	Average
AA	115	120	140	125	73.6	76.7	89.5	79.9
AB	53.3	38.0	52.3	48	34.7	24.7	34.0	31.1
AC	85	80	82	82	53.6	50.4	51.7	51.9

[1]Tested at age of 28 days

[2]AA is combination of high-strength brick and cement mortar with grade A workmanship. AB is combination of medium-strength brick and cement-lime mortar with grade B workmanship. AC is the same combination as AB but with grade A workmanship.

from reference (22)

are difficult. An attempt to evaluate the effect of workmanship was performed in 1938 by Whittemore et al.[22] who defined excellent or grade A workmanship to be a wall with completely filled bed joints and poor or grade B workmanship to be a wall with bed joints that were not completely filled. The mortar and brick properties are given in Tables 3.11 (1) and (2). The test results are given in Table 3.11 (3). The two series of walls AB and AC with the same mortar and brick had grade B and A workmanship, respectively. The walls (AB) with grade B workmanship had flexural strengths 60% of those of the grade A walls (AC).

Although the objective of the test series performed at the Structural Clay Products Institute[20] was to evaluate the effect of mortar joint width, by Whittemore's definition this was an evaluation of the effect of workmanship on solid units. The strength of the walls with poor workmanship according to Whittemore's definition was 55% and 81% of the strength of the walls with excellent workmanship for 8 inch and 6 inch units, respectively.

3.4 Effect of Wall Pattern

One of the architectural features of masonry is that a variety of wall patterns can be obtained with the various sizes, shapes and colors of masonry units. These patterned walls generally are not used as load bearing shear walls, therefore their capacity to withstand out-of-plane or transverse loadings is of major importance. In a series of tests performed by the Portland Cement Association in 1963[23] the effect of various wall patterns was investigated. The nine wall patterns used in the tests are shown in Fig. 3.4. The walls were 8 ft. high and 4 ft wide and tested with the ASTM E-72-55 test setup. The walls were constructed from concrete block units of various sizes. All

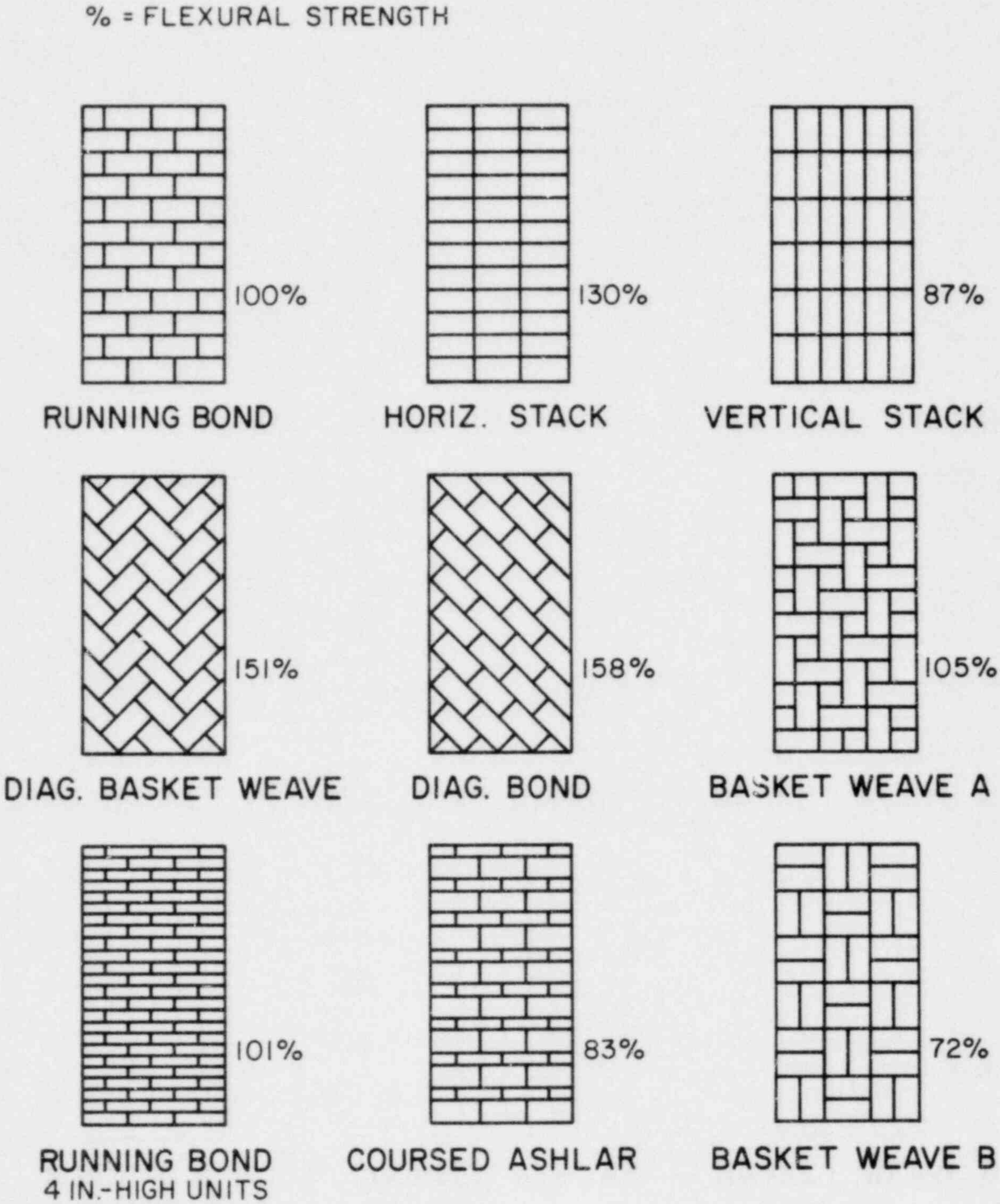

FIG. 3.4 CONCRETE MASONRY PATTERNS FOR STRUCTURAL TESTS
From Reference (18)

the walls were tested such that they spanned vertically. The top six walls shown in Fig. 3.4 were also tested with a vertical compressive load of 85 psi. Four of the walls (standard, horizontally stacked, diagonal basket weave and 4 inch running bond) also were tested such that they spanned horizontally, and in addition the same four walls were tested with horizontal joint reinforcement.

The results of the tests are given in Table 3.12 for Type M and Type S mortar. For walls spanning vertically the two diagonal types of bond increased the flexural strength by approximately 50%. The horizontally stacked bonded wall, surprisingly, increased the flexural strength by 30% whereas the vertically stacked bonded wall decreased the flexural strength by 13%. The effect of wall pattern was more dramatic for walls spanning horizontally. The strength of the horizontally stacked bonded wall was 28% of that of the standard 8 inch running bond wall, while the corresponding value for the diagonal basket weave wall was 60%. The wall with 4 inch high units and running bond had an increase in strength of 30% when compared with the wall with 8 inch high units.

3.5 Effect of Reinforcement

Although only a few investigations have been performed to determine the effect of reinforcement, two distinct and different types of reinforcement have been considered. The first is joint reinforcement, i.e. horizontal reinforcement placed in the mortar joints. It is effective for a wall spanning horizontally between vertical supports. The second type is vertical reinforcement which is placed in the cores of hollow units and in the grouted core of cavity walls. It is effective for walls spanning vertically between horizontal supports. The effect

Table 3.12
Transverse Strength of Masonry Patterned Walls

Wall pattern	Mortar type	Vertical span transverse strength lb. per sq. ft.				Horizontal span transverse strength				
		No compressive load			Compressive load, 85 psi	Unreinforced			Horizontal reinforcement, lb. per sq. ft.	
		lb. per sq. ft.	Percent of standard	Average*		lb. per sq. ft.	Percent of standard	Average*	16-in. c-c	8-in. c-c
8-in. running bond (standard)	M	60.0	100		425.0	127.0			149.4	203.0
						136.0	100			
				100		127.0		100		
	S	34.7				123.0	100		149.9	202.3
		32.2	100							
Horizontal stacked bond	M	85.0	141	130	405.0	47.7	37	28	130.0	191.2
	S	39.9	120			29.2	24		131.3	190.0
Vertical stacked bond	M	60.6	101	87	357.5					
	S	24.6	74							
Diagonal basket weave	M	89.0	148		410.5	69.5	56			
				151		76.9	67	60		
	S	51.7	155			65.8	57			
Diagonal running bond	M	103.0	172	158	429.0					
	S	48.1	144							
Basket weave A	M	69.9	117	105	400.0					
	S	30.7	92							
Basket weave B	M	42.9	72	72						
		44.5	72							
	S	24.4	73							
Coursed ashlar	M	43.3	72	83						
		55.5	93							
	S	26.3	79							
		34.7	104							
4-in. running bond	M	65.0	108			169.4	129		160.0	
				101		173.0	133	130	193.0	196.0
	S	31.3	94			158.0	128		186.6	194.7

*Average for Type M and S mortars

from reference (23)

of joint reinforcement was evaluated by both the Portland Cement Association (PCA)[23] and Cox and Ennega[8]. The effect of vertical reinforcement was evaluated by Scrivener[24] and the Masonry Institute of America[25].

In the tests performed by the PCA and described in the previous section horizontal joint reinforcement was included in the mortar bed joints at 8 inches and 16 inches center to center in walls with different bond patterns. The walls were tested with a horizontal span of 8 ft. with a test setup similar to Fig. 2.1.

A comparison of the results obtained for the unreinforced walls for different bonding patterns is shown in Table 3.12. The horizontal joint reinforcement had the most dramatic effect on the horizontally stack-bonded walls. For type M mortar and reinforcement 16 inches center to center, the transverse strength increased from 47.7 lb/sq. ft. to 130 lb/sq. ft., a 171% increase. For the type S mortar the increase was from 29.2 lb/sq. ft. to 131.3 lb/sq. ft. a 333% increase. The corresponding transverse strengths with reinforcement 8 inches center to center were 191.2 lb/sq. ft. and 190 lb/sq. ft., respectively. For the 8 inch high standard running bond walls, the percentage increase in transverse strengths over unreinforced walls for reinforcement placed at 16 inches center to center and 8 inches center to center were 15% and 54%, respectively. For the 4 inch high unit standard running bond walls the corresponding increases in transverse strength were 10% and 20%, respectively. It should be noted that all three walls with different bonding patterns had approximately the same transverse strength when horizontal reinforcement was placed at 8 inches center to center - the range of values was 190 to 203 lb/sq. ft.

Table 3.13

Summary of Recommendations

Wall type	Average moment at rupture, ft-lb per ft of height	$L = \sqrt{\frac{8M}{W}}$	L in ft for a safety factor of 2	Remarks
A	860	18' 6"	13	
B	1200	22' 0"	--	18' 0" design span
C	1140	21' 4"	15	
D	1280	22' 7"	--	18' 0" design span

from reference (8)

Cox and Ennega[8] investigated the effect of horizontal joint reinforcement on two different types of masonry construction. They used a test setup similar to that shown in Fig. 2.1, where the walls spanned (8 ft.) horizontally between vertical supports. The two types of construction used in the investigation were a 4 in. x 2 in. x 4 in. clay brick cavity wall and an 8 in. x 8 in. x 16 in hollow concrete block wall. The panels were 3 ft. 4 in. high and 8 ft. long. The cavity walls were designated as type A and B. The type A specimen had minimal horizontal joint reinforcement consisting of 1/4 inch Z bar ties for each 3 sq. ft. of wall area. The type B specimen had reinforcement in each bed joint consisting of 3/16 inch longitudinal wire with 9 gage web members with a drip or crimp located at the center of each web member. The C and D type walls were constructed from hollow concrete block units. The C walls were unreinforced while the D walls had standard joint reinforcement consisting of 9 gage longitudinal wires with 9 gage web members in each joint.

A summary of the results is given in Table 3.13 and the moment-deflection curves for the four types of walls are given in Fig. 3.5. The results for cavity walls (A and B) indicate that the joint reinforcement increases the load at which rupture occurs by approximately 40%, and the ultimate strength by approximately 100%. Furthermore, failure of the unreinforced walls occurs at a deflection soon after rupture (i.e. brittle failure) whereas the reinforced walls are able to carry load from a deflection of 0.04 inch at rupture to 0.25 inch at ultimate load (i.e. ductile behavior). A similar type of behavior was observed for the hollow concrete block walls. Joint reinforcement increased the rupture load by 12% and the ultimate strength by 36%.

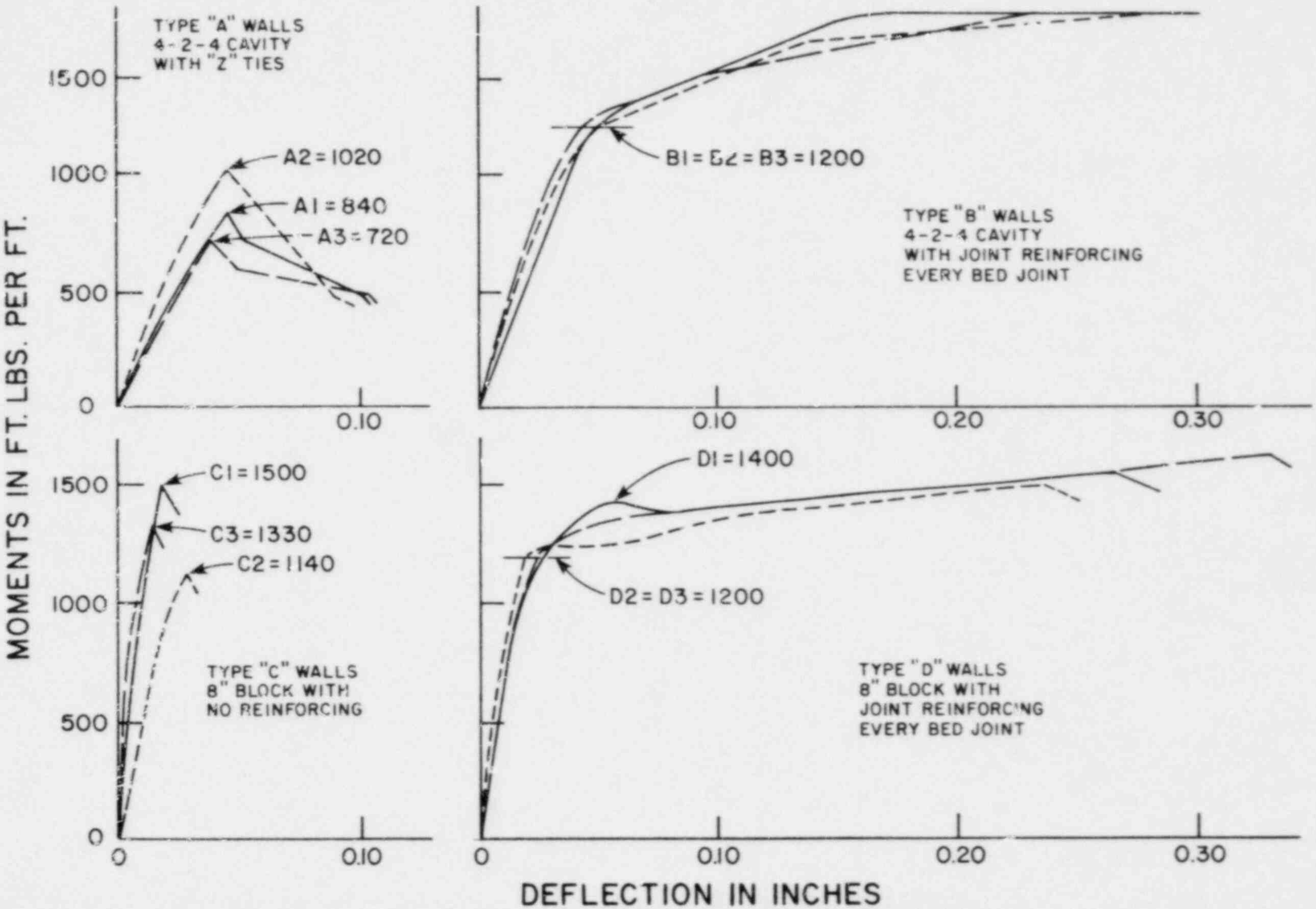

FIG. 3.5 MOMENT-DEFLECTION DIAGRAMS FOR BLOCK WALLS From Reference (6)

For the unreinforced walls the rupture and ultimate loads and deflections are the same indicating a brittle failure whereas for the reinforced walls there is an increase of 20% from the rupture to the ultimate load. The deflection at rupture is 0.03 inch and 0.27 inch at ultimate, indicating a ductile type of behavior.

Cox and Ennega included in their results spans at which a 20 psf wind loading would cause failure, see Table 3.13. Applying a factor of safety of two would result in spacing transverse supports 13 to 15 ft. apart for nonreinforced walls; however, they recommended 12 ft. spacing in compliance with the "American Standard Building Code Requirements for Masonry"(26). They also considered a span of 18 ft. to be reasonable for walls with horizontal reinforcement in each bed joint for both types of walls.

Scrivener(24) conducted two series of tests on 10 ft. high walls with 4 1/2 inch thick clay brick units and vertical reinforcing in the cores of the bricks. In the first series of tests the walls were tested in a horizontal plane with a face load applied by an air bag. The air bag reacted against the floor slab and the walls were simply supported at their ends. This was a somewhat artificial test as the dead load of the walls was incorrectly applied. In the second series of tests(27) the walls were kept in their natural vertical orientation and the face load was applied by an air bag in a manner similar to that shown in Fig. 2.1. The load was applied cyclically by changing the air bag from one face to the other. The walls contained varying amounts of vertical reinforcement as shown in Table 3.14. A typical cyclic load-deflection curve is given in Fig. 3.6. Included in the results of Table 3.14 are the theoretical yield loads which were calculated by the method described in Section 4.5.

Table 3.14

Cyclic Face Loading of Reinforced Brick Walls

- Test Results and Wall Details

Wall Reinforcement	Yield Loads (lb/ft^2)	
	Theoretical	Experimental
None	-	32
2 - 3/8" diam.	31	33
3 - 3/8" diam.	46	42
4 - 3/8" diam.	61	64
3 - 1/2" diam.	77	84

Bricks: McSkimmings 4¼" reinforcing and lattice bricks.

Walls: Brickwork 10' high x 5' wide supported on RC beams at base and top.

Reinforcing: Vertical deformed bars in grouted cores, lapped with starter bars from RC beams.

from reference (23)

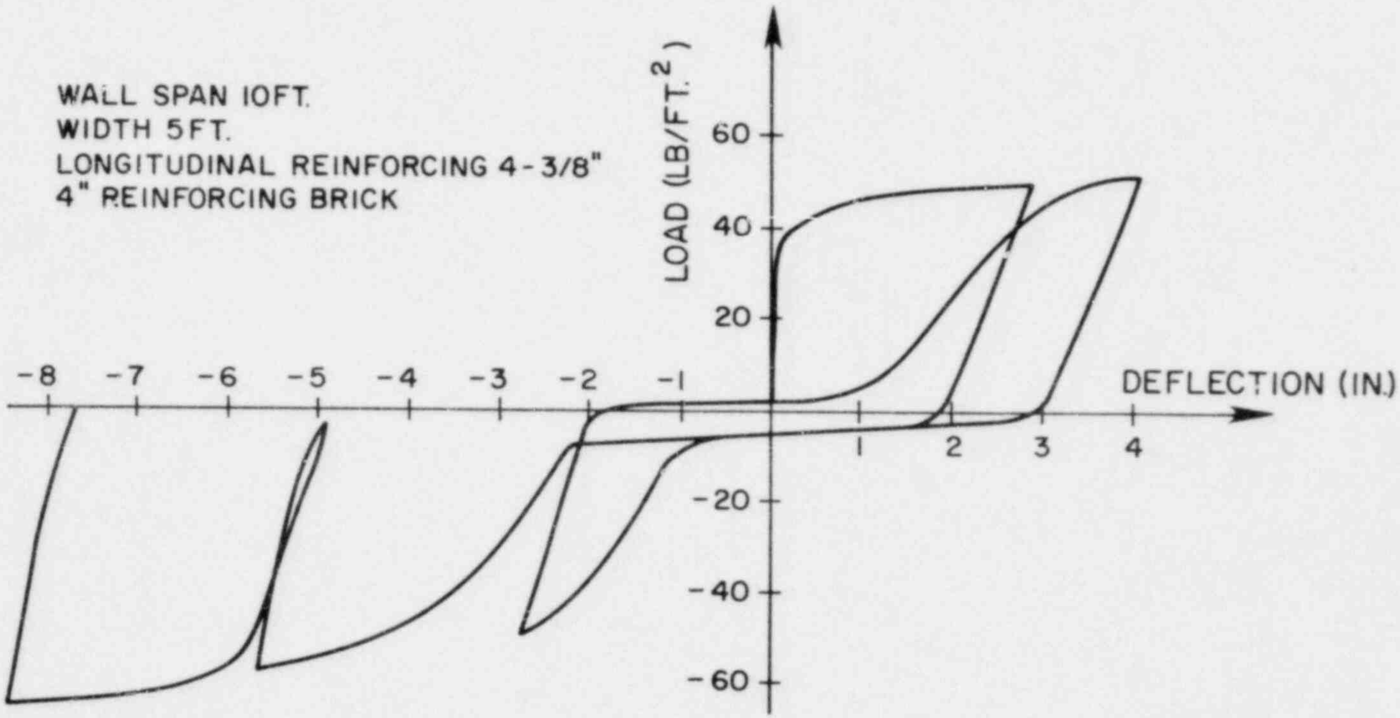

FIG. 3.6 LOAD-DEFLECTION HYSTERESIS OF REINFORCED MASONRY WALL UNDER CYCLIC LOADING

From Reference (23)

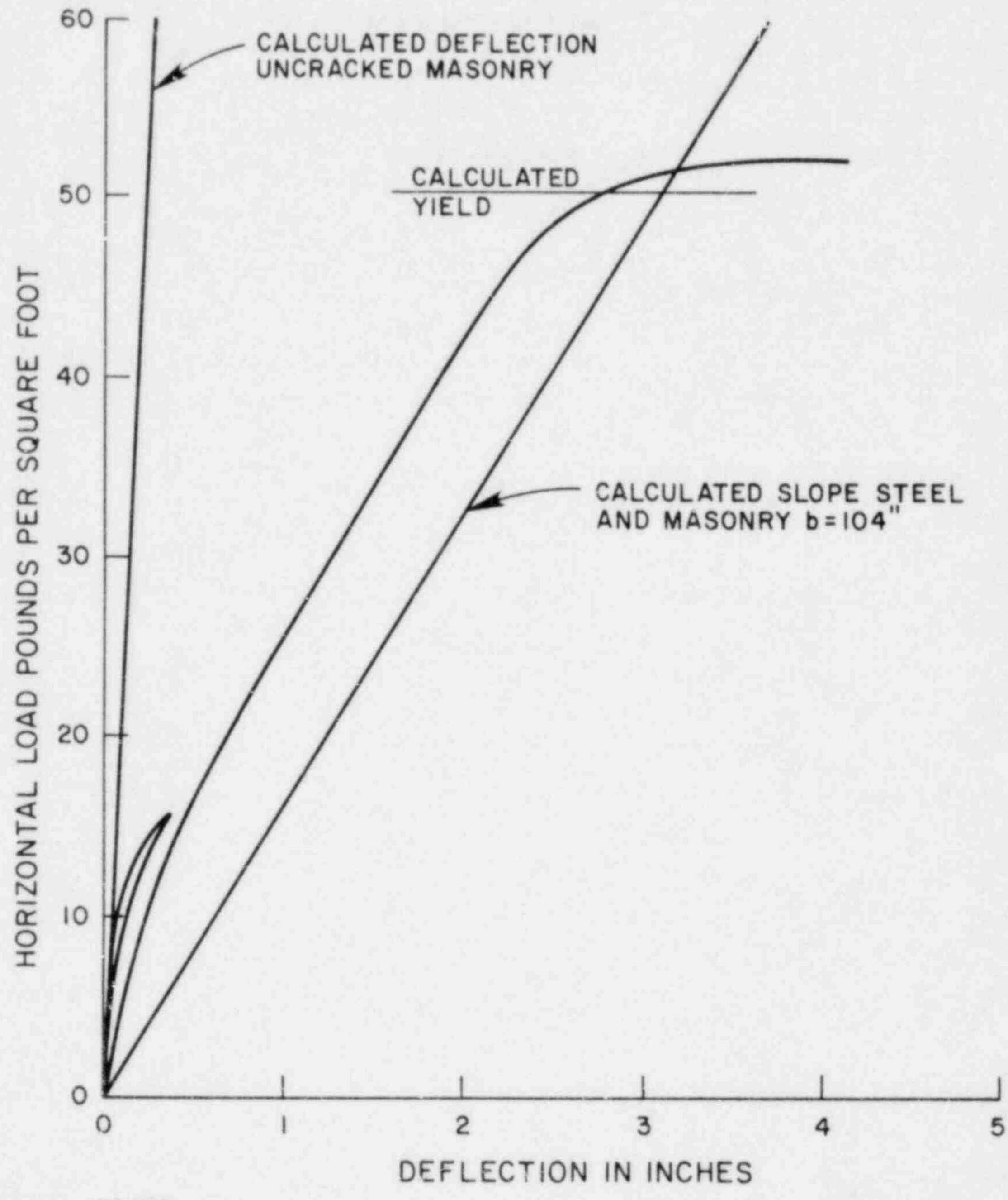

NOTES:

1 - #7 BAR EACH END OF WALL - BARS 8'-0" O.C.
EFFECTIVE DEPTH = 4" (MEASURED)
TEST REBOUNDED @ 15.6#/□' TO 2.6#/□'

FIG. 3.7 MONOTONIC LOADING TEST RESULT

From Reference (25)

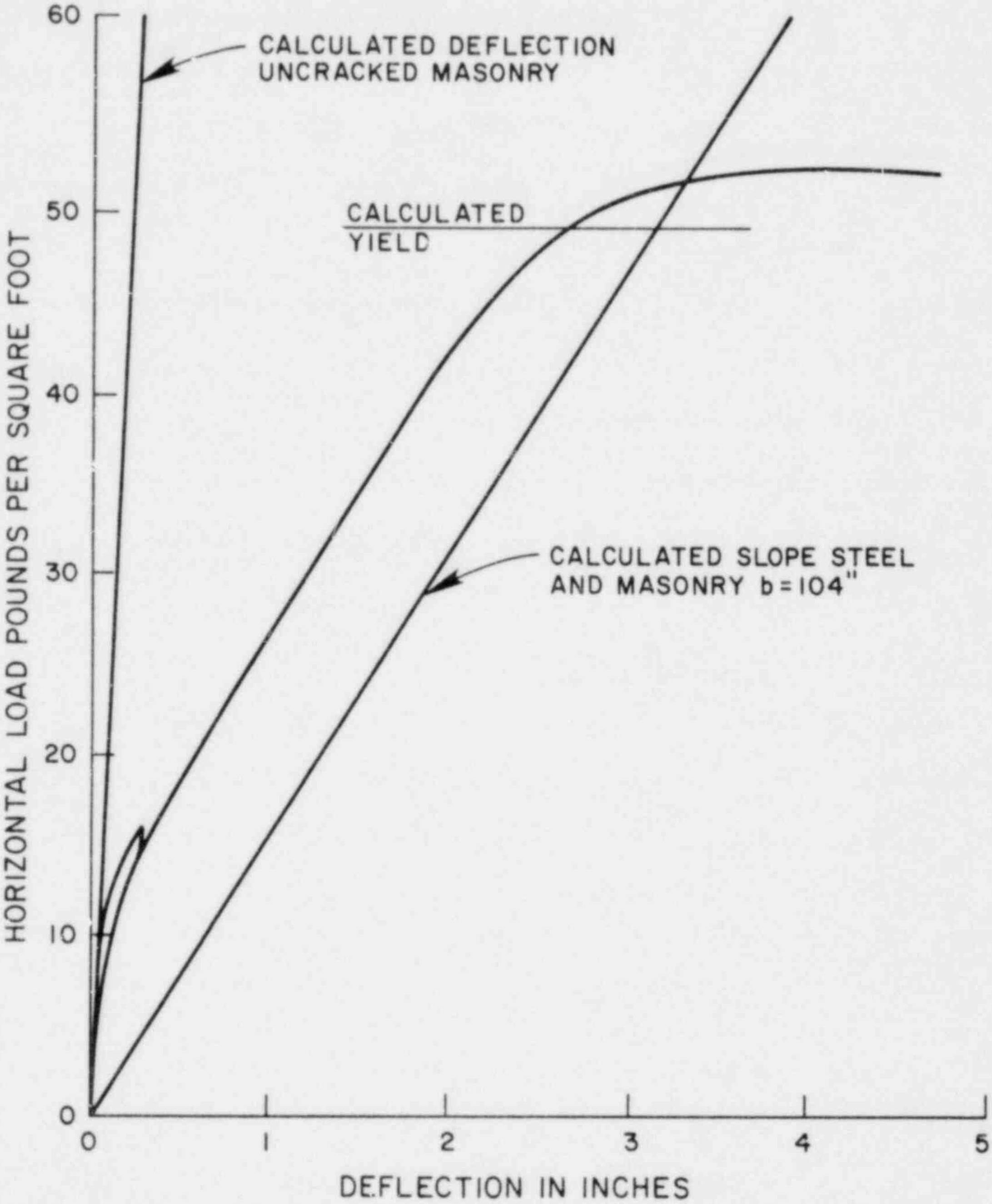

NOTES:

VERTICAL BARS @ 24" O.C.
EFFECTIVE DEPTH = 3.9" (MEASURED)
TEST REBOUNDED @ 15.6#/□' TO 2.6#/□'

FIG. 3.8 MONOTONIC LOADING TEST RESULT

From Reference (25)

The two main points resulting from this test series are as follows: First, the theoretical yield load was within 10% of the experimental yield load for all walls. Secondly,the cyclic load deflection curves showed highly ductile behavior characterized by large inelastic deflections. Scrivener noted that even with deformations of 6 inches and greater there was never any sign of bricks separating from the wall. The hysteresis loops were narrow because of the positioning of the reinforcement at the center of the wall.

In a series of eight tests performed by Dickey and Mackintosh[25] the spacing of vertical reinforcement in hollow concrete block walls was evaluated. The test specimens were 20 ft. high and 8 ft. 8 in. long constructed from both 8 inch and 6 inch units. The walls were tested in a manner similar to that shown in Fig. 2.1. Each wall had a bond beam at the top and a bond beam at 7 ft. 2 in. from the foundations.

The objective of the test series was to determine the effect of the spacing of vertical reinforcing on the flexural resistance of reinforced concrete masonry walls. All walls contained the same area of vertical steel 1.2 sq. in. and only the spacing varied. Also included was a stack bonded test specimen. The force-deflection relationships for the walls with re-bar at 8 ft. and 2 ft. spacing are shown in Figs. 3.7 and 3.8, respectively. It is clear that the wall with bars 2 ft. center to center was able to maintain load over a larger deflection (5 inches) as compared to 4 inches for the wall with bars 8 ft. center to center, but the ultimate load of the two walls was the same. It is interesting to compare the force-deflection relationships obtained in the cyclic tests (Fig. 3.6) and the monotonic tests (Fig. 3.7). There appears to be a more ductile behavior in the walls tested cyclically. Dickey and Mackintosh concluded that vertical reinforcing for walls laid in running bond functions for stress and deflection over the total width as effectively at 8 ft. spacing as it does at 2 ft. spacing

3.6 Effect of Added Vertical Load

Yokel et al.(6) performed an extensive series of tests on the transverse strength of masonry walls with a combination of transverse and vertical loads. The relationships between the vertical compressive load and the transverse load for ten types of construction (listed in Table 3.6) are shown in Figs. 3.9 (1) to (10). The walls were loaded axially with a uniform load and the transverse load was applied uniformly over the face of the wall with the test setup shown in Fig. 2.1.

A brief summary of the manner in which the walls failed is now given. Both the 8 in. hollow concrete block walls with 1:3 mortar and high-bond mortar failed by tensile cracking along horizontal joints near midspan when the compressive bearing stress ranged from 0 to 359 psi to 449 psi, respectively. For vertical compressive loads greater than these values, vertical splitting occurred along the ends of the walls near the top or the bottom as shown in Fig. 3.10. Eight inch solid concrete block walls with 1:3 mortar failed along a horizontal joint at or near midspan, under combined loading in which the superimposed vertical compressive load ranged from 0 to 552 psi, as shown in Fig. 3.11.

The general trend in the failure of the 4-inch brick walls, as listed in Table 3.8, is similar to that of concrete block walls. Under combined loading conditions with small vertical compressive loads,

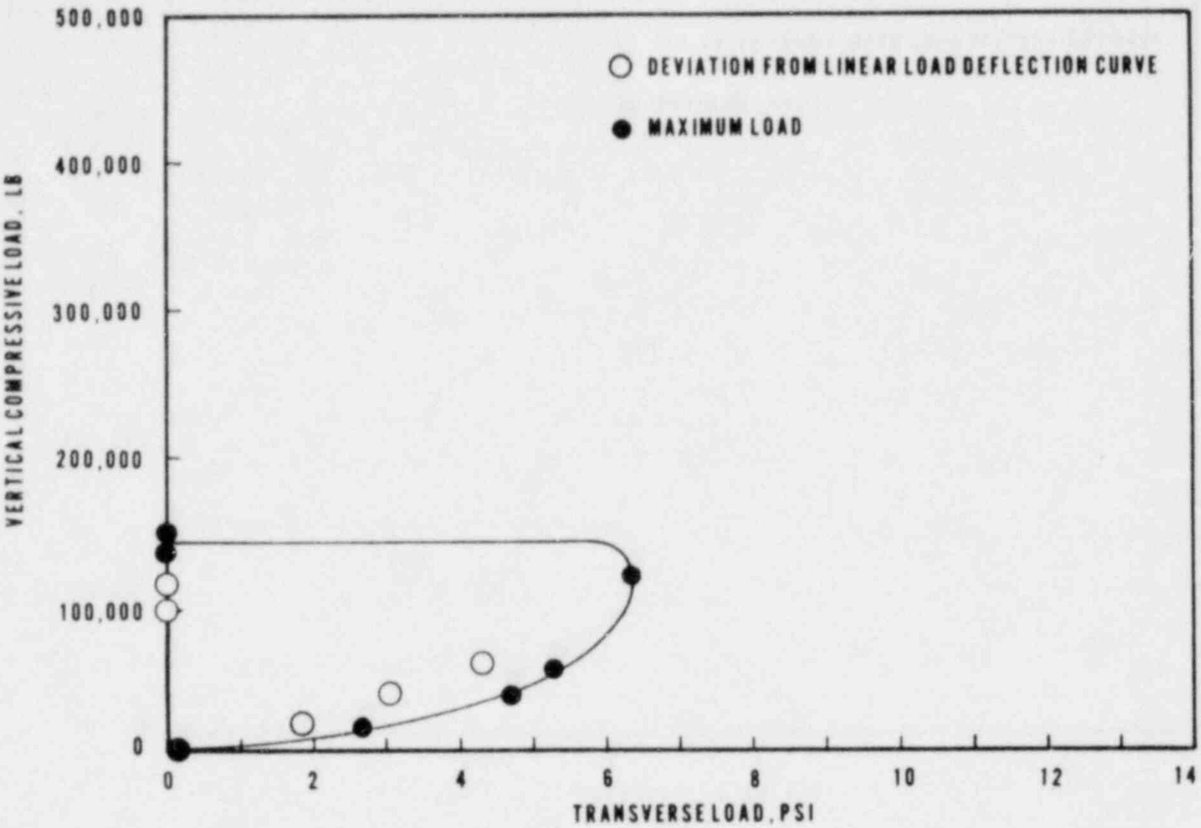

FIG. 3.9(1) RELATIONSHIP BETWEEN VERTICAL COMPRESSIVE LOAD AND TRANSVERSE LOAD FOR 8-IN HOLLOW CONCRETE BLOCK WALLS WITH TYPE N(1:3) MORTAR

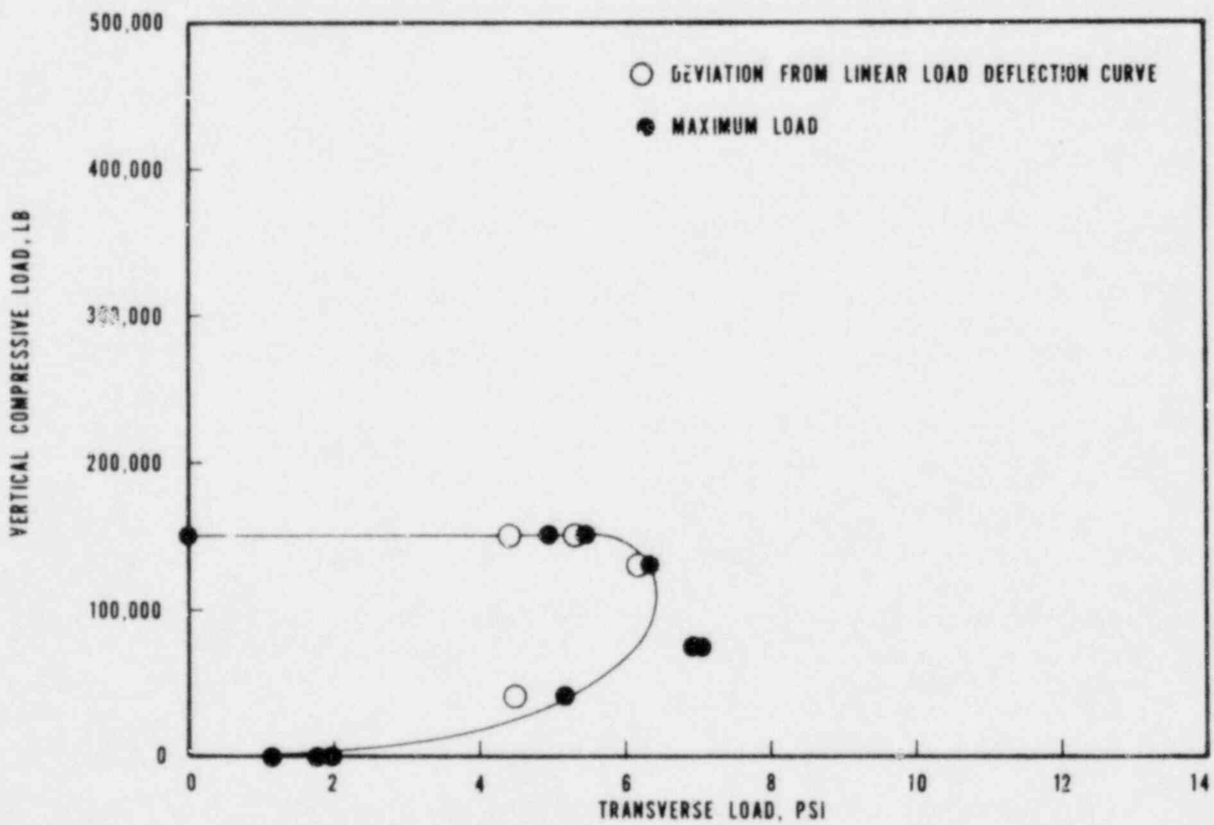

FIG. 3.9(2) RELATIONSHIP BETWEEN VERTICAL COMPRESSIVE LOAD AND TRANSVERSE LOAD FOR 8-IN HOLLOW CONCRETE BLOCK WALLS WITH HIGH BOND MORTAR

From Reference (4)

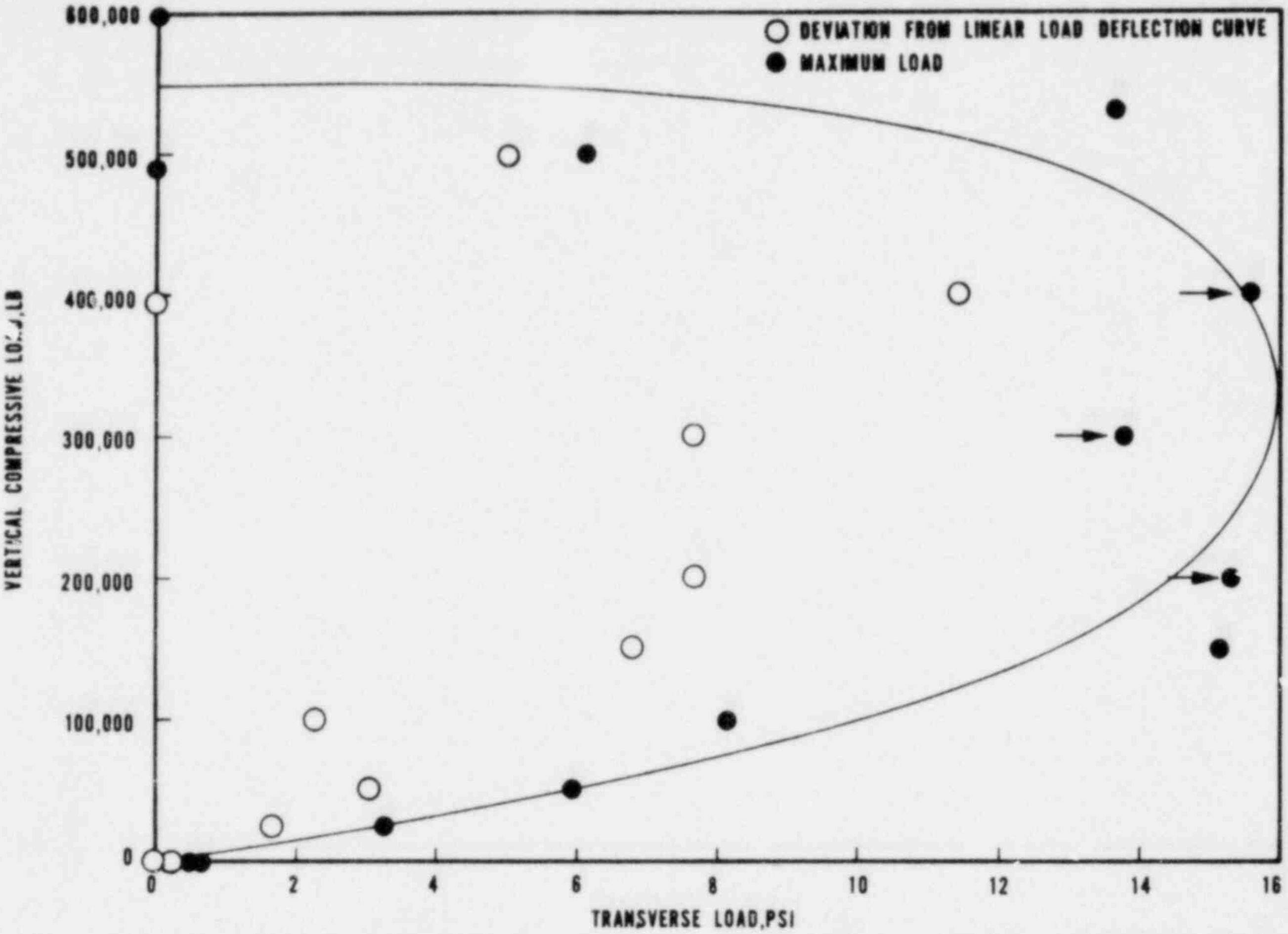

FIG. 3.9(3) RELATIONSHIP BETWEEN VERTICAL COMPRESSIVE LOAD AND TRANSVERSE LOAD FOR 8-IN SOLID CONCRETE BLOCK WALLS WITH TYPE N(1:3) MORTAR

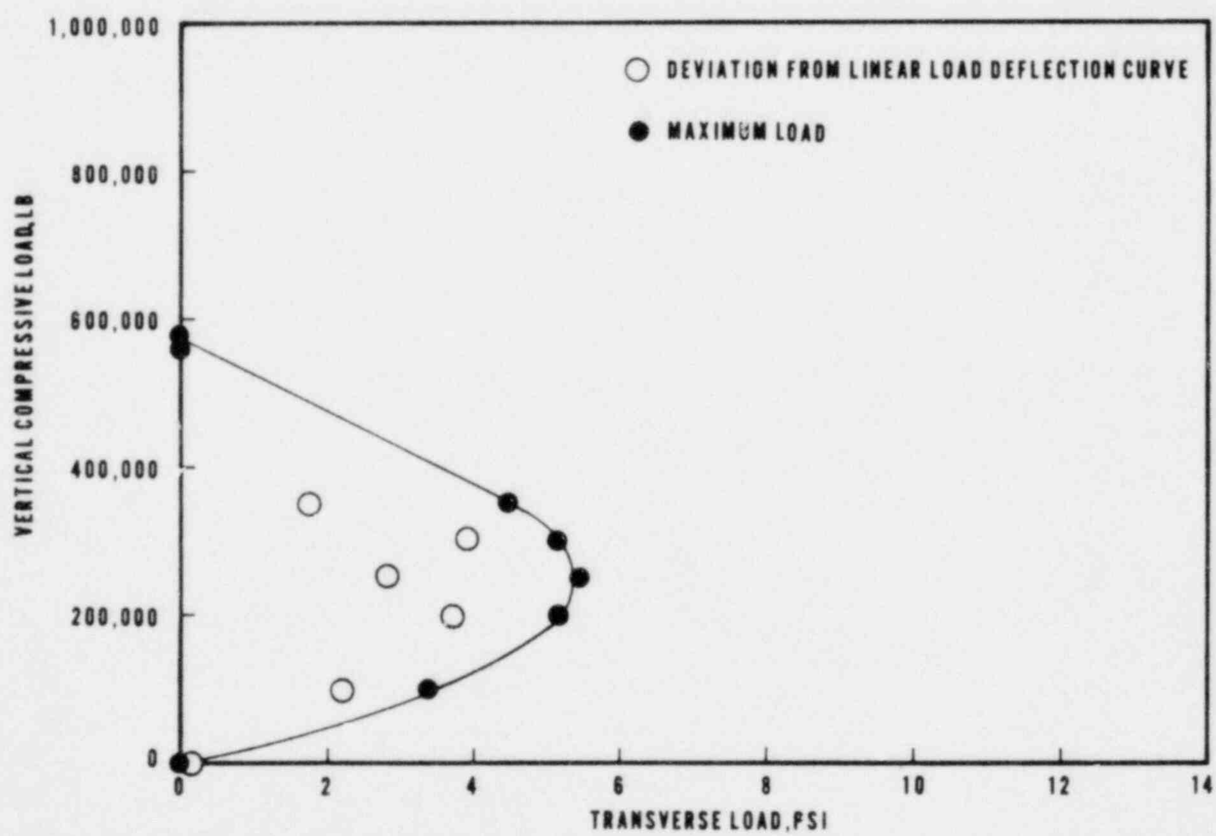

FIG. 3.9(4) RELATIONSHIP BETWEEN VERTICAL COMPRESSIVE LOAD AND TRANSVERSE LOAD FOR 4-IN BRICK A WALLS WITH 1:1:4 MORTAR

From Reference (4)

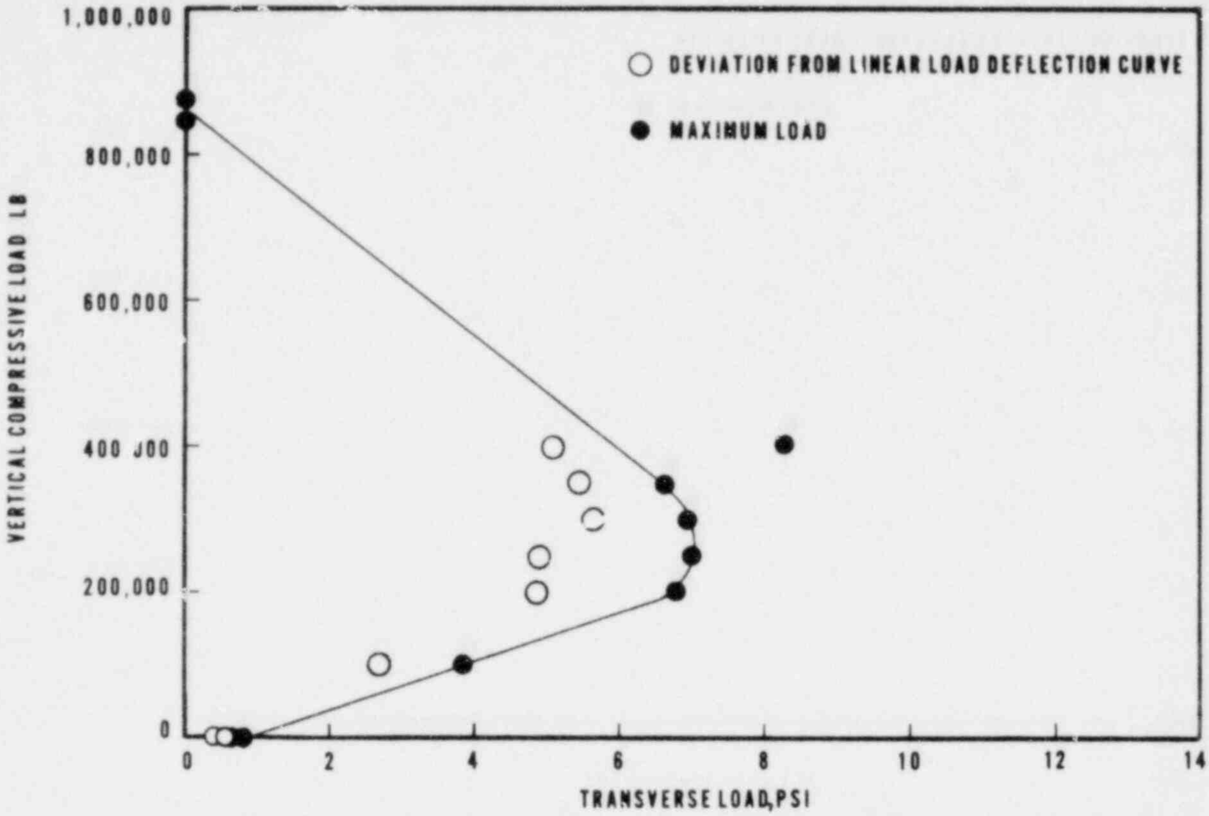

FIG. 3.9(5) RELATIONSHIP BETWEEN VERTICAL COMPRESSIVE LOAD AND TRANSVERSE LOAD FOR 4-IN BRICK A WALLS WITH HIGH BOND MORTAR

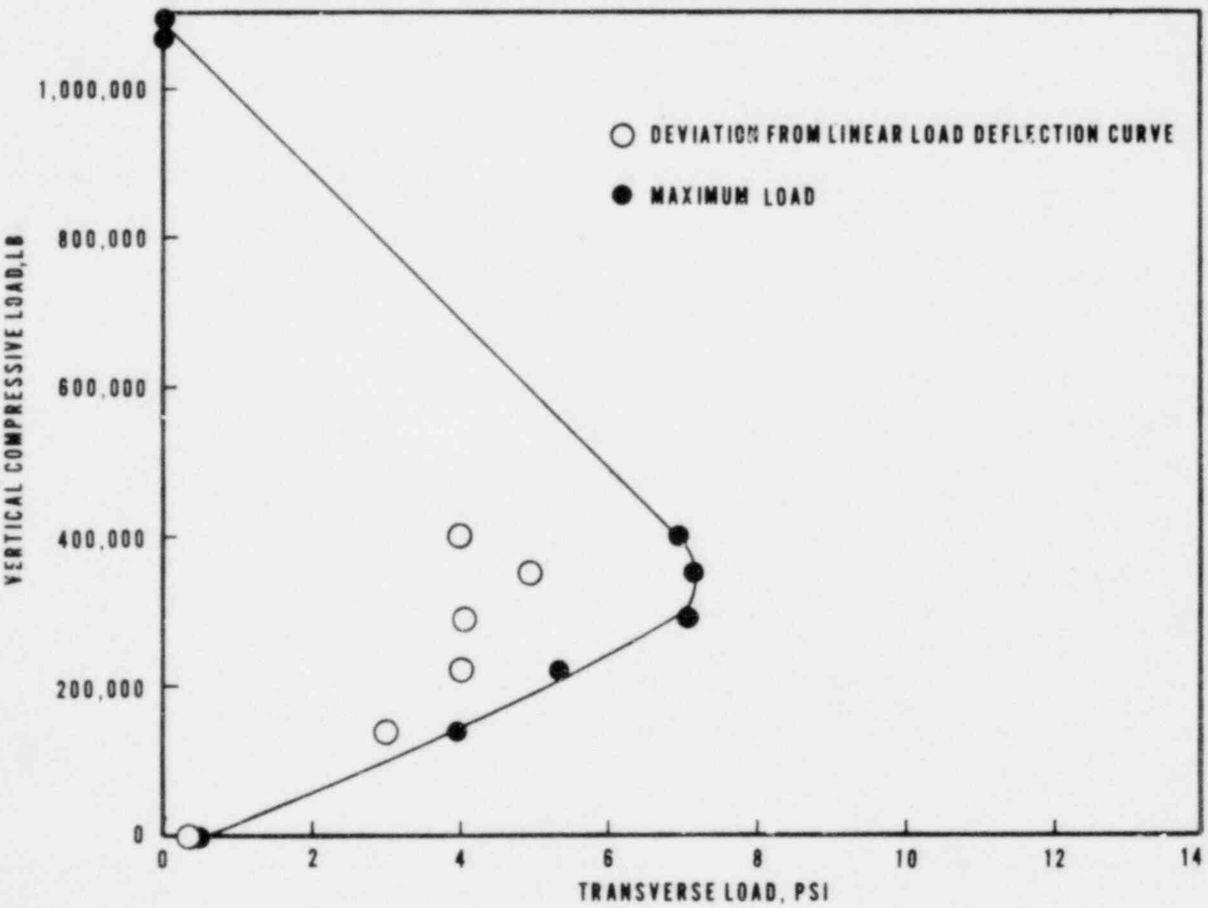

FIG. 3.9(6) RELATIONSHIP BETWEEN VERTICAL COMPRESSIVE LOAD AND TRANSVERSE LOAD FOR 4-IN BRICK S WALLS WITH HIGH BOND MORTAR

From Reference (4)

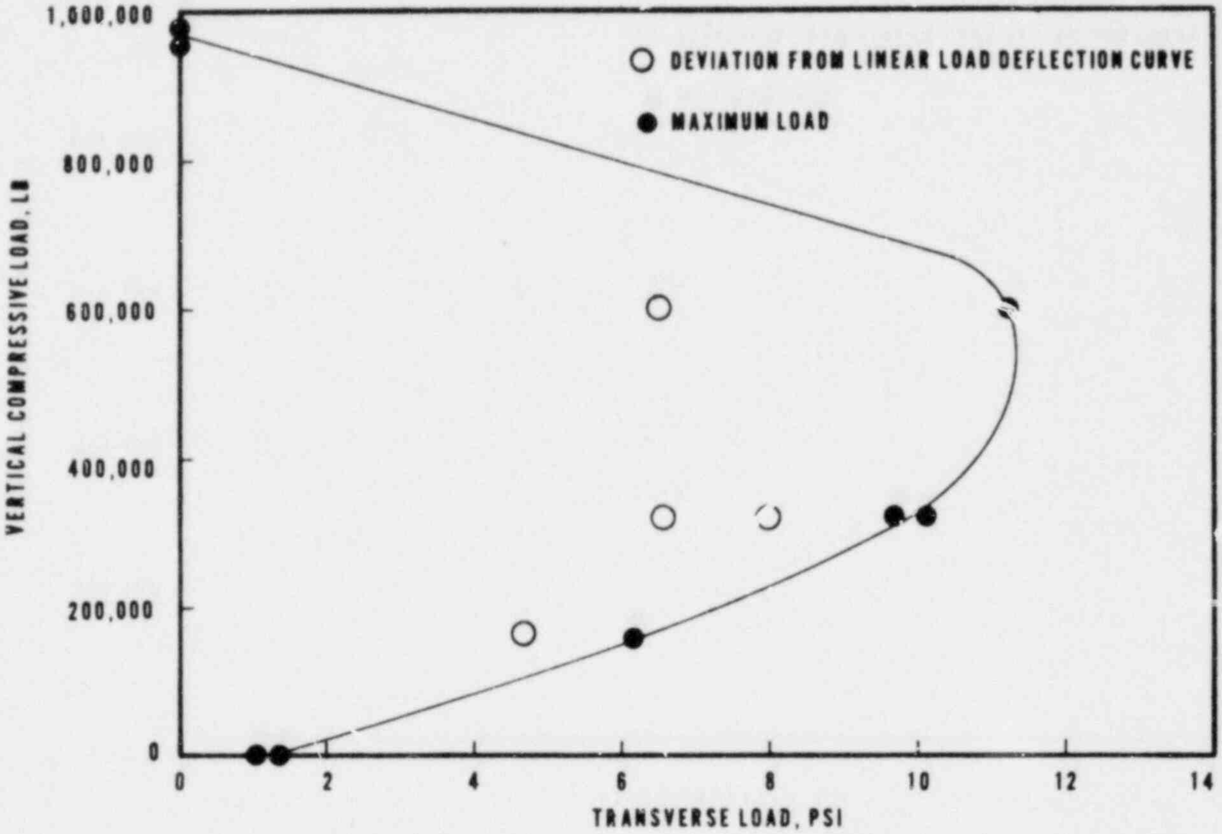

FIG. 3.9(7) RELATIONSHIP BETWEEN VERTICAL COMPRESSIVE LOAD AND TRANSVERSE LOAD FOR 4-IN BRICK B WALLS WITH HIGH BOND MORTAR

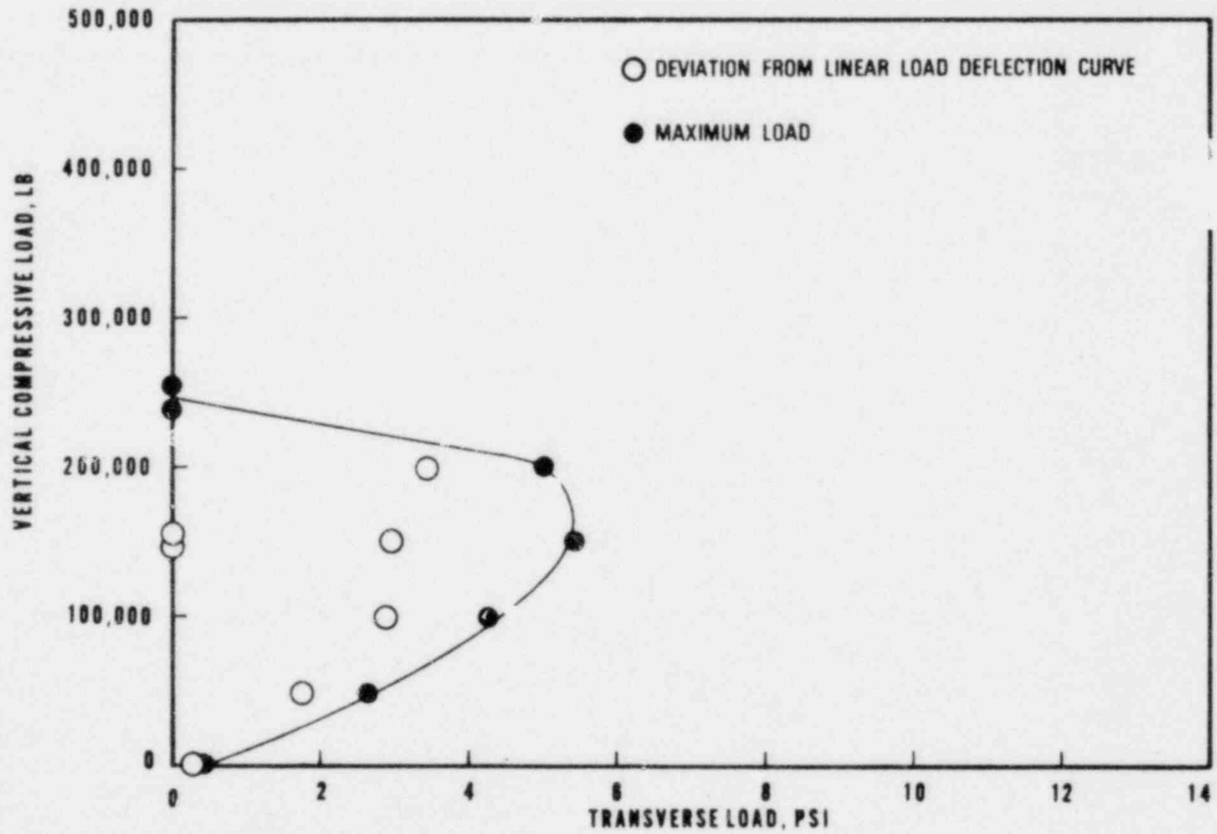

FIG. 3.9(8) RELATIONSHIP BETWEEN VERTICAL COMPRESSIVE LOAD AND 4-2-4 IN CAVITY BLOCK AND BLOCK WALLS WITH TYPE N(1:3) MORTAR

From Reference (4)

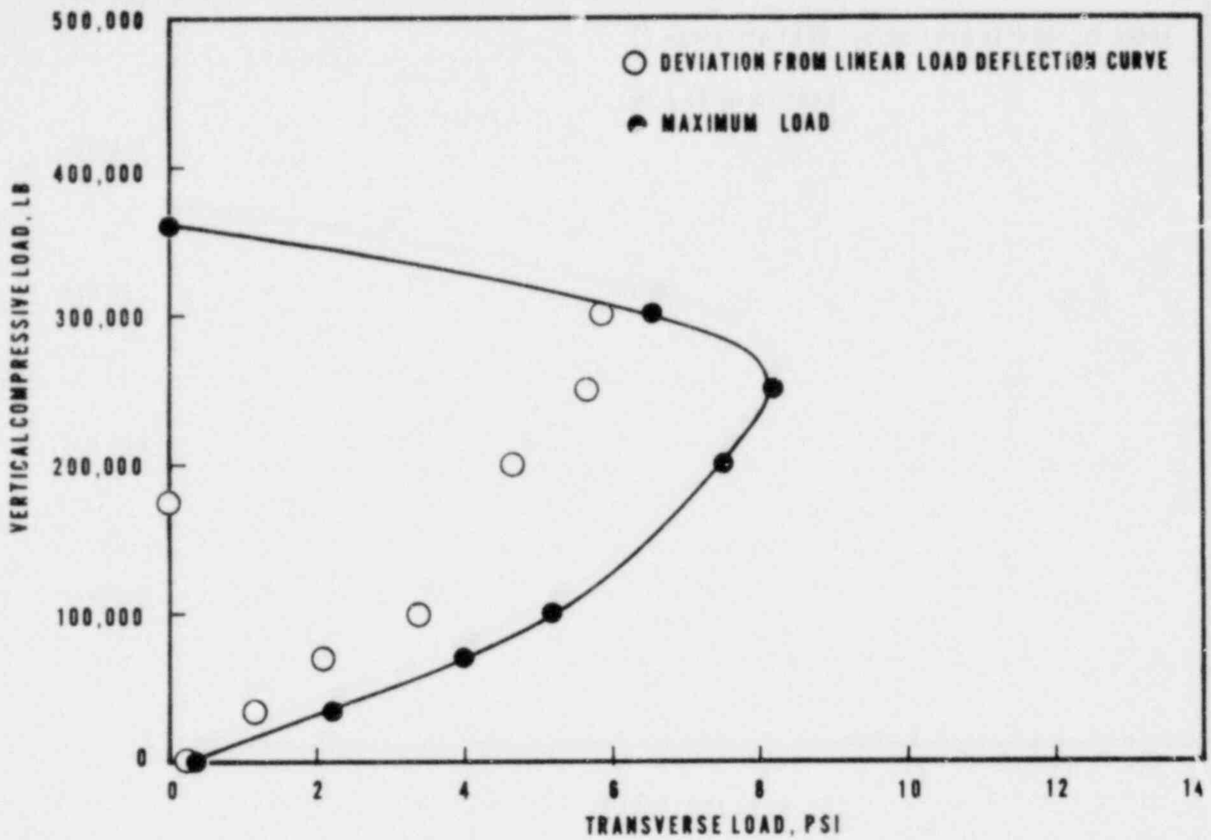

FIG. 3.9(9) RELATIONSHIP BETWEEN VERTICAL COMPRESSIVE LOAD AND TRANSVERSE LOAD FOR 4-2-4 IN CAVITY BRICK AND CONCRETE BLOCK WALLS WITH TYPE N(1:3) MORTAR

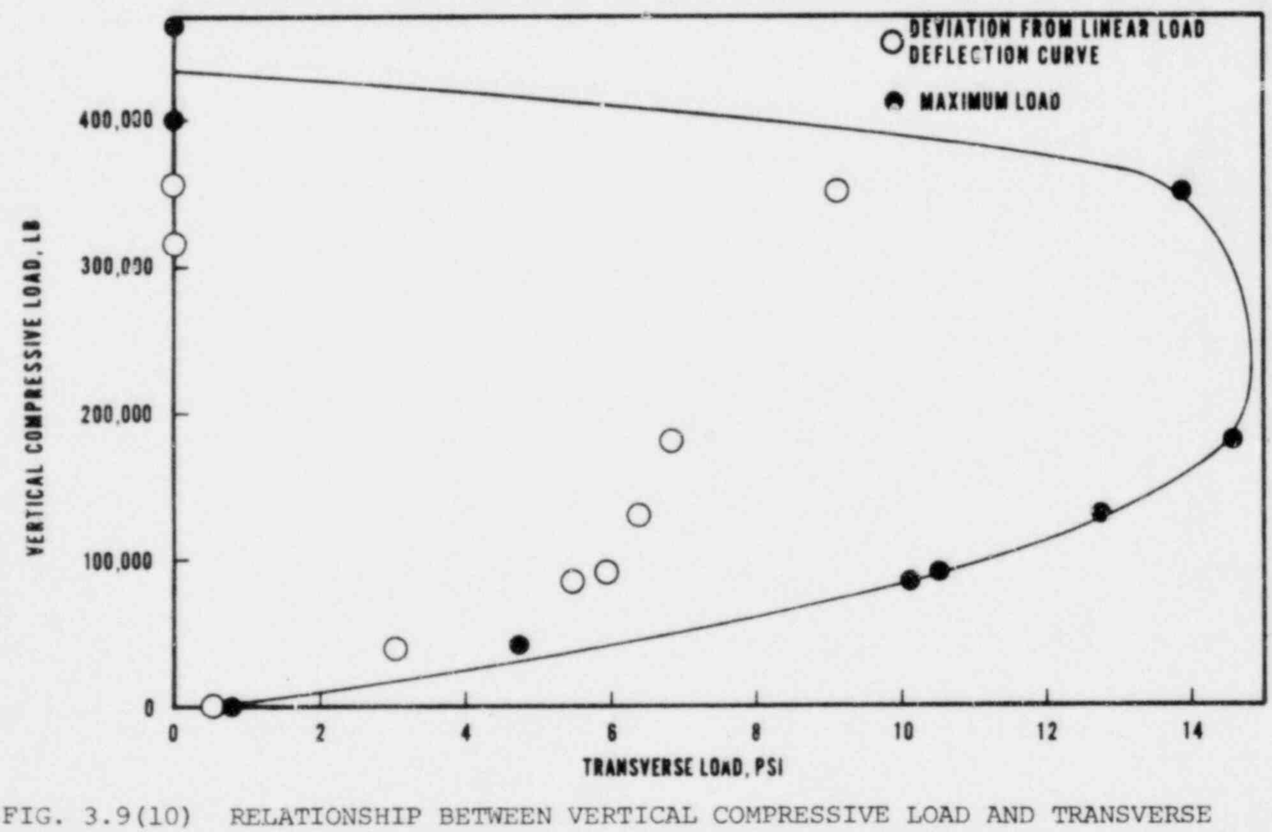

FIG. 3.9(10) RELATIONSHIP BETWEEN VERTICAL COMPRESSIVE LOAD AND TRANSVERSE LOAD FOR 8-IN COMPOSITE BRICK AND CONCRETE BLOCK WALLS WITH TYPE N(1:3) MORTAR

From Reference (4)

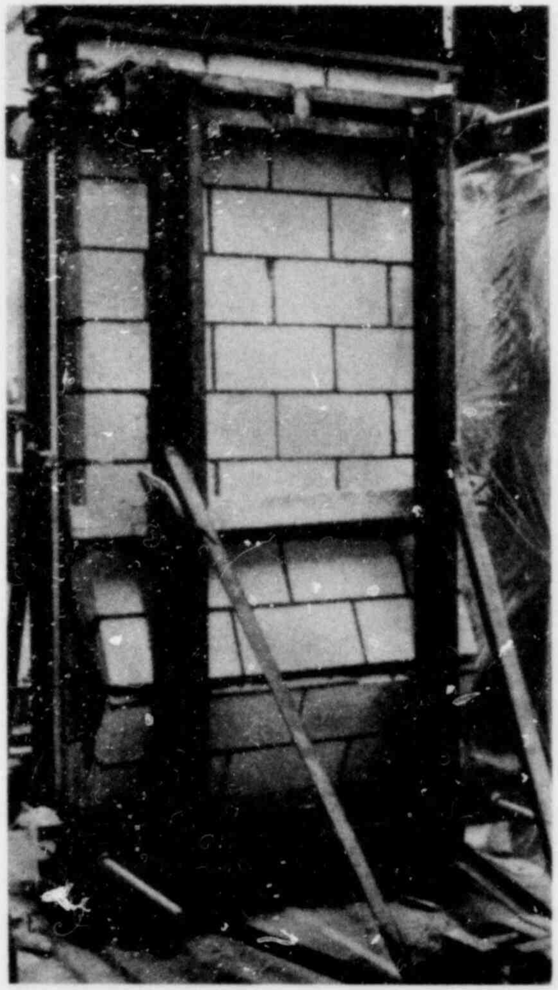

FIG. 3.10 FAILURE OF 8-IN HOLLOW CONCRETE BLOCK WALL (SPECIMEN 2-8)

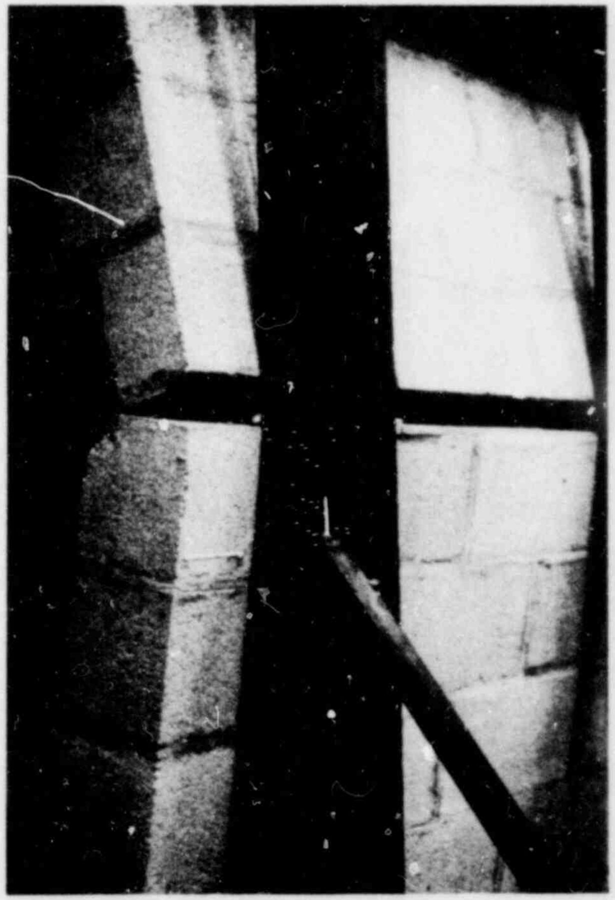

FIG. 3.11 FAILURE OF 8-IN SOLID CONCRETE MASONRY WALL

From Reference (6)

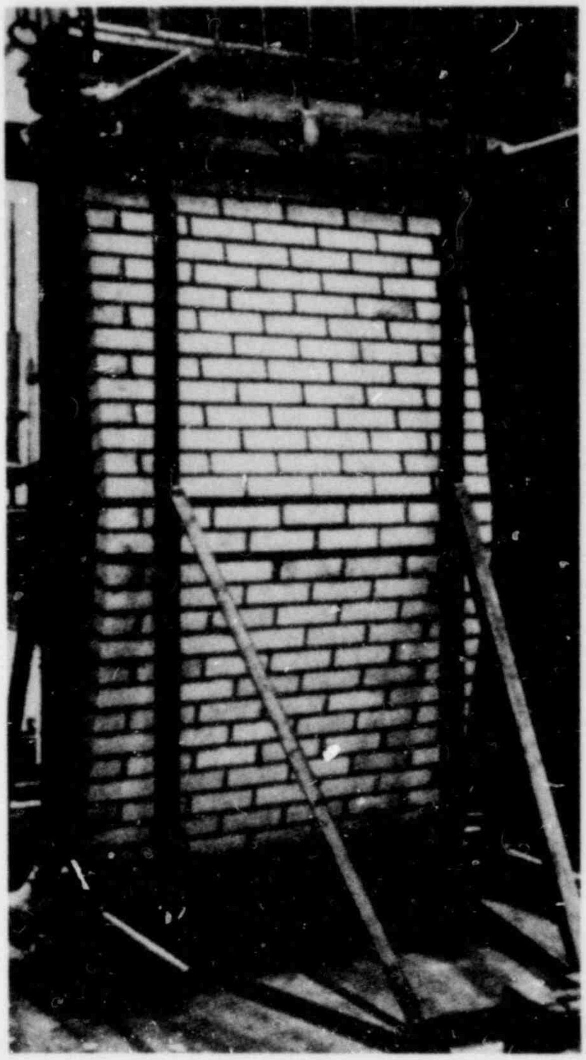

FIG. 3.12 TYPICAL FAILURE OF BRICK WALLS WITH LOW VERTICAL COMPRESSIVE LOADS

From Reference (6)

failure occurred on the tensile face of the wall with cracking along a horizontal joint near midspan, as shown in Fig. 3.12. An increase in the vertical compressive load resulted in flexural failures that were initiated on the compressive side of the specimen. At very high vertical loads failure occurred suddenly with crushing as shown in Fig. 3.13.

For the 4-2-4 in. cavity hollow concrete block or brick-block walls, tensile failure due to combined loading occurred near midspan in walls to which a low compressive load was applied. An increase in the vertical compressive load resulted in buckling of the ties and subsequent crushing of the masonry for the brick-block walls. At high vertical compressive loads, failure occurred by crushing accompanied by some splitting of the concrete masonry units near the top of the wall as shown in Fig. 3.14.

In the case of 8 inch composite brick and hollow concrete block walls, tensile failure occurred on the block face along a horizontal joint near midspan for walls having low vertical loads. For high compressive loads, these walls either failed by crushing of the concrete units or flexural loading had to be suspended because of the limited capacity of the horizontal loading equipment.

It is clear from these test results that the addition of a vertical compressive load to the walls increases the transverse strength of the walls which fail in flexure. Figure 3.15 shows load-deflection curves for 20, 60 and 120 kip compressive loads, with the dashed line referring to the 20-kip case. Note that at this small vertical load the wall apparently exhibits considerable ductility. This may be attributed to the loss in stiffness with section cracking and not to

FIG. 3.13 TYPICAL FAILURE OF BRICK WALLS WITH HIGH VERTICAL COMPRESSIVE LOADS

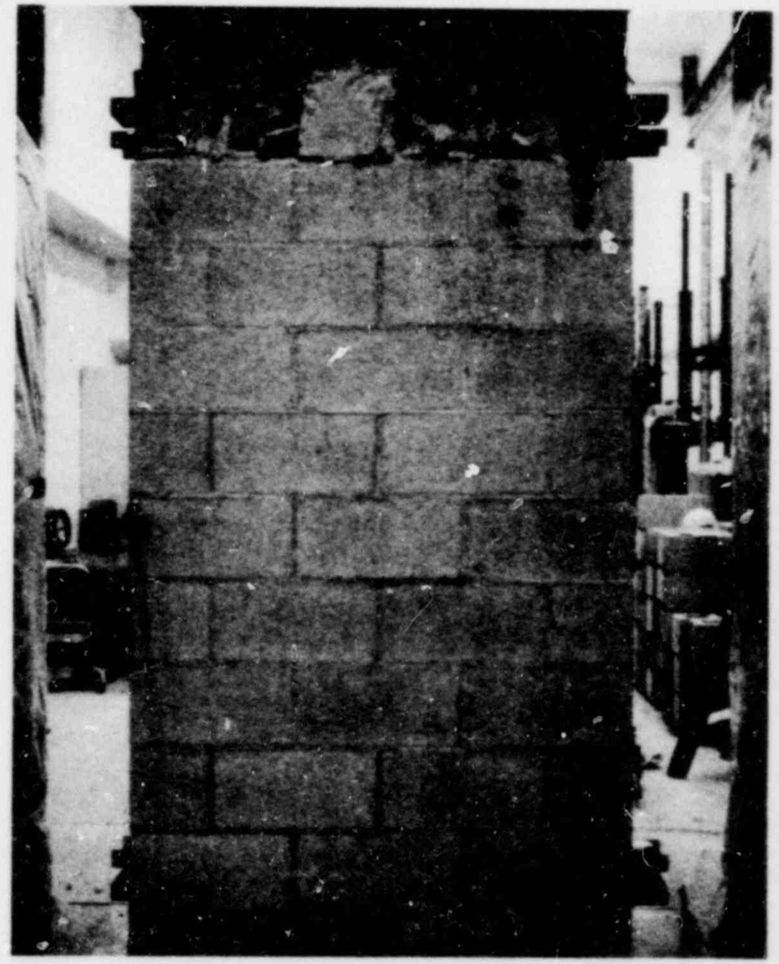

FIG. 3.14 FAILURES OF BRICK-BLOCK CAVITY WALLS

From Reference (6)

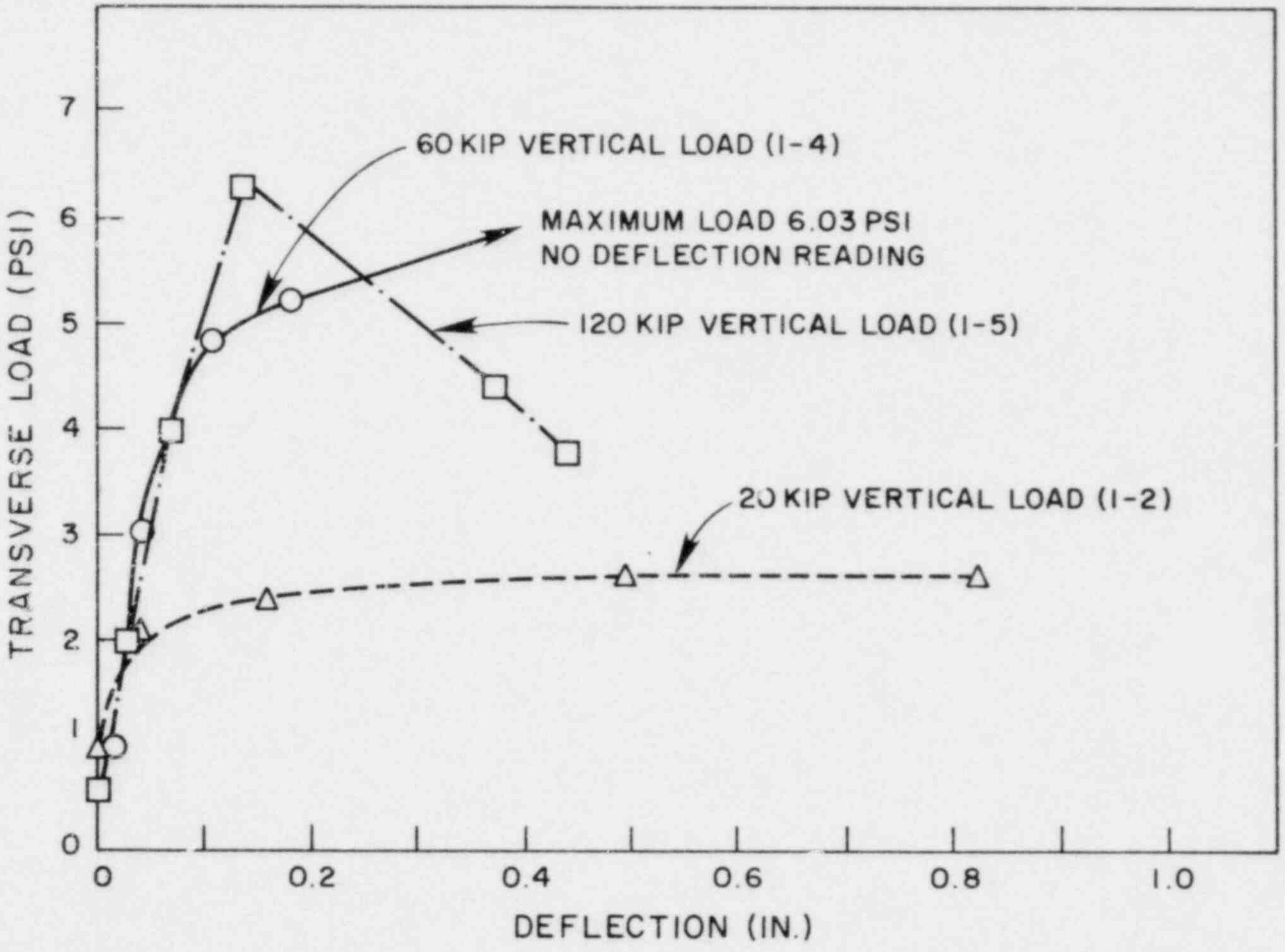

FIG. 3.15 LOAD-DEFLECTION CURVES FOR 8-IN HOLLOW CONCRETE BLOCK WALLS WITH TYPE N MORTAR
From Reference (4)

any real ductility of the materials. Large additional deflections can then develop without a significant increase in moment. At higher compressive loads, failure tends to be more brittle, as is illustrated in Fig. 3.15 by the dashed-dotted line which refers to the 120 kip vertical load.

In tests performed by the Portland Cement Association six walls that had been tested by transverse loads on a vertical span were repaired by a polyester resin adhesive and were then retested with a combined transverse load and an 85 psi uniform compressive load. The test results are shown in Table 3.12. The addition of a vertical compressive load to the walls tested in flexure across a vertical span proved to be an effective method of increasing the flexural strength. These tests show that use of the bearing load carrying capacity of a wall is one way of increasing the stability of the wall for transverse loads.

3.7 Comparison Between Small Scale Wallette Tests and Full Scale Wall Tests

While performing expensive full-scale tests it is important to determine their correlation with small-scale tests that can easily be performed in test laboratories. The most simple test having a failure mechanism similar to the mortar joint tensile failure in flexural tests is the wallette test shown in Fig. 2.3. Three different series of investigations have been performed to evaluate the correlation that exists between wallette and full scale transverse tests.

The Structural Clay Products Institute[20] performed a series of tests on 6 inch and 8 inch thick clay brick walls. The wallettes were 24 in. x 24 in. and were tested with the setup shown in Fig. 2.3

The walls were wide and spanned 7 ft. 6 in. between vertical supports. They were tested with the air-bag system shown in Fig. 2.1. The results of the two series of tests are given in Table 3.15. The 4S, 6S and 8S specimens were all solid clay units with full bed joints. The range of the ratio

(modulus of rupture of walls)/(modulus of rupture of wallettes)

was 1.1 to 1.3. For hollow units, 6H and 8H, the ratio was 0.92 for the 6 inch units and 1.6 for the 8 inch units. Except for the 6 inch hollow units the modulus of rupture of the wallettes was lower than that of the full scale walls with the best correlation found with the solid units.

The Structural Clay Products Research Foundation[28] performed a similar series of tests of 4 inch wide structural clay facing tiles. The wallettes were 16 inches high and the walls were 4 ft. wide and spanned 7 ft. 6 in. between vertical supports. The results are given in Table 3.16. The ratios of the modulus of rupture of the walls to wallettes varied between 0.47 and 0.7. For this series of tests, the modulus of rupture of the wallettes was substantially higher than that of the walls. This is opposite to the trend observed in the tests on the clay brick units.

Johnson and Mathys[29] performed a series of comparative tests using various types of hollow clay tiles with a type S mortar. All the horizontally cored units, designated with an H, were laid with full bed joints while the vertically cored units, designated with a V, were laid with a face shell bedding. Three flexural wallettes two units high were built with each type of unit and were tested according to ASTM-E 149. For each type of unit six wall specimens 4 ft. x 8 ft. were constructed. Three of the specimens were tested with the span

Table 3.15

Transverse (Flexural) Strength of Single-Wythe 6 and 8-in. Clay Masonry Walls

Specimen		Wallettes (24 in. by 24 in.)[1]				Walls (7-ft 6-in. Span)			
Series	Thickness, t in.	Ultimate Load, P lb	Modulus of Rupture[2] f'_t psi	Average f'_t psi	V %	Ultimate Load, q psf	Modulus of Rupture[2] f'_t psi	Average f'_t psi	V %
4S (control)	3.63	444 449 280	118 119 75	104	24	45 55 30	143 175 95	138	29
6S	5.50	2035 1230 1885	155 94 144	131	25	76 111 116	106 155 162	141	22
8S	7.50	4265 3500 3585	165 135 138	146	11	229 217 253	172 163 190	175	8
6H	5.56	1030 1124 1215	77 84 91	84	8	42 59 68	57 81 92	77	24
8H	7.56	548 873 1172	21 34 46	34	36	80 64 73	59 47 54	53	11

(1) Except for 4S series which were nominal 16 in. by 16 in.

(2) Based on gross cross-sectional areas

Table 3.16

Transverse Strength of 4-in. Structural Clay

Facing Tile Wallettes and Walls

Series	Wallettes						Walls							
	No.	Total Load	Modulus of Rupture f'_t	$\overline{X}$	s	v	No.	Ultimate Load[1]	Modulus of Rupture f'_t	$\overline{X}$		s		v
										Ultimate Load	Modulus of Rupture	Ultimate Load	Modulus of Rupture	
		lb.	psi	psi	psi	%		psf	psi	psf	psi	psf	psi	%
6T	1	568	194	184	8.95	4.9	TT-10	25	75	29	86	4.73	14.93	16.5
	2	523	179				TT-11	27	80					
	3	519	178				TT-12	34	103					
6TC	1	542	186	175	15.72	9.0	TT-4	43	130	41	123	4.36	13.34	10.6
	2	533	182				TT-5	44	132					
	3	457	157				TT-6	36	108					
8WC	1	827	210	221	12.23	5.5	TT-1	44	137	47	147	3.51	10.02	7.4
	2	925	234				TT-2	51	157					
	3	860	218				TT-3	47	146					

[1]Over 7.5-ft span.

from reference (28)

Table 3.17
Ultimate Transverse Strength

Type	WALLETTES			WALLS SPAN NORMAL TO BED JOINT					WALLS SPAN PARALLEL TO BED JOINT				
	Modulus Rupture			Modulus Rupture					Modulus Rupture				
	Gross, per sq. in.	Net, per sq. in.	V as a %	Gross, per sq. in.	Net, per sq. in.	V	F net x 10^6 per sq. in.	V as a %	Gross, per sq. in.	Net, per sq. in.	V	F net x 10^6 per sq. in.	V as a %
(1)	(2)	(3)	(4)	(5)	(6)	(7)	(8)	(9)	(10)	(11)	(12)	(13)	(14)
4 in. H	91.5	79.2	19.6	130.5	178.3	13.3	2.25	5.7	253.3	360	21.6	2.93	7.5
4 in. V	44.4	54.9	6.5	63.1	86.0	16.9	--	--	149.3	203.6	16.9	2.35	1[illegible].9
6 in. H	111.2	74.6	23.0	64.4	109.0	17.8	1.16	14.1	94.0	159.2	4.8	1.55	3.6
6 in. V	98.4	189.9	23.1	77.2	114.5	23.4	--	--	210.1	310.9	7.3	1.52	2.6
8 in. H	72.8	47.3	33.5	57.1	124.9	12.2	--	--	80.8	176.5	15.8	6.75	30.0
8 in. V	107.4	166.8	31.8	40.5	88.5	23.5	--	--	64.9	141.7	9.2	6.11	25.5

from reference (25)

perpendicular to the bed joints (vertical span) and three were tested with the span parallel to the bed joints (horizontal span). The typical mode of failure of both the wallettes and walls (vertical span) was a bond failure at the tile-mortar interface near the mid-height of the vertical span. The results of the tests are given in Table 3.17. The ratio of the modulus of rupture of the walls (vertical span) to wallettes ranged from 0.38 to 1.4, which is a clear indication that for this series of tests no correlation exists between the two types of tests.

In conclusion, it is apparent from the limited number of tests performed that no definite trend exists between the results obtained from wallette and full size wall tests.

A comparison of the transverse strengths of standard running bond walls for vertical span and horizontal span shows that the horizontally spanned walls are more than two times stronger than the vertically spanned walls using type M mortar. The same observation was made in reference (8), which states that "the strength in horizontal span was found to be several times greater than the strength reported by other experimenters for vertical span".

4. FORMULATIONS TO PREDICT THE TRANSVERSE STRENGTH OF MASONRY WALLS

4.1 Introduction

The objective of most experimental research projects is to validate or improve a theoretical model. Because of the complexities associated with the non-homogeneity of masonry structural members, accurate theoretical models are difficult to develop and in many cases empirical or simplified relationships have been developed in their place. With respect to the transverse strength of masonry walls, several different theoretical approaches have been used. The most extensive work has been performed by Yokel et al.[6,30,31] who evaluated the theoretical capacity of unreinforced walls in a manner similar to that for concrete columns. In a correlation of the experimental results with their theory, inclusion of the slenderness effect of the walls produced reasonable agreement.

Both Scrivener[27] and Dickey[25] worked with reinforced masonry walls; they used formulations similar to those used for reinforced concrete beams and obtained reasonable correlation with experiments. Cajdert and Losberg[41] and Haseltine and Hodgkinson[42] used an analogy with the yield line theory for reinforced concrete slabs and performed tests on both reinforced and unreinforced walls with several different boundary conditions. Baker[43] used another method commonly used for reinforced concrete slabs; that of assuming the strength of a wall is given by the strength of two independent strips spanning in either direction. Baker performed experiments with one-third scale model panels simply supported on all edges.

Each of the above formulations and its correlation with experiments are described in the following sections.

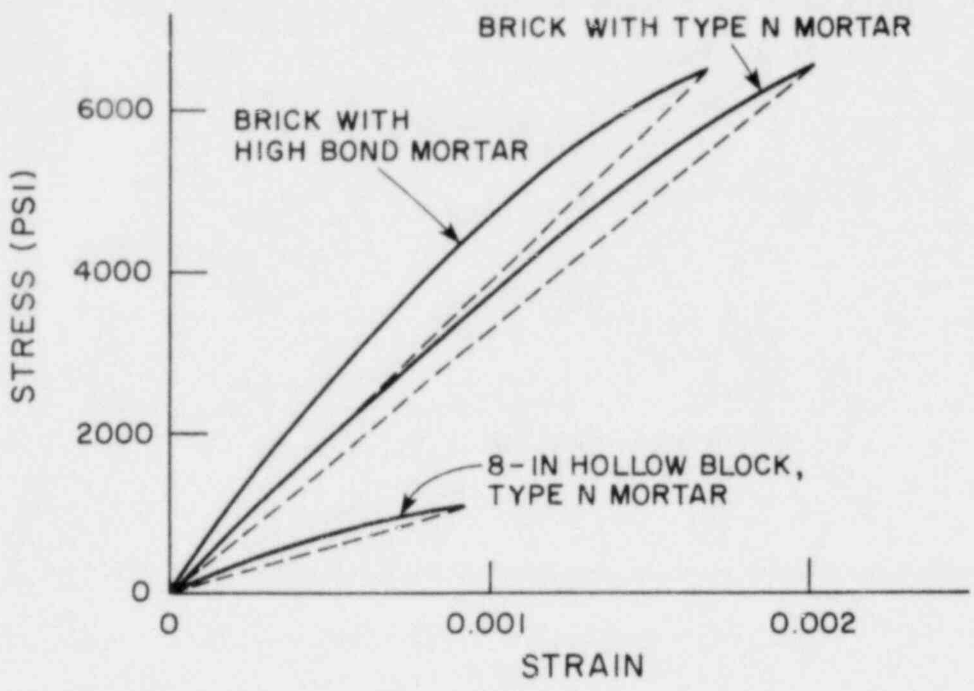

FIG. 4.1 STRESS-STRAIN PROPERTIES OF MASONRY

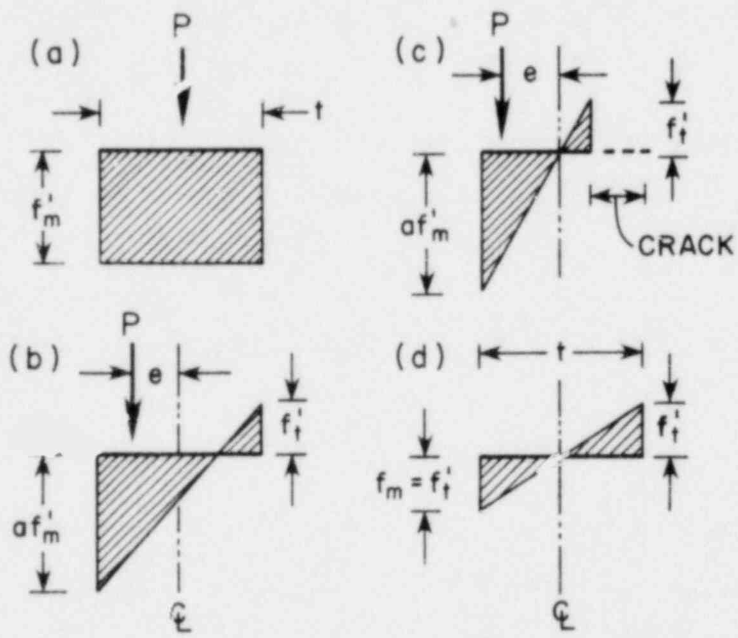

NOTE: t = wall thickness
f'_t = flexural tensile strength of masonry
f'_m = compressive strength of masonry
a = flexural compressive strength coefficient

FIG. 4.2 STRESS DISTRIBUTION AT FAILURE UNDER VARIOUS VERTICAL-LOAD AND MOMENT COMBINATIONS

From Reference (4)

4.2 Cross-Sectional Capacity of Unreinforced Walls

The moment capacity of a cross section of a wall is not only a function of the tensile and compressive strengths of the masonry but also of the vertical load acting on the cross section. If the flexural, tensile and compressive strengths and the stress-strain properties of the masonry are known, an interaction curve between vertical load and moment can be drawn.

Yokel et al. show typical stress-strain curves for three different types of masonry, see Fig. 4.1. In order to simplify the analysis, a linear stress-strain relationship is assumed as shown by the dashed line in Fig. 4.1. Instead of this basic assumption, Meinheit[32] suggested that a stress-strain relationship more like that of concrete would give better agreement with experimental data.

If it is assumed that a plane section of the wall remains plane in flexure, and that a linear stress-strain relationship as shown in Fig. 4.1 is a valid approximation for masonry up to the point of failure, then the stress distribution at failure over a cross section under an eccentric vertical load can be determined as shown in Fig. 4.2. Figure 4.2(a) shows the stress distribution at failure under axial loading. In Fig. 4.2(b), the load eccentricity is increased to a point where, at failure, the section develops its flexural tensile strength at one wall face and its flexural compressive strength at the other wall face. If the load eccentricity is increased further, the stress distribution at failure will be associated with a cracked section as shown in Fig. 4.2(c). Finally, Fig. 4.2(d) shows the stress distribution at failure for pure flexure, when no resultant vertical load acts on the cross section. In this last case, the capacity depends entirely on the flexure tensile strength of the masonry.

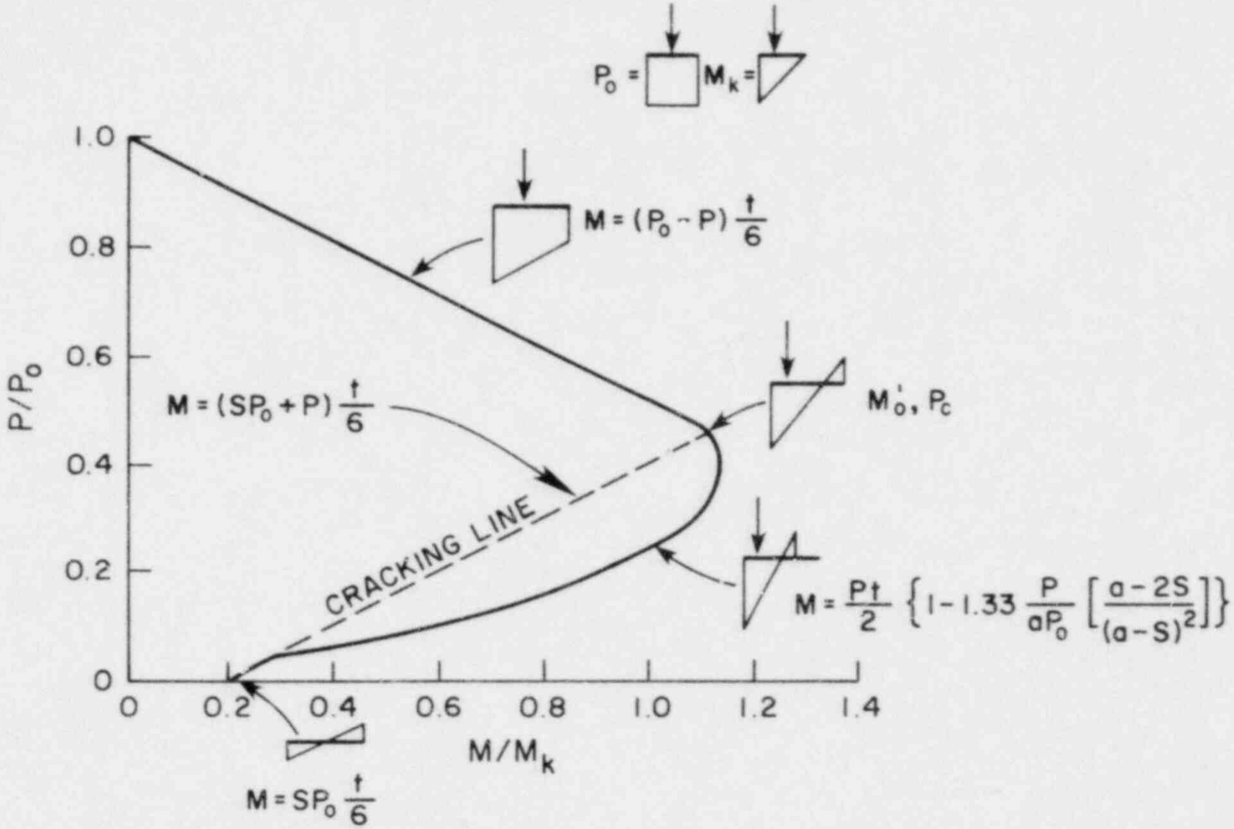

NOTE: P_o = axial load capacity $P_o = f_m' bt$

M_k = moment capacity $M_k = P_o t/_{12}$ which corresponded to the stress distribution in Fig. 4.2(b)

t = thickness of wall

b = width of wall

s = ratio of tensile strength to axial compressive strength of masonry (f_t'/f_m')

FIG. 4.3 CROSS SECTIONAL CAPACITY OF RECTANGULAR PRISMATIC SECTION WHEN $f_t' = 0.1f_m'$ AND $af_m' = f_m'$ (a=1)

From Reference (4)

Figure 4.3 shows an interaction curve for a solid rectangular section. The interaction curve is based on the assumption that flexural compressive strength equals the compressive strength under axial compression ($f'_m = a\ f'_m$, or $a = 1$). Typical stress distributions, associated with different portions of the curve, are shown in the figure and also the equations of these curves are shown. Further details of these interaction curves are discussed by Yokel and Dikkers[30].

4.3 Slenderness Effects Of Unreinforced Walls

The effects of slenderness on the moment capacity of walls are shown in Figs. 4.4 and 4.5. Figure 4.4 shows the free body of the upper half of a deflected wall under axial and transverse loads. The effective moment at any point along the height of this wall will be determined by the location of the line of action of the vertical force, relative to the location of the deflected centerline of the wall. Figure 4.5 shows a wall which is free to rotate at its upper and lower ends and is subjected to an eccentric vertical load which has a thrust line parallel to the axis of the wall. The moment acting on this wall is P e at the upper and lower ends of the wall. At midheight, the moment is equal to $P(e + \Delta)$. Thus the deflection of the slender wall causes a moment magnification equal to $P\Delta$. The moment magnification can be predicted approximately as

$$P(e + \Delta) = Pe \frac{1}{1 - \frac{P}{P_{c}}} \tag{4.1}$$

where $P_{cr} = \pi^2\ EI/h^2$ (Euler load)

E = modulus of elasticity

I = moment of inertia of cross section

h = total height of wall.

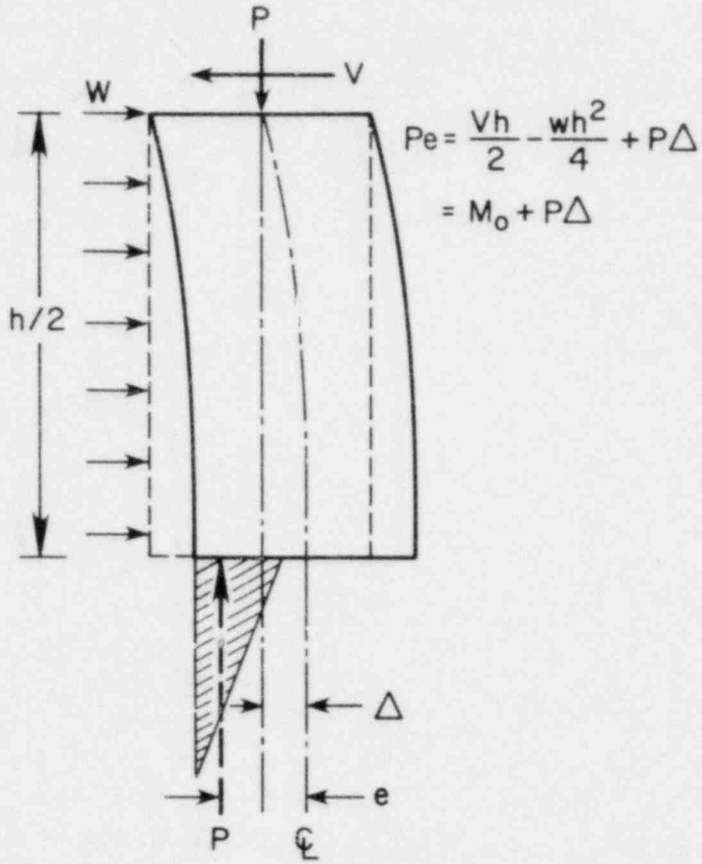

FIG. 4.4 SLENDERNESS EFFECTS ON EQUILIBRIUM
From Reference (30)

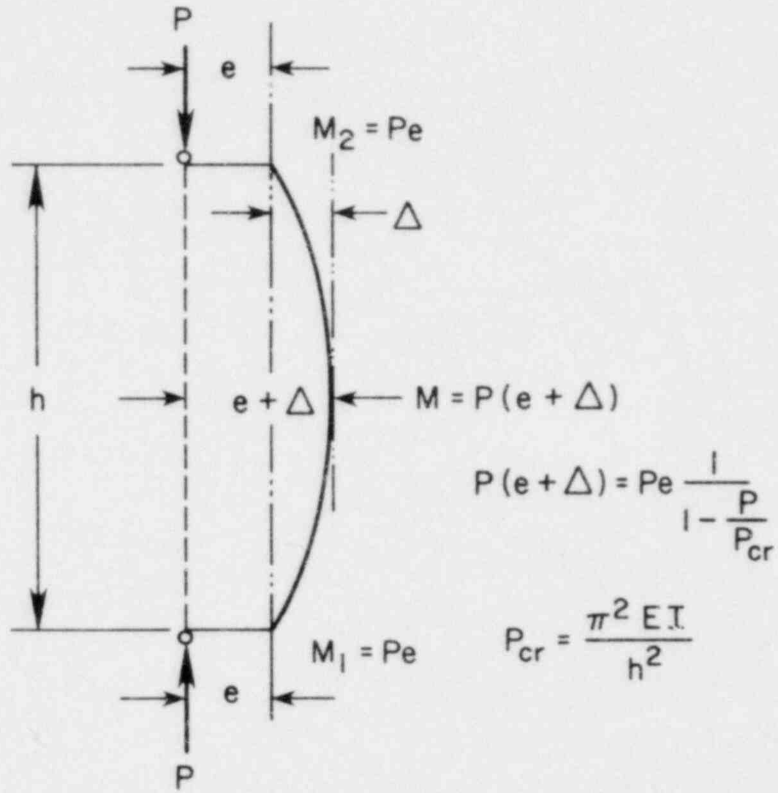

FIG. 4.5 SLENDERNESS EFFECT
From Reference (30)

The condition shown in Fig. 4.5 is not likely to occur in an actual building. A more realistic case is shown in Fig. 4.6 which shows an eccentrically loaded wall which is more or less fixed at its base and more or less free to rotate at the top. In this case the moment is not magnified as much as in Fig. 4.5, and if the wall is very stiff the moment may not be magnified at all.

An approximate prediction of moment magnification for any combination of end eccentricities and end fixities is given by[6,31,33]

$$M = M_o \frac{C_m}{1 - \frac{P}{P_{cr}}} \tag{4.2}$$

where M = maximum moment acting on the wall,

M_o = maximum moment imposed by external force.

(For an eccentric vertical load $M_o = P\,e$ and for a transverse load $M_o = \frac{wh^2}{8}$).

$C_m = 0.6 + 0.4\, M_1/M_2 \geq 0.4$,

where M_1 = the smaller end moment acting on the wall

M_2 = the greater end moment acting on the wall

$P_{cr} = \pi^2\, EI/(kh)^2$ critical load

k = length coefficient by which height is adjusted to equivalent height as shown in Fig. 4.7.

In Eq. (4.2), C_m is equal to zero for the case shown in Fig. 4.5 and for the case of transverse loading.

In order to estimate the value of the critical load P_{cr} in Eq. (4.2), the flexural wall stiffness EI is also important. Yokel et al.[31] in a study of vertically loaded unreinforced and reinforced

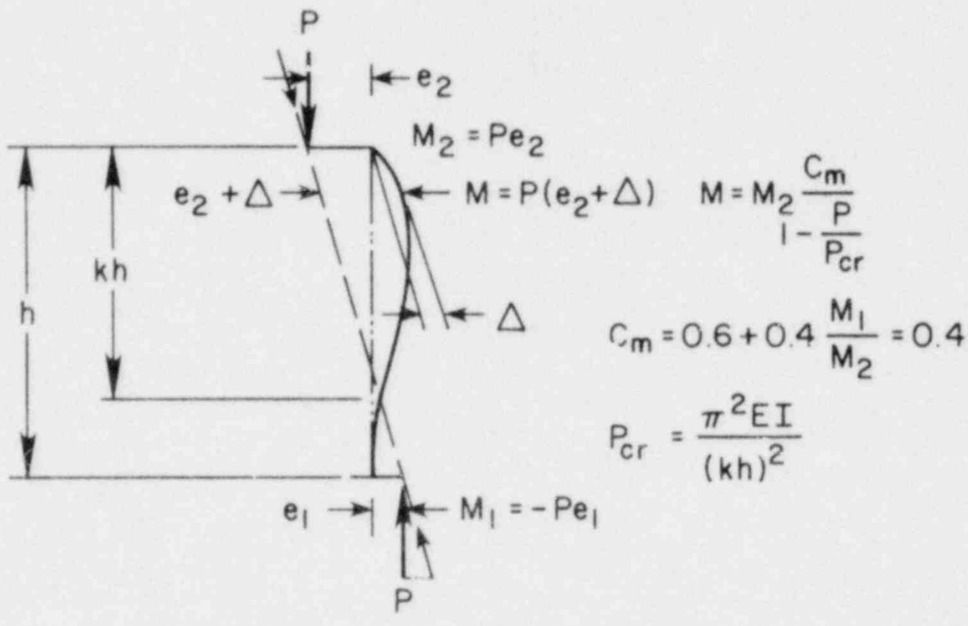

FIG. 4.6 EFFECT OF END CONDITIONS
From Reference (30)

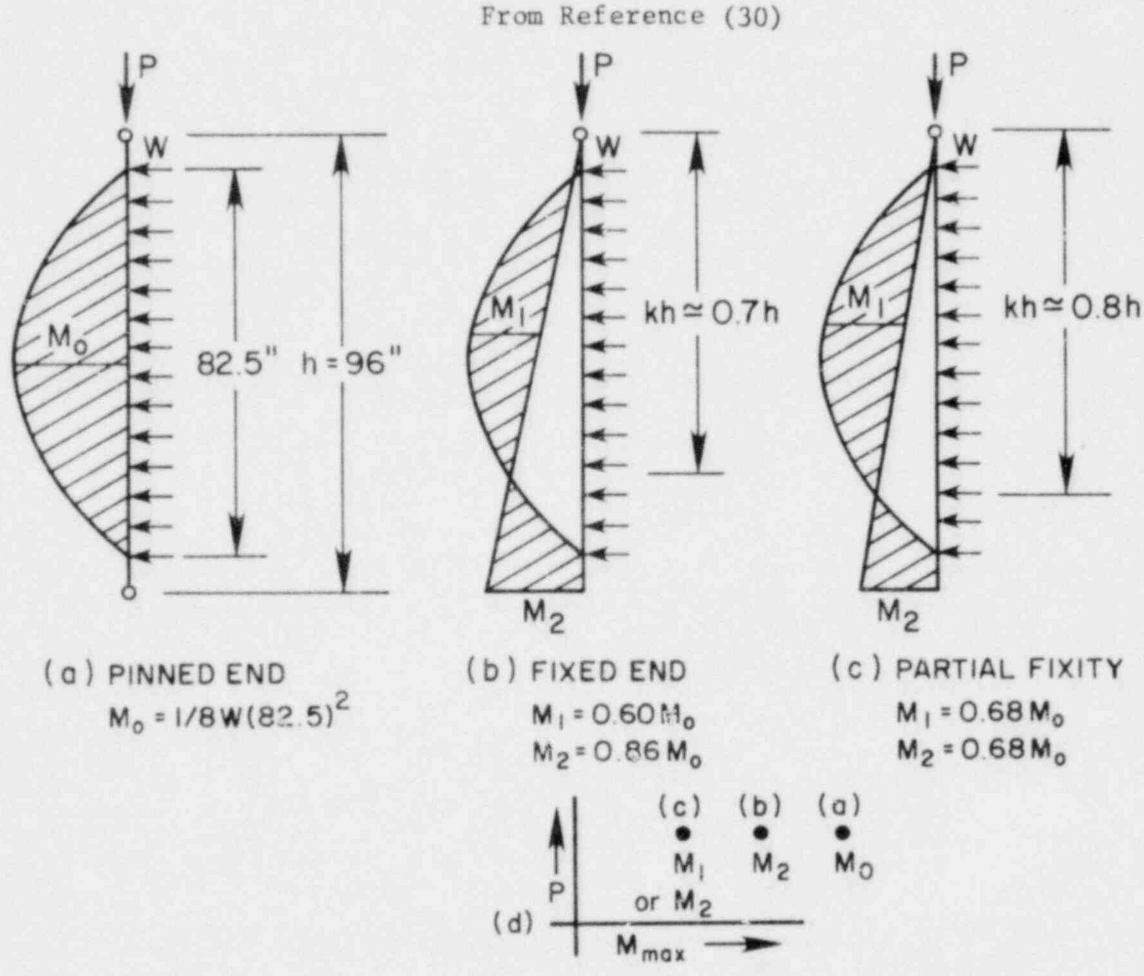

FIG. 4.7 INFLUENCE OF END CONDITIONS
From Reference (30)

concrete masonry walls suggested the following expressions to approximate to EI:

$$EI = E_i I_n/2.5 \text{ (reinforced masonry)} \tag{4.3}$$

$$EI = E_i I_n/3.5 \text{ (unreinforced masonry)} \tag{4.4}$$

where E_i = initial tangent modulus of elasticity

I_n = moment of inertia of uncracked net section.

For transverse loading combined with a vertical load for brick walls, Yokel[6] proposed that

$$EI = E_i I_n \left(0.2 + \frac{P}{P_o}\right) \leq 0.7\, E_i I_n,$$

where P_o = short wall axial load capacity determined on the basis of prism strength.

4.4 Correlation Between Theory And Experiments For Unreinforced Walls

Figure 4.8 shows an example of correlation of theory developed from Sections 4.2 and 4.3 with the combined vertical and transverse load tests on 4 inch brick walls with type N mortar conducted by Yokel et al.[6]. The test results are shown by solid circles and heavy horizontal lines. The left ends of these heavy lines represent the maximum moment caused by transverse load. The length of the horizontal line itself represents the added moment, equal to the product of the vertical load and the wall deflection at the point of maximum moment (mid-height). The magnitude of this added moment was computed using the horizontal deflections, measured at the time of wall failure.

The solid curve in Fig. 4.8 is the calculated cross-sectional capacity which is shown in Fig. 4.3 and should be compared with the

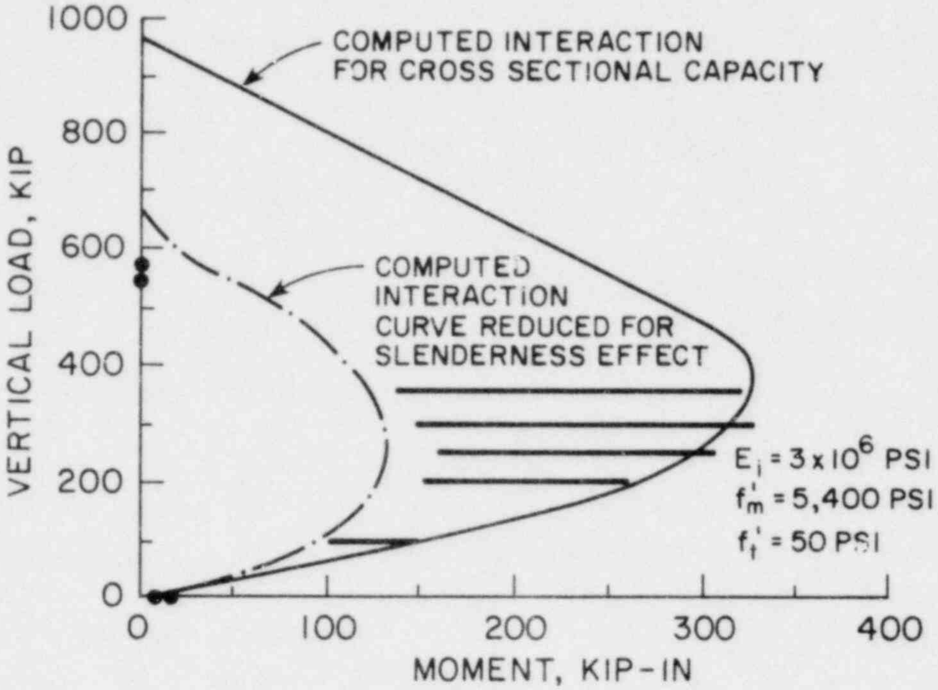

FIG. 4.8 4-IN BRICK WALLS WITH TYPE N MORTAR UNDER VERTICAL AND TRANSVERSE LOAD

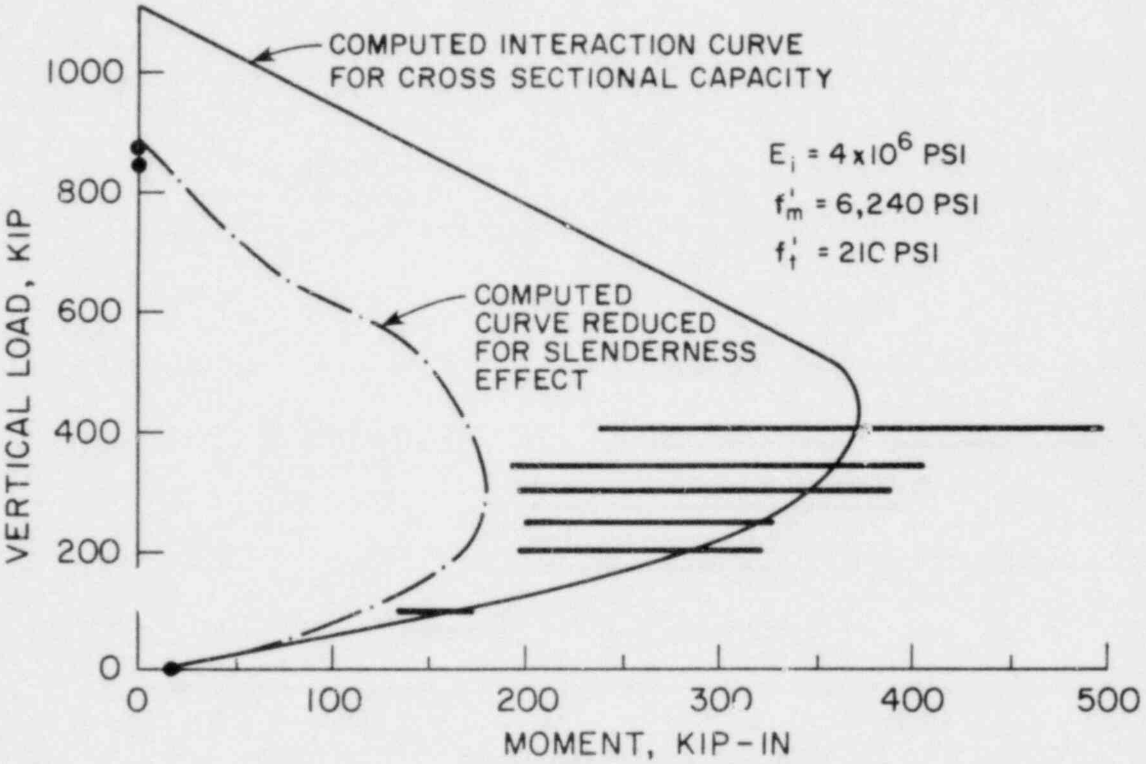

FIG. 4.9 4-IN BRICK WALLS WITH HIGH BOND MORTAR UNDER VERTICAL AND TRANSVERSE LOAD

From Reference (26)

right end of the horizontal line. The broken curve represents the wall capacity, computed by reducing the cross sectional capacity for slenderness effect in accordance with the theory discussed in Section 4.2. This reduced curve corresponds to the left ends of the horizontal solid lines. The intersection of the broken curve with the vertical load axis corresponds to the two solid circles on the load axis, which show the test results under vertical load without transverse load. Note that the theoretical curves closely predict the actual magnitude, as well as the trend of the test results. Slenderness effects are considerable in this case and their magnitude is well predicted by theory.

Similar comparisons are shown in Fig. 4.9 for 4 inch brick walls with high-bond mortar, and in Figs. 4.10 and 4.11 for 8 inch hollow block walls with type N mortar and high-bond mortar, respectively. The 4 inch brick walls with high-bond mortar show fair agreement between theoretical curves and test results, whereas the 8 inch hollow concrete walls show that the theoretical short-wall interaction curves (solid curves in Figs. 4.10 and 4.11) underestimate the wall strength for all panels. The reduced interaction curves (broken curves) predict moment capacities equal to or smaller than the observed reduced capacity

Figure 4.12 also compares the observed transverse strength of the walls with the theoretical interaction curves for 8 inch solid concrete block walls with type N mortar. All panels except one exceed the reduced moment capacity (dashed line) predicted on the basis of the axial prism test.

In the case of cavity walls or composite walls, theoretical interaction curves are somewhat different from those of single wythe

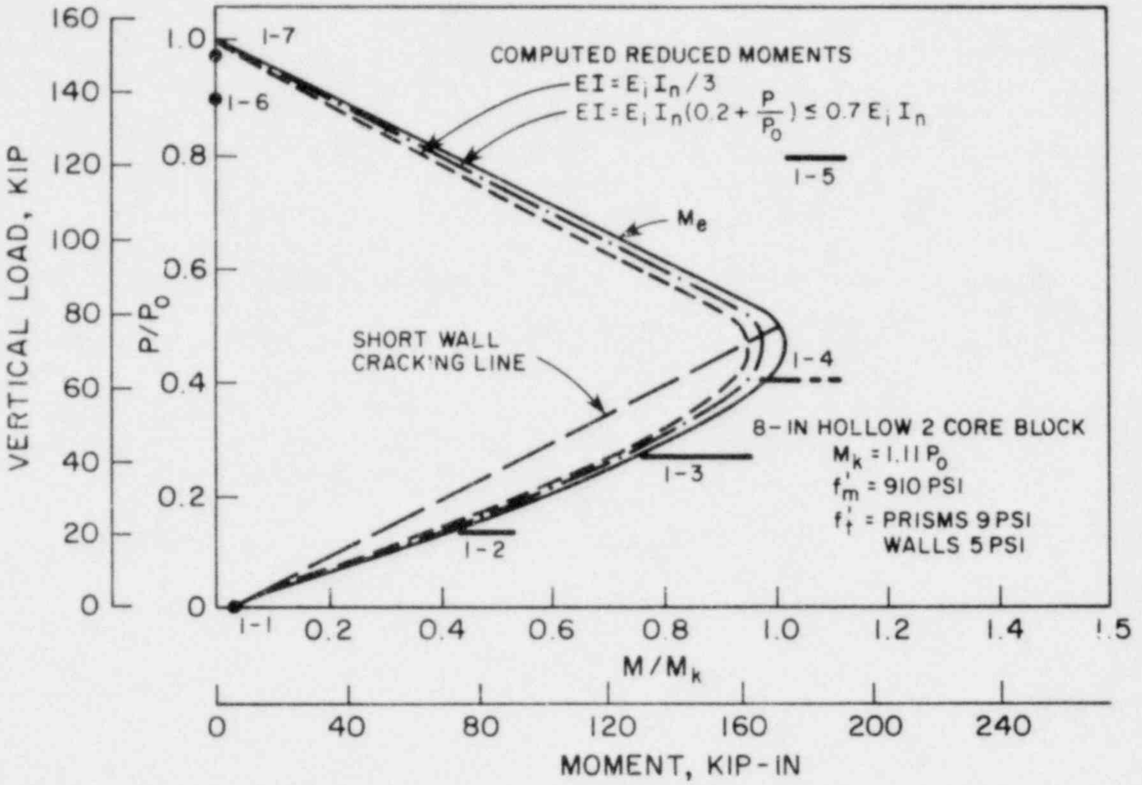

FIG. 4.10 8-IN HOLLOW BLOCK WALLS WITH TYPE N MORTAR, CORRELATION WITH PRISM STRENGTH

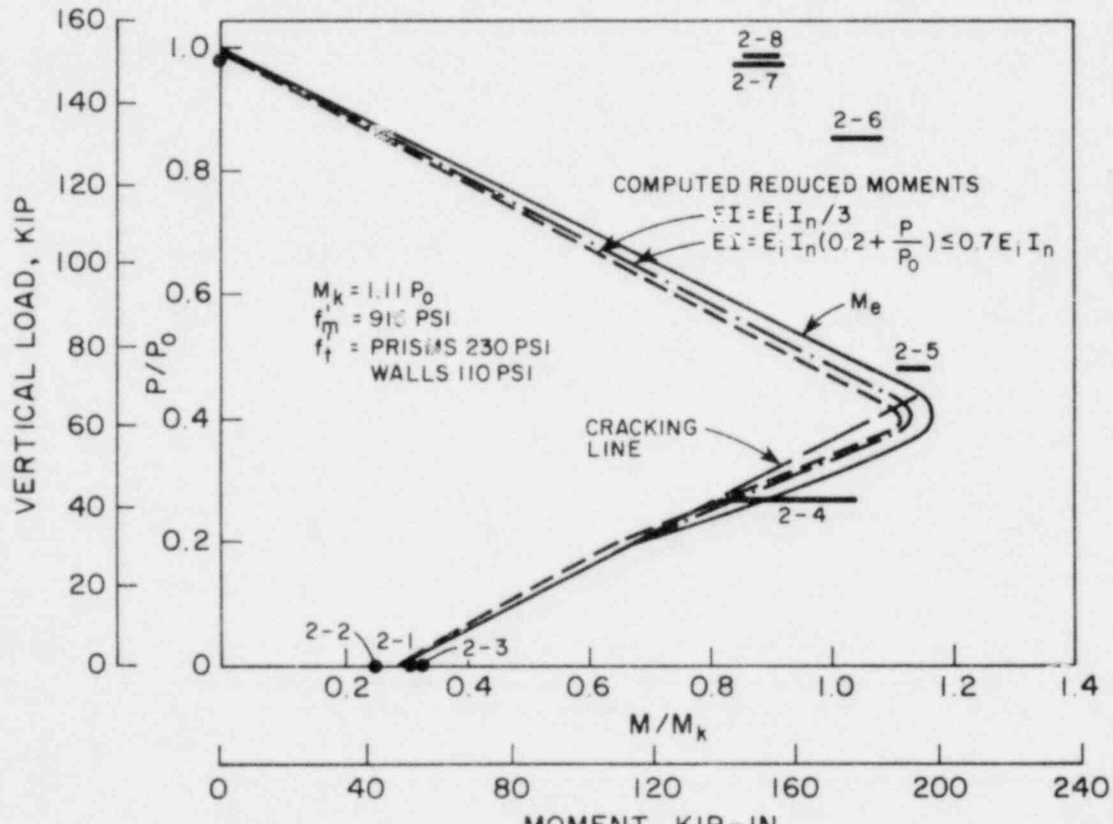

FIG. 4.11 8-IN HOLLOW CONCRETE BLOCK WALLS WITH HIGH BOND MORTAR, CORRELATION WITH PRISM STRENGTH

From Reference (4)

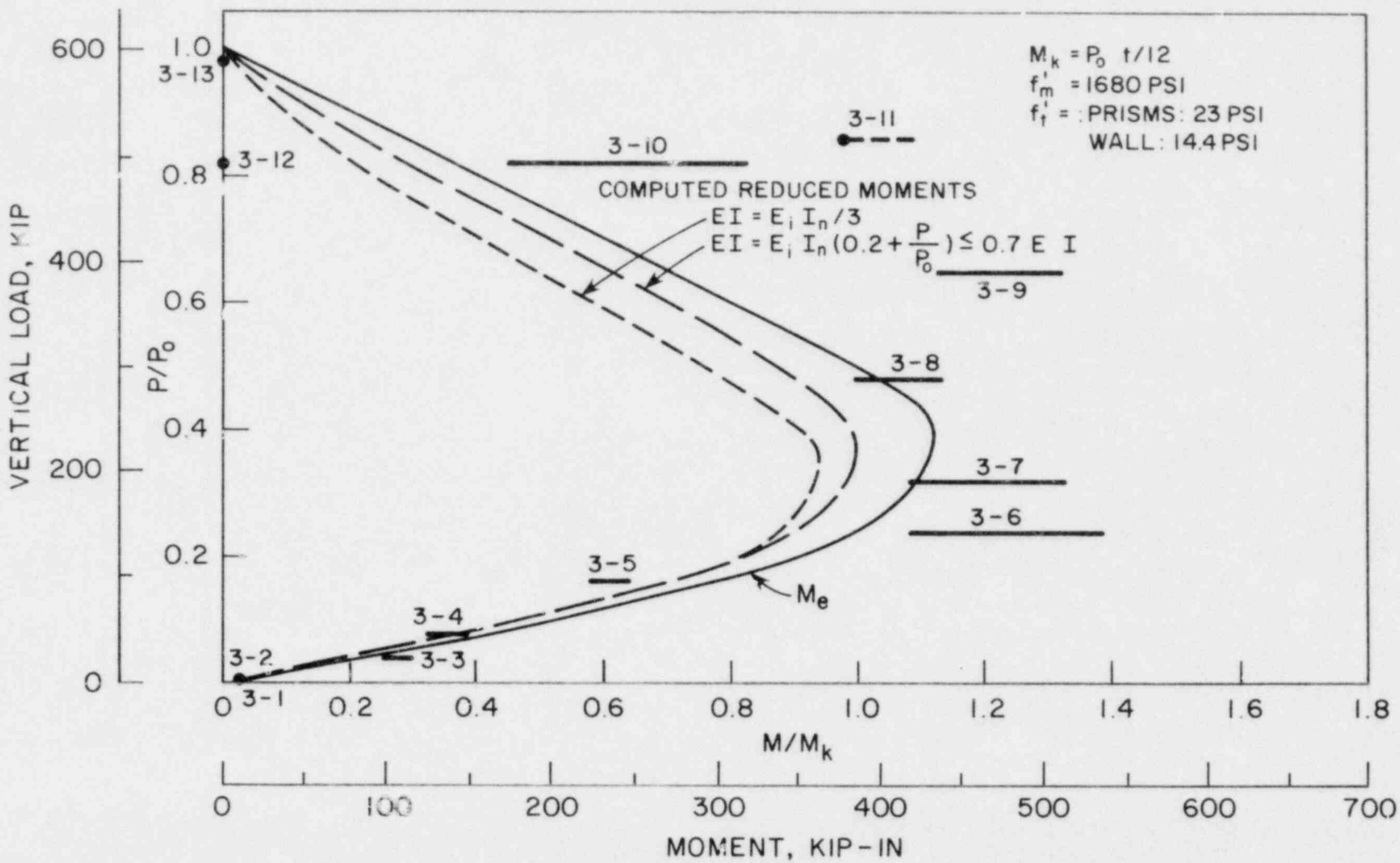

FIG. 4.12 8-IN SOLID CONCRETE BLOCK WALLS WITH TYPE N MORTAR, CORRELATION WITH PRISM STRENGTH From Reference (4)

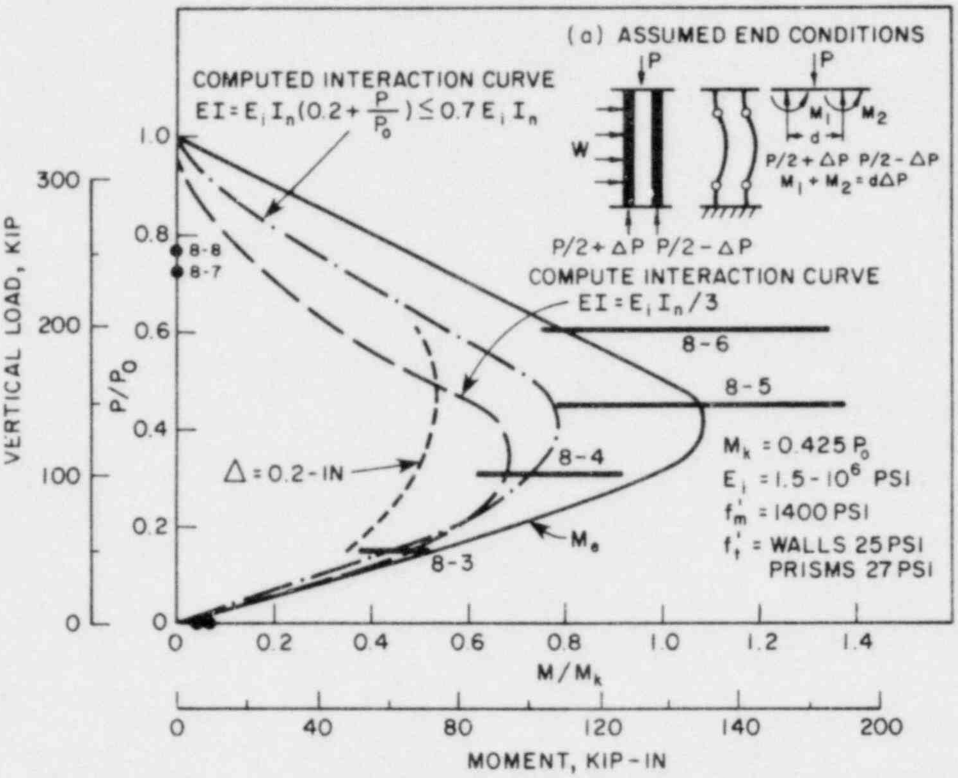

FIG. 4.13 4-2-4 IN CONCRETE BLOCK CAVITY WALLS, CORRELATION WITH PRISM STRENGTH

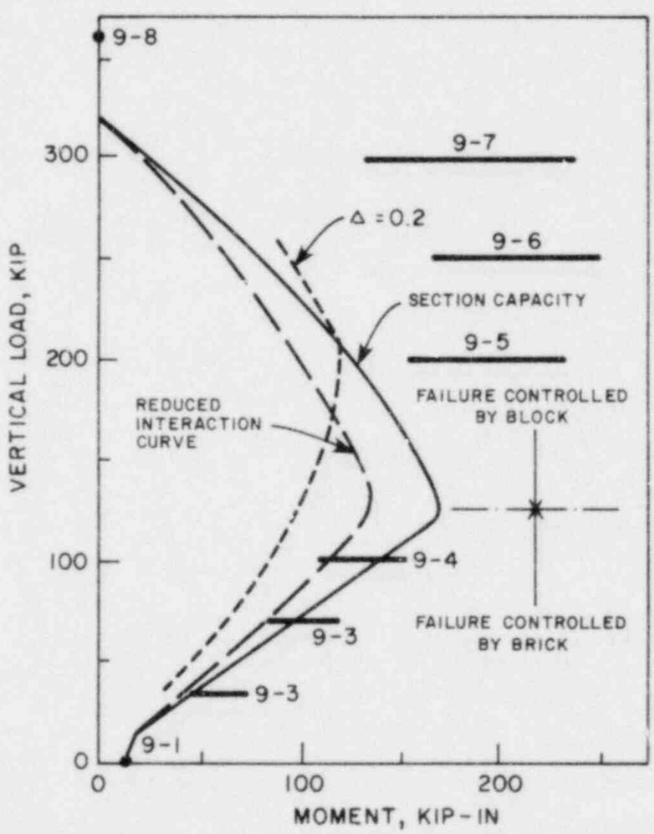

FIG. 4.14 4-2-4 IN BRICK AND CONCRETE BLOCK CAVITY WALLS, CORRELATION WITH PRISM STRENGTH

From Reference (4)

walls, but similar comparisons can be developed. The results of tests[6] of 4-2-4 in. concrete block cavity walls are plotted in Fig. 4.13 together with interaction curves computed on the basis of prism tests. The assumption was made that each wythe takes one half the vertical load and one half the moment. P_o was computed on the basis of the average strength obtained from prism tests on the 4 inch hollow block. Moments were computed conservatively, assuming that partial top-end fixity existed and this produced about one half the pin-ended moment, see Fig. 4.13(a). The analytical curve for section capacity reflects the tests reasonably well. It can be seen from the magnitude of the observed added moments which are due to deflection at failure (length of the horizontal solid line), that slenderness effects are an important factor in this wall system.

The prediction of wall capacity for brick-block cavity walls is more difficult and complicated because of the two different material properties and associated load transfer mechanism. Details of these prediction formulae are given by Yokel et al.[6], whose final results are shown in Fig. 4.14. Figure 4.14 shows that up to P = 100 kip, the moment capacity is controlled by the brick. In this range the computed reduced moment capacity (dashed line) agrees well with the test. The total moment capacity, which is shown by the solid line is somewhat less than observed capacity (right ends of the solid horizontal lines) and consequently the magnitude of the measured slenderness effect is larger than that of the computed effect. Above an axial load of 100 kips the computed strength underestimates observed wall strength considerably. In this range it is thought that strength is controlled by the concrete block which forms the back face with respect to the transverse load.

Yokel et al. summarized their extensive investigations with the following conclusions:

(1) Transverse strength of masonry walls is reasonably predicted by evaluating the cross-sectional capacity and reducing that capacity to account for the added moment caused by wall deflection. The general trend of the test results is in good agreement with theory, and the magnitude of individual test results is conservatively predicted.

(2) Cross-sectional moment capacity of wall panels was conservatively predicted by a theoretical interaction curve which was based on compressive prism strength and linear strain gradients.

(3) Slenderness effects, computed by the moment magnifier method as modified to account for section cracking, predicted closely the slenderness effects observed in the 4 inch thick brick walls, and reasonably predicted these effects for concrete masonry walls, concrete block cavity walls, and brick and block cavity walls.

(4) The qualitative observation was made that with large eccentricities the flexural compressive strength of masonry exceeds the compressive strength developed in pure one-dimensional compression by a significant margin, and that flexural compressive strength increases with increasing strain gradients.

(5) The transverse strength of cavity walls was conservatively predicted by assuming that each wythe carries its proportional share of vertical loads and moments, and that transverse loads, but not shear forces parallel to the plane of the wall, are transmitted by the ties.

(6) The transverse strength of composite brick and block walls was approximately predicted by assuming that the walls act monolithically.

(7) Whenever walls did not fail by stability-induced compression failure, their axial compressive strengths were reasonably predicted by

prism tests. In the case of concrete masonry with high-bond mortar, compressive tests with prisms capped with high strength plaster overestimated wall strength, while prisms set on fiberboard showed good correlation with wall strength.

(8) Flexural tensile strength of all the wall panels tested equaled or exceeded 1/2 of the flexural strength as determined by prism tests.

4.5 Flexural Capacity Of Reinforced Masonry Walls

Scrivener[27] suggested that a reinforced brick wall could be considered as a lightly reinforced wide beam, with the brick weak in tension similar to concrete. The yield load (ultimate load) can be predicted to within a few percent by considering the section in this way and applying ultimate moment theory (as for reinforced concrete). The stress strain curve for brick is assumed to be the same as that for concrete so that the concrete constant 0.59 in the Whitney equation can be used. The ultimate moment M_u is

$$M_u = A_s f_y (d - 0.59 A_s f_y/f'_c b) \tag{4.5}$$

where A_s = cross-sectional area of steel

f_y = yield stress of steel

d = depth to center of gravity of steel

b = beam width

f'_c = brick crushing strength.

A comparison between the theoretical ultimate loads calculated by Eq. 4.5 and the transverse load tests performed by Scrivener are discussed in Section 3.4 and are shown in Table 3.12.

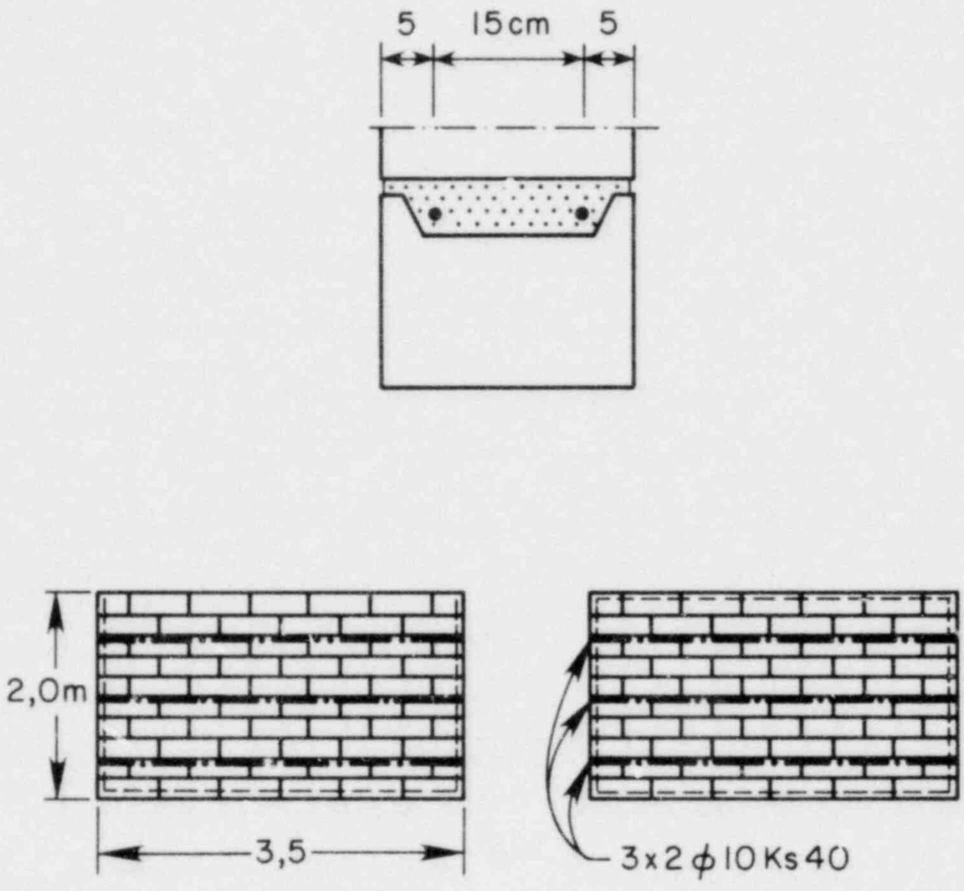

365:7, 865:10   865:8, 865:11

FIG. 4.15 WALL TEST SPECIMENS

From Reference (39)

The maximum difference between the predicted and experimental results for the four tests performed is 11%. Although only a few tests were performed the agreement between the predicted and experimental results is good. As the walls did not have a vertical load, the formulation used by Scrivener is only applicable for low rise walls. Development of a formulation for reinforced walls with a vertical load is obviously required and this should be validated with tests.

4.6 Reinforced Concrete Slab Theories Applied To Masonry Walls

Cajdert and Losberg[41] conducted transverse load tests of 3.5m (11.5 ft) wide, 2.0m (6.5 ft) high and 0.25m (9.8 in.) thick clay block walls. Two of the walls were supported along three edges (upper edge free), the other two walls were supported along four edges. For each support condition, an unreinforced wall and a wall reinforced with 2-ϕ10 mm deformed bars in every third horizontal joint (0.1% of total area) were tested as shown in Fig. 4.15. The transverse load was applied uniformly by a plastic air-bag system. The crack loads and ultimate loads of the four walls are shown in Table 4.1.

The theoretical crack loads in Table 4.1 were calculated according to the theory of elasticity for isotropic plates with Poisson's ratio assumed to be 0.20. This value is based on individual tests of unreinforced masonry beams. The measured wall crack loads are in good agreement with theoretical values, except for the reinforced wall laterally supported along three edges (No. 865:10 in the Table), where the horizontal reinforcement obviously delayed e crack formation at the free edge. The horizontal strain for an unreinforced masonry wall is mainly concentrated at the head joints while, in the reinforced wall, the strain shows a smoother distribution along the wall because

Table 4.1

Comparison of Test Results vs. Yield Line Theory

Wall No.	Supporting edges	Reinforcement	Age at testing, days	Crack load, kp/m^2			Ultimate load, kp/m^2		
				meas. q_m	calc. q_c	q_m/q_c	meas. q_m	calc. q_c	q_m/q_c
865:7	3	unreinforced	28	4[illegible]	480	0,94	550	660	0,84
865:8	4	unreinforced	28	1200	1140	1,05	1300	1580	0,82
865:10	3	3x2 Ø 10 Ks40	24	800	480	1,67	1550	1190	1,30
865:11	4	3x2 Ø 10 Ks40	24	1150	1140	1,01	2150	2290	0,94

from reference (41)

of the reinforcement, (see Fig. 4.16). The theoretical ultimate loads in Table 4.1 were derived by using an analogy with the yield line theory for reinforced concrete slabs. This simple analogy gives about ± 20% deviation between measured and calculated ultimate loads. The assumed yield line pattern is shown in Fig. 4.17.

Haseltine and Hodgkinson[42] also carried out transverse load tests of masonry walls which were supported along two, three and four edges. They concluded that the yield line theory could be a satisfactory means of designing panel walls in brick work, although this is surprising in view of the brittle nature of the material. They stated that the calculations for random yield line cases would probably be very tedious, and suggested that using elastic plate theory as developed by Timoshenko provides a safe estimation of the strength of a wall which would be considerably easier for the designer.

Baker[43] carried out some experimental work with one-third scale models of brick panels with simple supports on all sides and no in-plane restraint. The models were subjected to a uniform lateral face load and Baker proposed a simple empirical method to predict the load capacity of masonry walls under transverse loadings. In this method the total load capacity of a panel is assumed to be the sum of the load capacity of two independent strips spanning vertically and horizontally. That is,

$$\omega = \frac{8\,M_V}{h^2} + \frac{8\,M_H}{\ell^2} \qquad (4.6)$$

where ω = load capacity of the wall

M_V = ultimate moment of resistance per unit width of brick work spanning vertically

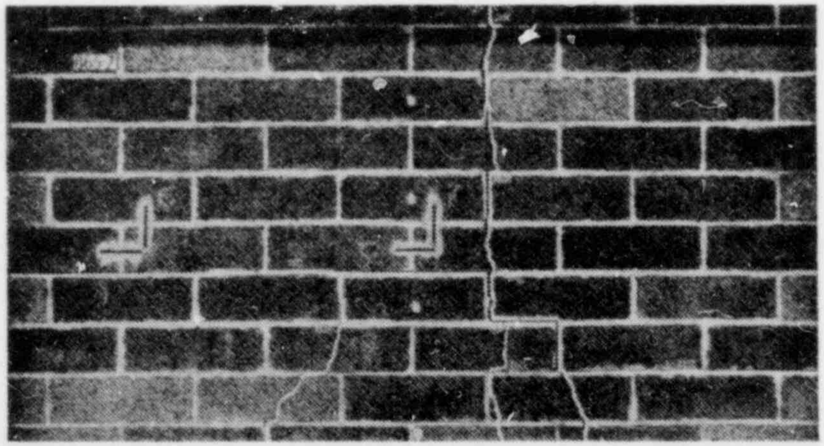

WALL SUPPORTED AT 3 EDGES, UNREINFORCED

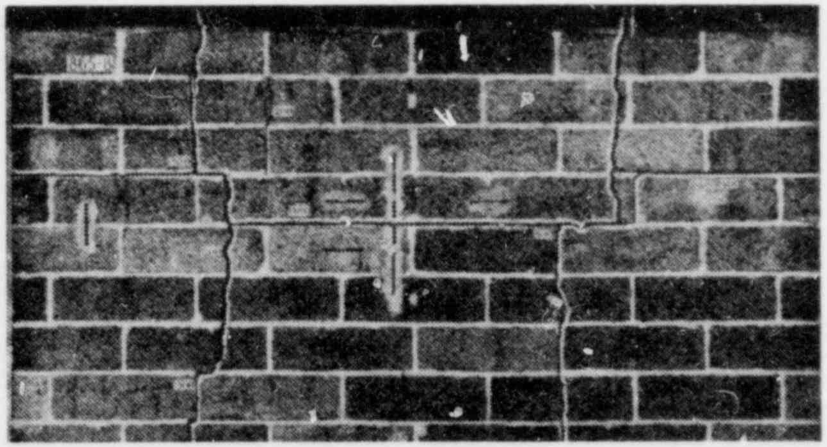

WALL SUPPORTED AT 4 EDGES, UNREINFORCED

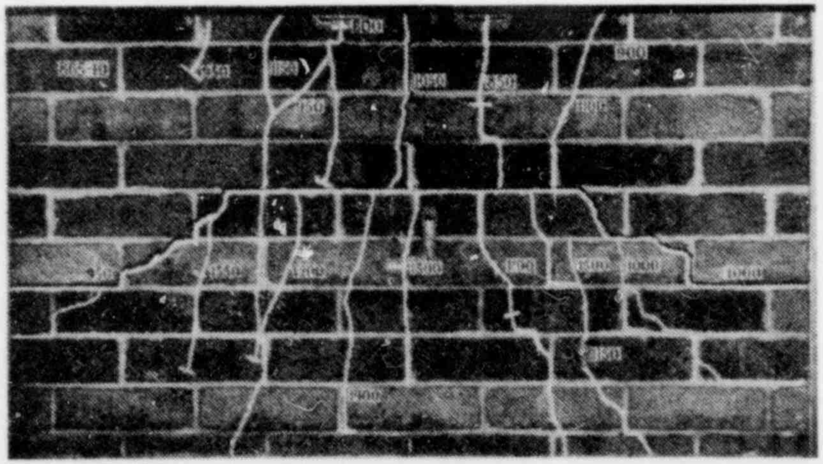

WALL SUPPORTED AT 3 EDGES, REINFORCED

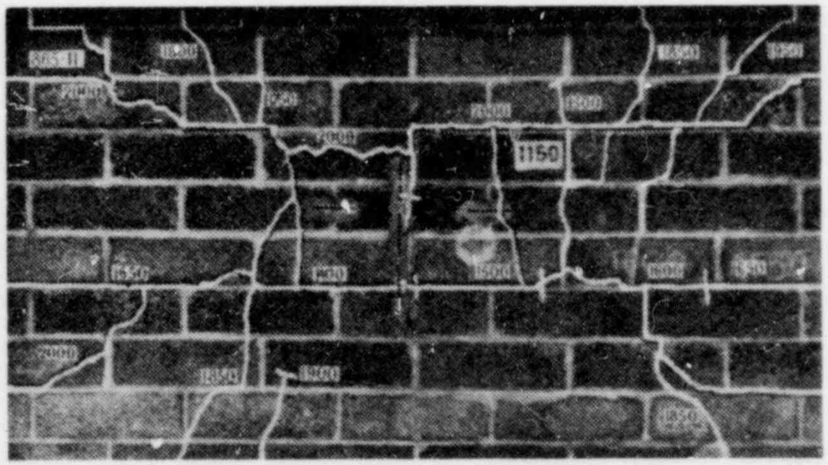

WALL SUPPORTED AT 4 EDGES, REINFORCED

FIG. 4.16 WALL TEST SPECIMENS
From Reference (41)

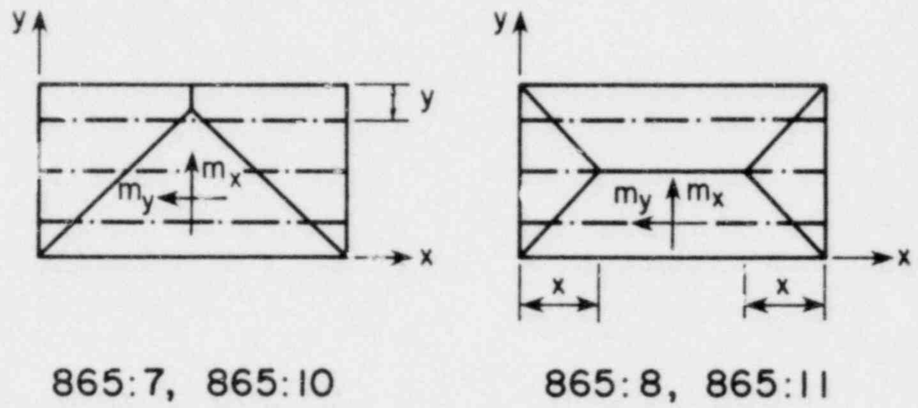

FIG. 4.17 ASSUMED YIELD LINE
From Reference (39)

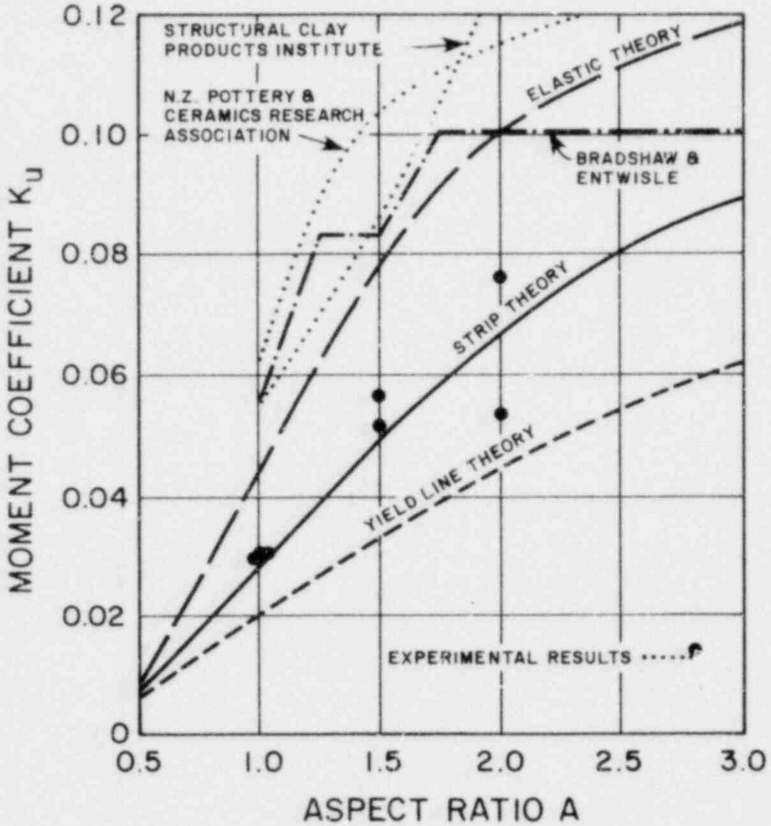

FIG. 4.18 ULTIMATE LOAD EVALUATION

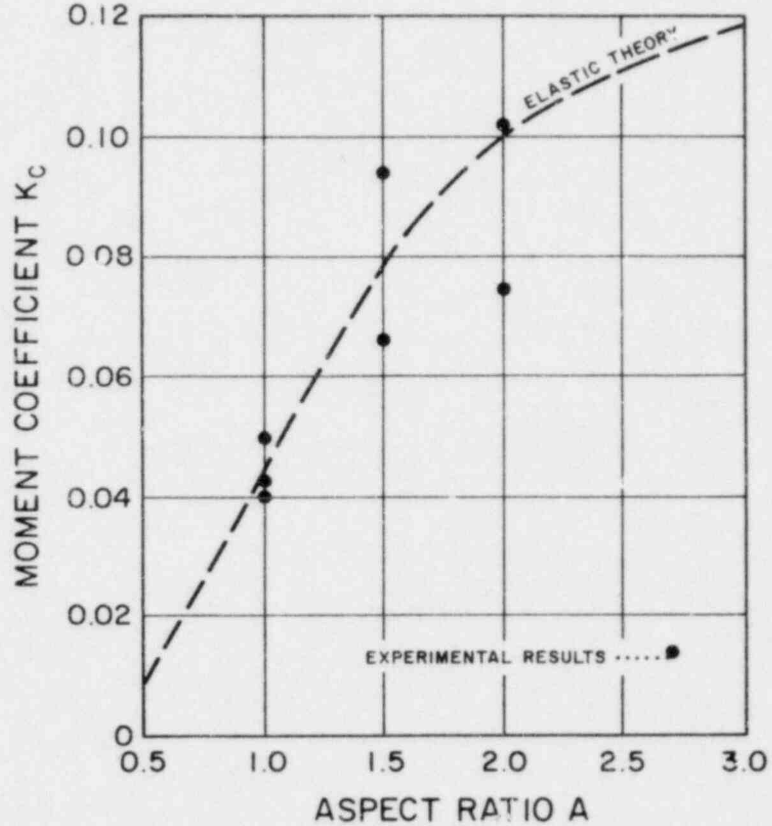

FIG. 4.19 CRACKING LOAD EVALUATION
From Reference (41)

M_H = ultimate moment of resistance per unit width of brick work spanning horizontally

h = vertical span of panel

ℓ = horizontal span of panel.

This theory is compared with experimental results in Fig. 4.18, and with results by the elastic theory and the yield line theory. In the figure the ordinate is the non-dimensional moment coefficient k_u, where k_u = (section modulus) x (modulus of rupture, spanning vertically)/$\omega_u \ell^2$ or $k_u = M_V/\omega\ell^2$. The aspect ratio of the wall is ℓ/h. Elastic theory underestimates the ultimate load but gives a reasonable prediction of cracking load, shown in Fig. 4.19. The ultimate load is overestimated by the yield line theory for a strength ratio (M_H/M_V) equal to 2, the value specified by most codes. Ultimate load was closely predicted by the strip theory of Eq. (4.6). Baker concluded that this theory may allow for the reserve strength after initial cracking in an empirical way with sufficient accuracy for practical design.

5. DISCUSSION OF TEST RESULTS IN RELATION TO CURRENT DESIGN PRACTICE

5.1 Introduction

The ultimate objective of most experimental masonry research projects has been to ensure that design codes provide sufficient safety in the design of masonry buildings. Code provisions are formulated or changed by the collective judgment of groups of competent engineers based on relevant available information. Inherent in this procedure is a significant time lag between the availability of relevant research results and their inclusion in an appropriate form in code provisions. Consequently the purpose of this chapter is to examine code requirements and design practices to see how they relate to research information currently available. Part of the material (Sections 5.2, 5.3 and 5.6) for this chapter is taken directly from the summaries and conclusions of an extensive investigation performed by Yokel et al.(6)

5.2 Determination Of The Transverse Strength Of Unreinforced Masonry Walls

The material in this section is a direct reproduction of material presented in reference 6.

Two wall properties must be evaluated in order to determine the transverse strength of masonry walls:

1. The capacity of the wall cross section to resist combined bending and axial loads.

2. The effect of wall slenderness on load capacity.

It has been shown by Yokel(6) that the moment capacity of a wall cross section is not only a function of the tensile and compressive strength of the masonry but also of the vertical load acting on the cross section. Thus an interaction curve can be developed which shows the maximum moment capacity as a function of vertical load. Such an interaction curve can be developed if flexural tensile and compressive strengths and the stress-strain properties of the masonry are known. The cross-sectional capacity can be conservatively determined by assuming a flexural compressive strength equal to the compressive strength of prisms under axial loading, a linear stress-strain relationship for masonry, and a flexural tensile strength equal to 50 percent of the modulus of rupture as determined by prism tests. This procedure is conservative since it appears that most specimens developed flexural compressive strengths in excess of the strength of axially loaded prisms, and that the assumption of a linear stress-strain relationship will underestimate the moment that the cross section is actually capable of developing.

In Yokel's study, the capacity of wall cross sections was evaluated directly, by testing eccentrically loaded prism specimens and indirectly, by adding the moment exerted by the axial load on the deflected wall to the moment exerted by transverse loads.

Slenderness effects were caused by the additional moments which the vertical loads impose on the deflected wall. Not only will the vertical load impose added moments on the walls, which will equal the product of the vertical load and transverse deflections relative to the line of action of the vertical load, but the vertical load will also act to increase the magnitude of transverse deflections. These slenderness effects, which will magnify the moments acting on the walls, can be approximately predicted by the moment magnifier method, provided that EI, the stiffness of the wall, is correctly estimated.

Slenderness effects have been successfully and conservatively predicted for slender brick walls by using the moment magnifier method with an equivalent stiffness which may be predicted either by Eq. 5.1 or Eq. 5.2. Equation 5.1 is somewhat simpler while Eq. 5.2 shows better agreement with test results for the entire range of vertical loads that the wall can support. No extensive data are available on slender concrete block walls. Transverse strength can be reasonably well predicted however, by using Eq. 5.1 or Eq. 5.2 to predict slenderness effects for solid block walls, and by making the conservative assumption for hollow block that the cracking line represents ultimate strength.

$$M_0' = M_e \left(1 - \frac{P}{P_{cr}}\right)$$

where
$$P_{cr} = \frac{\pi^2 EI}{(0.8h)^2}$$

and
$$EI = \frac{E_i I_i}{3} \tag{5.1}$$

or
$$EI = E_i I_i \left(0.2 + \frac{P}{P_o}\right) \leq 0.7 E_i I_i \tag{5.2}$$

The moment magnifier equation [Eq. 4.2] uses a coefficient C_m, which accounts for the shape of the deflection curve and a coefficient k, which accounts for end fixity. In the special case where moments are caused by transverse loads, the coefficient C_m is taken as 1. However, in the case where transverse moments are caused by eccentric vertical loads, a case which was not covered by Yokel's investigation, the moment magnifier equation is also applicable,with a factor C_m which will depend on the relationship between vertical load eccentricities at the wall supports. Thus the moment magnifier method could be applied to determine transverse strength under all practical loading conditions.

The practical procedure in an actual design problem would be to determine cross-sectional capacity on the basis of flexural compressive and tensile strengths, cross-sectional geometry, and the vertical load at which transverse strength is to be determined, and then to reduce this capacity to account for slenderness, on the basis of wall length, end-support conditions, and wall stiffness "EI" at the design vertical load.

Yokel suggested that the following equations may be used to predict ultimate and cracking strength. The ultimate transverse moment imposed on the wall in the direction of transverse loads, M_0', can be taken as

$$M_0' = M_e \left(1 - \frac{P}{P_{cr}}\right)$$

The maximum end moment opposite to the direction of transverse loads, M_{end}, will be

$$M_{end} = M_e'$$

where M_e = maximum moment capacity of the wall in the direction of transverse loads,

M_e' = maximum moment capacity of the wall opposite to the direction of transverse load,

P = applied axial load,

P_{cr} = critical load for stability-induced compressive failure, computed on the basis of a modified EI, accounting for section cracking and reduced stiffness at maximum stress, where

$$EI = E_i I_n \left(0.2 + \frac{P}{P_o}\right) \leq 0.7 E_i I_n \quad \text{or} \quad EI = \frac{E_i I_n}{3}$$

E_i = initial tangent modulus of elasticity of masonry,

I_n = moment of inertia based on uncracked net section,

P_o = short-wall axial load capacity.

The transverse cracking strength of a wall, M_c, can be determined by the following equation:

$$M_c = (M_t + Pe_k)\left(1 - \frac{P}{0.7 P_{cro}}\right)$$

where

M_c = moment at which cracking occurs,

M_t = maximum moment considering tensile strength with zero vertical load,

e_k = distance from centroid to edge of kern,

P_{cro} = critical load for stability-induced compression failure computed on the basis of E_i and I_n; $0.7 P_{cro}$ is recommended as critical load for uncracked walls.

In view of the loss of moment of inertia after cracking of hollow block walls, it is recommended that the ultimate strength of slender hollow concrete block walls equals the cracking strength.

5.3 Discussion Of Present Design Practice For Unreinforced Walls

The material in this section is a direct reproduction of material presented in reference 6.

Present masonry design is based entirely on working stresses. Even though design provisions were developed with specific margins of safety relative to ultimate strength in mind, comparison of hypothetical ultimate strength computed on the basis of design practice standards with ultimate strength actually achieved is not necessarily the only criterion by which the design provisions should be judged.

Three different design standards will be considered:

(1) The ANSI Standard Building Code Requirements for Masonry(26)

(2) Building Code Requirements for Engineered Brick Masonry developed by SCPI(34)

(3) Design Specifications for Load-Bearing Concrete Masonry developed by NCMA(35) and proposed recommendations developed by ACI Committee 531(36)

5.3.1 ANSI Standard Building Code Requirements

The ANSI building code requirements (A41.1-1953) limit allowable slenderness as follows:

Type of masonry	h/t Ratio (based on nominal dimensions)
Hollow unit walls	18
Solid unit walls	20
Cavity walls	18*

These limits may be compared with a nominal h/t of 24 for the brick walls, and a nominal h/t of 12 for the block walls as well as the cavity walls tested in Yokel's(6) program. Consequently, these design requirements permit the construction of walls that will be subject to considerable slenderness effects, particularly in the case of cavity walls. On the other hand, this standard does not contain any provisions for stress reduction to account for these slenderness effects. To assure

*t in cavity walls is the sum of both wythe thicknesses.

a safe design, permitted allowable stresses are extremely low, compensating for potential slenderness effects. Such a procedure, which does not account for such an important variable, requires a very high margin of safety which penalizes short walls and therefore leads to uneconomical design.

For composite walls, this standard limits the allowable stress to that permitted for the weakest of the combinations of units and mortars of which the member is composed. There are no provisions for considering the location of the vertical load with respect to the weakest wall materials.

5.3.2 SCPI Standard For Engineered Brick Masonry

In the present SCPI Standard (1969), the following equation is used for the computation of allowable vertical loads on nonreinforced brick walls:

$$P = C_e C_s \; (0.20 \; f_m') \; A_g$$

where C_e and C_s are determined from the following equations:

For $\quad e \leq \frac{1}{20}, \; C_e = 1.0$

For $\quad \frac{t}{20} < e \leq \frac{t}{6}, \; C_e = \dfrac{1.3}{1 + \frac{6e}{t}} + \frac{1}{2}\left(\frac{e}{t} - \frac{1}{20}\right)\left(1 - \frac{e_1}{e_2}\right)$

For $\quad \frac{t}{6} < e \leq \frac{t}{3}, \; C_e = 1.95\left(\frac{1}{2} - \frac{e}{t}\right) + \frac{1}{2}\left(\frac{e}{t} - \frac{1}{20}\right)\left(1 - \frac{e_1}{e_2}\right)$

where

e = maximum eccentricity,

e_1 = smaller eccentricity at lateral supports,

e_2 = larger eccentricity at lateral supports,

t = wall thickness.

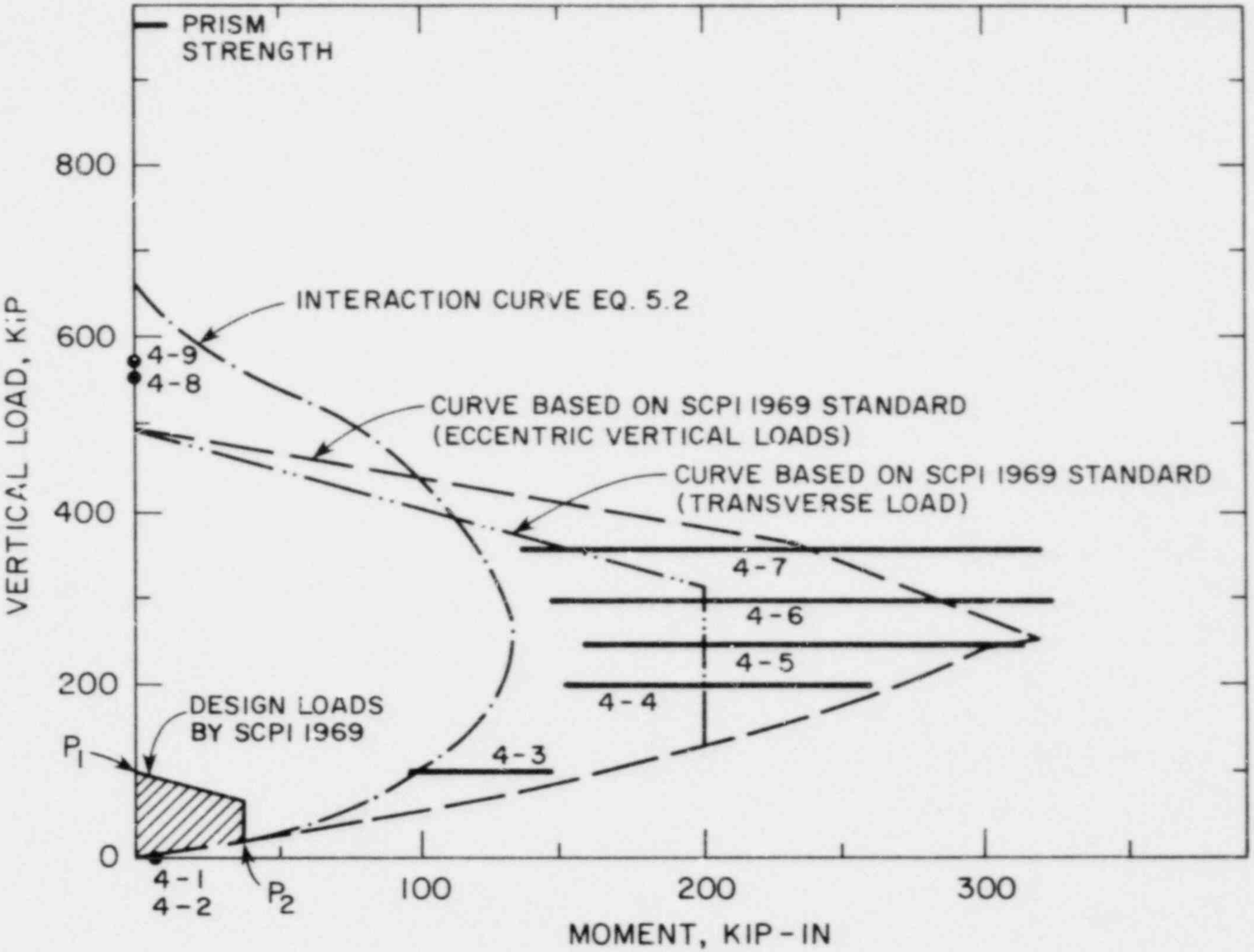

FIG. 5.1 COMPARISON OF DESIGN RECOMMENDATIONS FOR BRICK WALLS WITH YOKEL'S TEST RESULTS ON BRICK A WALLS WITH 1:1:4 MORTAR

From Reference (6)

Value of e_1/e_2 is positive for walls bent in single curvature and negative for walls bent in double or reverse curvature. For members subjected to transverse loads greater than 10 psf, e_1/e_2 is assumed as +1.0 in the computation of C_e.

$$C_s = 1.20 - \frac{\frac{h}{t}}{300}\left[5.75 + \left(1.5 + \frac{e_1}{e_2}\right)^2\right] \leq 1.0$$

Loads and moments at eccentricities in excess of t/3 are limited by allowable flexural tensile stresses.

Test results on Brick A walls with 1:1:4 mortar from Yokel's[6] work are compared in Fig. 5.1 with hypothetical ultimate strength curves based on the 1969 SCPI Standard. These curves were developed on the assumption that the ultimate loads are equal to $C_e\ C_s\ f'_m\ A_g$.

The dashed curve applicable to eccentric vertical loads was based on $e_1/e_2 = -0.4$ (assuming partial fixity at one end and a pinned condition at the other end). The axial load capacity predicted by this curve is in fair agreement with the test results obtained in this investigation and the capacity predicted by Eq. 5.2. However for smaller values of vertical load, there is considerable difference in the moment capacities. The reasons for these differences are discussed in the following paragraphs.

Figure 5.2 shows a comparison between the loading condition on the tested wall panels and the loading conditions which were used in SCPI tests. As shown, brick walls were subjected to eccentric vertical loads in the SCPI tests. If the moment magnifier method is applied to these two cases of loading, the following coefficients would be used:

Lateral loading: $C_m = 1$, $k = 0.8$

Vertical loading: $C_m = 0.5$, $k = 0.8$.

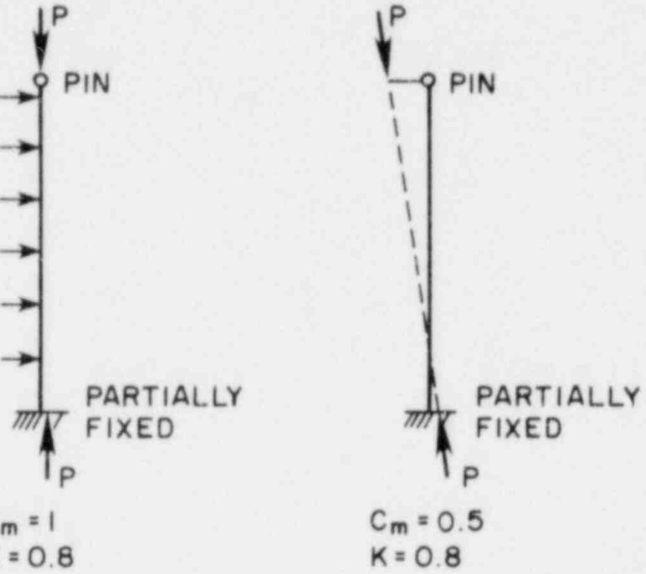

FIG. 5.2 COMPARISON OF LOADING AND END CONDITIONS
From Reference (6)

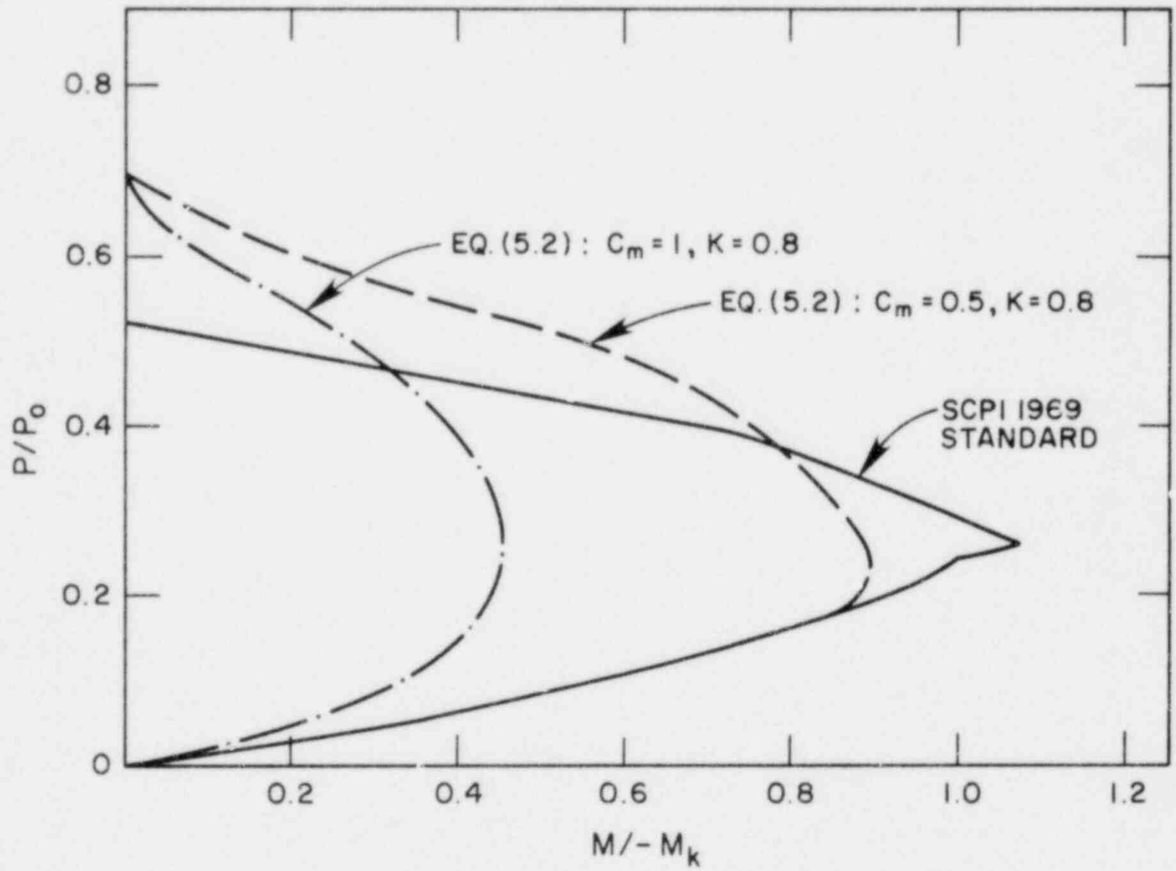

FIG. 5.3 PREDICTION OF SCPI 1969 CONDITIONS
From Reference (6)

The resulting predicted slenderness effects would be quite different for the two cases.

Figure 5.3 compares the SCPI curve with transverse strength predicted by the moment magnifier method using the coefficients $C_m = 0.5$ and $k = 0.8$. The predicted interaction curve for lateral loading is also shown for the sake of comparison. It can be seen that the moment magnifier curve for vertical load eccentricity approximately agrees with the SCPI curve.

It should be recognized that the SCPI test curve was developed on the basis of tests with eccentric vertical loads only. When slenderness effects are analyzed by considering added moments caused by deflections, it can be demonstrated that the case of lateral loading is not correctly simulated by eccentric vertical loads. However, this difference is generally not recognized in present design practice. Thus the moment magnifier method provides a more flexible approach for the prediction of slenderness effects under all loading conditions.

In the 1969 SCPI Standard, the case of transverse loading has been recognized as a result of Yokel's investigation. This loading condition corresponds to the dashed-dotted curve in Fig. 5.1 and is in reasonable agreement with the results obtained in Yokel's investigation.

The shaded area in Fig. 5.1 shows the allowable loads and moments in accordance with the case of transverse loading specified in the SCPI 1969 standard. These values are safe, however the margin of safety seems to decrease with increasing e/t. It is obvious that these recommendations provide a margin of safety by "scaling down" a hypothetical ultimate strength curve. This scaling down is along constant e/t lines. At the eccentricity of $e/t = 1/3$ the interaction curve is scaled down radially, which provides a rather slim margin of safety at that eccentricity. For loads larger than P_2 (Fig. 5.1), the margin of safety for transverse moments gradually increases. At load P_1 no moment is permitted, while actually a wall would be capable of supporting a much greater moment at that load than at load P_2, where the maximum transverse moment is permitted. The philosophy behind the method of scaling down the ultimate interaction curve is questionable and should be reexamined, considering all possible combinations of vertical loads and moments at ultimate loads, as well as at service loads.

5.3.3 NCMA and ACI Recommendations

These recommendations account for slenderness effects, but do not account for end or loading conditions. The following equations are recommended by NCMA and ACI for nonreinforced walls:

Axial load:

$$P = 0.20\ f'_m \left[1 - \left(\frac{h}{40t}\right)^3\right] A_n$$

where

A_n = net cross-sectional area of the masonry.

Eccentric loads:

$$\frac{f_a}{F_a} + \frac{f_m}{F_m} \text{ shall not exceed } 1$$

where

f_a = computed axial compressive stress,

$F_a = \frac{P}{A_n}$ = allowable axial compressive stress,

f_m = computed flexural compressive stress,

$F_m = 0.3\ f'_m$ = allowable flexural compressive stress.

Up to an eccentricity of $e/t = 1/3$, a cracked section may be assumed to compute bending strength in solid unit walls, neglecting the flexural tensile strength. In hollow unit walls, eccentricity is limited to a value which would produce tension.

In Fig. 5.4 allowable axial load (P_{all}) computed by the NCMA standard is compared with critical axial load computed for the 8 inch solid concrete block walls used in Yokel's program, where critical axial loads were assumed to equal 0.7 P_{cro}, (Eq. 5.2). Critical loads were computed for different h/t ratios for the pin ended case and for partial fixity as assumed in the interpretation of test results. It appears that the pin ended case is fairly close to the NCMA equation.

The slenderness reduction equation used by NCMA and ACI, which is also termed "empirical equation," considers only the geometry of the wall gross section. Variables which influence slenderness effects and which are not considered by the equation are f'_m/E, cross-sectional geometry, end fixity, and loading conditions. The justification for not considering some of these variables may be in part attributed to the fact that there is a linear relationship between f'_m and E within a certain range of masonry strength, and that end conditions are similar for most conventional masonry structures. It is questionable whether, with the increasing use of high strength masonry and of high rise masonry construction, it is still possible to disregard these variables without the use of unduly high margins of safety.

Interaction curves for ultimate and allowable loads are compared in Fig. 5.5 with test results and with interaction curves constructed in accordance with Yokel's investigation. It should be noted that the NCMA allowable flexural stress is 0.3 f'_m and the allowable compressive stress only 0.2 f'_m. These stresses when multiplied by 5, which may be

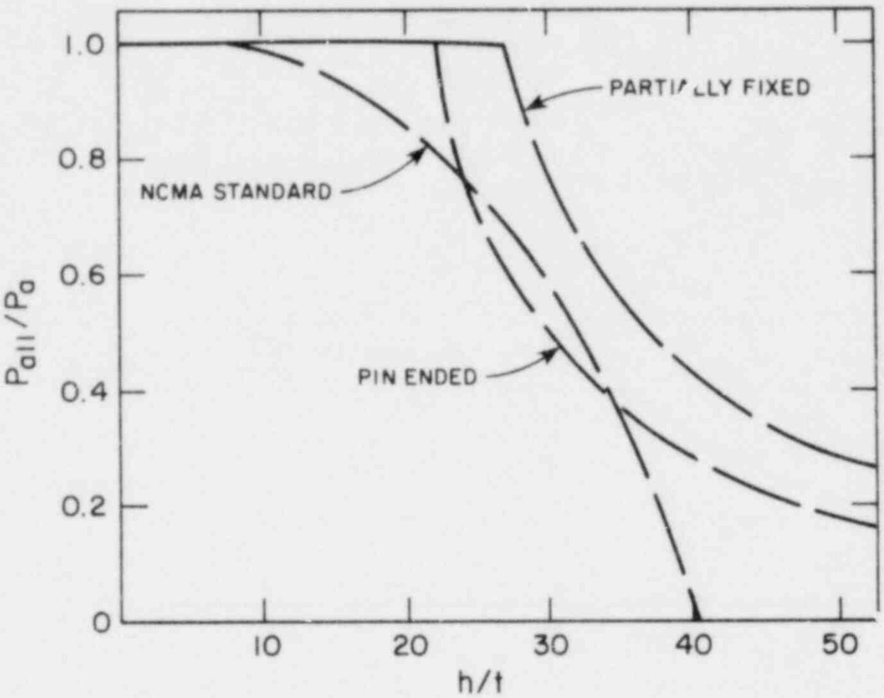

FIG. 5.4 NCMA EXPRESSION FOR SLENDERNESS EFFECTS
From Reference (6)

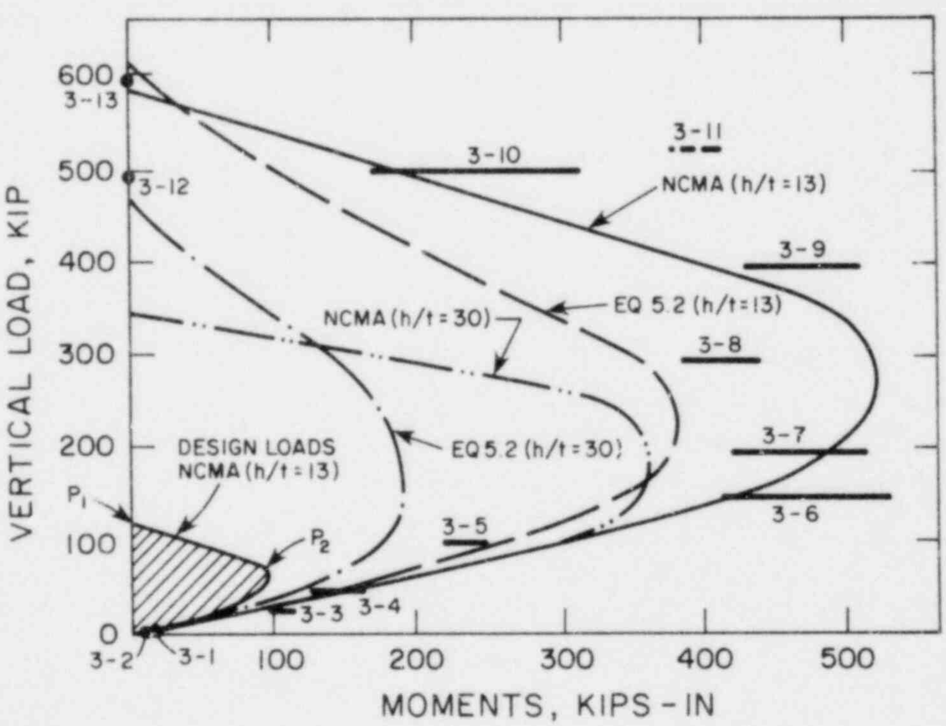

FIG. 5.5 COMPARISON OF NCMA RECOMMENDATIONS WITH YOKEL'S TEST RESULTS ON SOLID 8-IN CONCRETE BLOCK WALLS
From Reference (6)

considered the axial load margin of safety and assumed constant throughout the e/t range, will result in a short-wall interaction curve. This curve assumes an "a" value greater than 1 (flexural compressive strength is af'_m where f'_m is the prism compressive strength) for large e/t values, with a peak at P_o and a distortion which will result in greater ultimate moments at higher e/t ratios. This short-wall interaction curve is modified for slenderness by reducing the part of the total stress due to axial load (P/A), without at the same time reducing the stress caused by moments (Mc/I).

For the slenderness of the walls tested, the modification of the interaction curves is relatively minor. Curves were therefore constructed for an h/t ratio of 30, to provide a better comparison between Eq. 5.2 and the NCMA equation.

For the small slenderness ratio the moments predicted by the NCMA equation are greater, accounting for an "a" value which is greater than 1. These increased moments are less conservative than the moments predicted by the interaction curve at a = 1, and seem to show fairly good agreement with some of the tested panels, while overestimating the strength of other specimens.

Comparison of the two theoretical curves for h/t = 30 shows that the NCMA curve predicts a smaller axial load, but greater moments. While no slender concrete masonry walls were tested, it appears on the basis of the agreement between predicted and observed strength of the more slender brick walls that the NCMA curve probably overestimates the transverse strength of transversely loaded slender walls, even though the curve plotted by Eq. (5.2), which assumes a = 1, is very conservative. However, the NCMA equation is probably conservative for the case of eccentric vertical loads.

Allowable moments by the NCMA equation for an h/t ratio of 13 are shown in the shaded area in Fig. 5.5. As in the case of the SCPI equation, the philosophy of scaling down predicted ultimate interaction curves should be reexamined.

5.4 Determination Of The Transverse Strength Of Reinforced Masonry Walls

As with unreinforced walls, two wall properties must be evaluated in order to determine the transverse strength of reinforced masonry walls:

(1) the capacity of the wall cross-section to resist combined bending and axial loads,

and (2) the effect of wall slenderness on load capacity.

It has been shown by Scrivener[27] that the moment capacity of a reinforced wall cross-section with no vertical load is a function of the amount of reinforcement and the compressive strength of the masonry. Yokel[6] has further shown that for unreinforced walls the moment capacity is a function of the vertical load. This relation is clearly applicable to reinforced walls as well. Amrhein in his reinforced masonry engineering handbook[37] has developed working stress design formulations for the moment versus vertical load interaction diagram for reinforced walls. His formulations do not include the slenderness effects of the walls, however.

5.4.1 Discussion Of Present Design Practice For Reinforced Walls

The major U.S. code requiring reinforcement of masonry is the Uniform Building Code[38]. The UBC requirements for minimum reinforcement in walls are as follows:

Reinforcement. All walls using stresses permitted for reinforced masonry shall be reinforced with both vertical and horizontal reinforcement. The sum of the areas of horizontal and vertical reinforcement shall be at least 0.002 times the gross cross-sectional area of the wall and the minimum area of reinforcement in either direction shall be not less than 0.0007 times the gross cross-sectional area of the wall. The reinforcement shall be limited to a maximum spacing of 4 feet on center. The minimum diameter of reinforcement shall be 3/8 inch except that joint reinforcement may be considered as part of the required minimum reinforcement.

Further, the allowable axial stress for a wall is given by

$$f_m = 0.2\, f'_m \left[1 - \left(\frac{h}{40t}\right)^3\right]$$

where

f_m = compressive unit axial stress in masonry wall,

f'_m = ultimate compressive masonry stress. The value of f'_m shall not exceed 6000 pounds per square inch,

t = thickness of wall in inches,

h = clear unsupported distance between supporting or enclosing members (vertical or horizontal stiffening elements).

For combined axial and flexural loads the following interaction framework is used:

$$\frac{f_a}{F_a} + \frac{f_b}{F_b} < 1$$

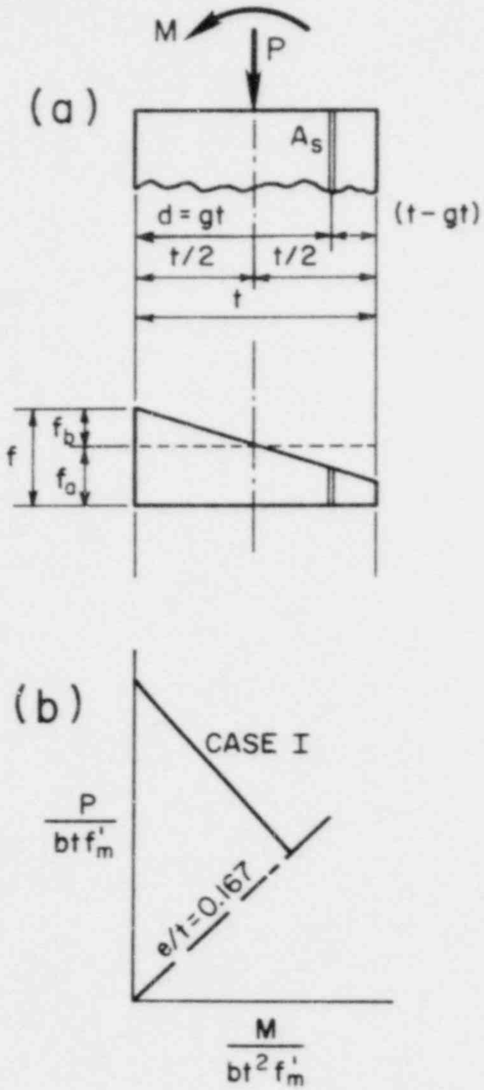

FIG. 5.6 INTERACTION, CASE I
From Reference (37)

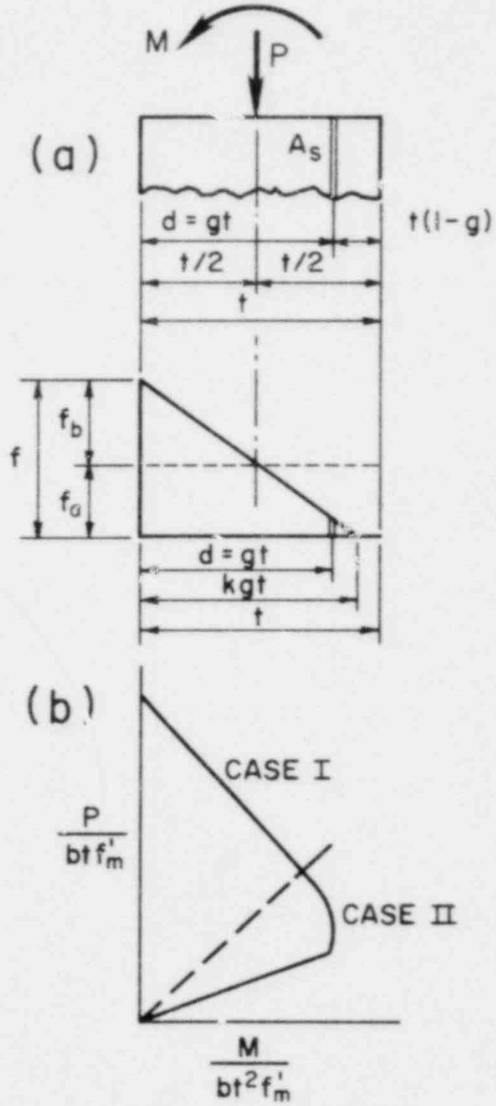

FIG. 5.7 INTERACTION, CASE II
From Reference (37)

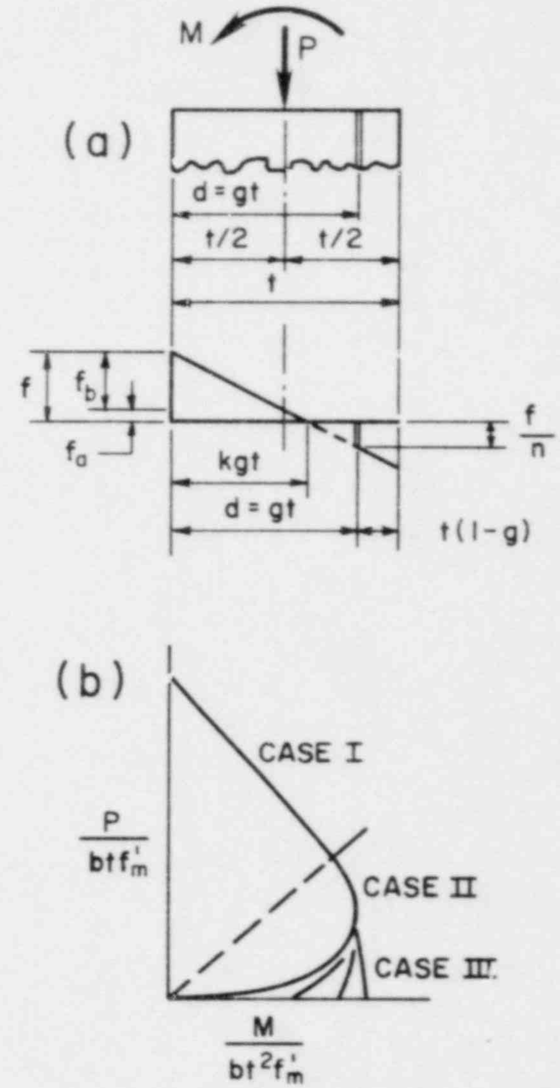

FIG. 5.8 INTERACTION, CASE III
From Reference (37)

where

f_a = computed axial compressive stress on the net area,

$F_a = \frac{P}{A_n} = f_m$ given above for walls,

f_b = computed compressive flexural stress,

$F_b = 0.33\ f'_m$ = allowable flexural compressive stress n.

The allowable load requirements are almost identical to those of the NCMA and ACI recommendations for unreinforced walls discussed in Section 5.3.3. The reinforcement requirements are additional and only affect the allowable loads in regions of low vertical load, as shown in the following three cases from reference 37.

Case I (Figure 5.6)

Compression on total cross-section of wall. Steel not credited with resisting any compression.

$$f_a = \frac{P}{bt} \text{ psi}$$

$$f_b = \frac{M}{S} = \frac{6M}{bt^2} \text{ psi.}$$

The load may have a maximum eccentricity of t/6 or e/t = 0.167, which is the location of the kern point, and there would then be zero stress on one edge.

Case II (Figure 5.7)

Compression on part of the wall with some compression between the face of the wall and steel. Line of zero stress is between the outside edge of the wall and the steel. The steel is not credited with resisting any compression. The moment is great enough or the load would have an eccentricity large enough, e/t > 0.167, to create an area that has no stress on it. Masonry is assumed not to resist tension.

$$f_a = \frac{P}{bt} \text{ psi}$$

$$f_b = \frac{2M}{bt^2\, kg\left(\frac{1}{2} - \frac{kg}{3}\right)} - f_a \text{ psi.}$$

Case III (Figure 5.8)

The moment is large enough to cause the steel to act in tension. The moment capacity is determined by the amount of steel (np) in the section.

$$f_a = \frac{P}{bt} \text{ psi}$$

$$f_b = \frac{\frac{M}{bt^2} - \frac{k}{2}\left(\frac{1}{2} - \frac{k}{3}\right) f_a - np\left(\frac{g - k}{k}\right)\left(g - \frac{1}{2}\right) f_a}{\frac{k}{2}\left(\frac{1}{2} - \frac{k}{3}\right) + np\left(\frac{g - k}{k}\right)\left(g - \frac{1}{2}\right)} \text{ psi.}$$

It is clear from Figure 5.8 that the wall reinforcement only affects the region of low vertical loads.

Slenderness effects are accounted for in the Uniform Building Code in the same way as in the NCMA criteria (Section 5.3.3) and the same comments are applicable. Only a small amount of research has been performed on lateral loadings on reinforced walls and it is clear that additional research is required. Scrivener's work indicates that the ultimate strength design concept is promising and justifies further research.

5.5 Flexural Tensile Stess

As the design of unreinforced masonry walls for transverse loads is often governed by the flexural tensile strength of mortar bed joints, it is of interest to compare the allowable tensile stresses specified in various national codes and to compare these values with test results.

Table 5.1 presents a list of allowable flexural tensile stresses specified in several current national codes.

It would appear that the 1973 Uniform Building Code (USA) and 1970 Canada Code permit considerably higher tensile stresses than are normal in Europe and other countries. The Switzerland Code is the most conservative, although it allows for the beneficial effect of dead load stress, with a maximum allowable stress of 56 psi. All codes except the British and Australian (which is based on the British) allow for different mortar strengths.

A plot of mortar compressive strength versus modulus of rupture from various investigations is given in Fig. 5.9. Also included in the figure are the Uniform Building Code allowable flexural tensile stresses normal to the bed joint for inspected masonry construction. As can be seen, a factor of two separates the code allowable values and the lowest test results.

5.6 Comparison Of Test Results With Existing Design Practice

These conclusions are directly reproducted from reference (6)

(1) The ANSI American Standard Building Code Requirements for Masonry do not take into account slenderness and end conditions and compensate for variability in wall strengths by high margins of safety.

(2) The design equations in the 1969 SCPI Standard account for end conditions as well as slenderness. The equations were developed on the basis of eccentric vertical load tests but also provide for the case of transverse loading.

Table 5.1

Allowable Flexural Tensile

Stresses in National Codes

(Unreinforced Brick Masonry)

Code	Mortar Type, Mortar Mix (C:L:S) or Strength	Allowable Stress in Tension in Flexure (psi)	
		Parallel to bed joints	Normal to bed joints
1973 USA Uniform Building Code Ref. (38)	M or S (2500 psi or 1800 psi)	72* (36)** 56* (28)**	36* (18)** 28* (14)**
1970 Canada National Building Code Ref. (39)	M or S N	72 56	36 28
Britain (and Australia) Ref. (39)	1:1:6 or better	20 (to be used with caution)	10
Germany Ref. (39)	1:0:4	28	Only exceptionally permitted
Switzerland Ref. (39)	1:2:8 1:0:3.2-3.7	14 5.95-12.4***	Not permitted
Japan Ref. (44)	1:0:3 or 1:2:5	32 or less than $\frac{f'_m}{53}$	

*Special inspection required

**No special inspection required

***At mid-height of a story height panel

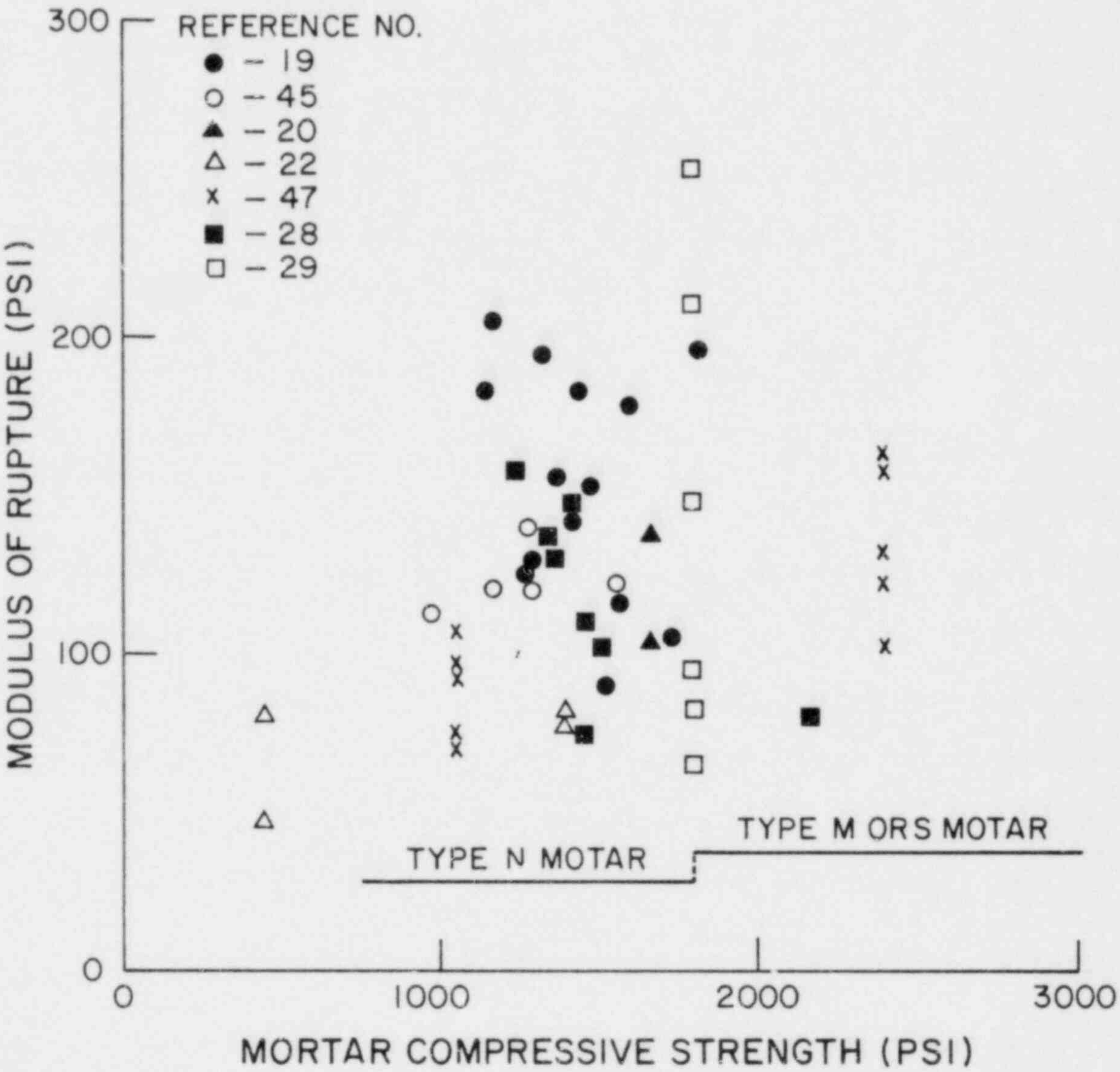

FIG. 5.9 EFFECT OF MORTAR COMPRESSIVE STRENGTH ON MODULUS OF RUPTURE OF BRICK WALLS

(3) The NCMA, ACI and UBC recommendations consider slenderness but not end conditions. The NCMA equations probably overestimate wall strength under transverse loading conditions.

(4) The interaction diagrams for ultimate transverse strength as a function of lateral loads, developed by SCPI and NCMA were scaled down radially to determine allowable working load. This scaling down in some cases results in extremely low factors of safety in bending, while the factor of safety under vertical loads is very high.

(5) Neither the NCMA nor the SCPI Standard provide for the design of composite (brick and block) walls. This type of construction is widely used.

(6) While existing design standards are primarily intended for the case of eccentric vertical loads, and in most cases do not account for end conditions, the moment magnifier method, if used for the prediction of transverse wall strength, could cover both the case of eccentric vertical loading and the case of transverse loading and could also account for end conditions.

6. SUMMARY AND CONCLUSIONS

The survey of forty-seven references presented in the preceding chapters indicates the extent of information currently available on transverse strength of masonry walls. Several trends and conclusions can be drawn from the results presented and these are summarised in the following paragraphs. Some areas, where additional information is desirable, are also included.

The three major factors influencing the transverse strength of masonry walls are applied vertical load, bond strength between the masonry unit and the mortar and amount and distribution of reinforcement

(1) Vertical Load. Below the vertical load P_c, (designated on a moment vs vertical load interaction diagram as the cracking load), an increase in compressive load increases the transverse strength of a wall. This increase in strength is associated with a trend towards a more brittle mode of failure. For critical loads greater than P_c, an increase in vertical load causes a decrease in the transverse strength of a masonry wall.

(2) Reinforcement. The addition of reinforcement increases both the strength and ductility of masonry walls loaded transversely. As might be expected horizontal or joint reinforcement is most effective for walls spanning horizontally whereas vertical reinforcement is most effective for walls spanning vertically.

(3) Bond Strength. An increase in the bond strength between the masonry unit and the mortar increases the transverse strength of a masonry wall. The bond strength between the mortar and masonry unit

is affected by several parameters including the strength and surface roughness of the masonry unit; the initial rate of absorption of the masonry unit; the strength, width and thickness of the mortar joint, and the workmanship. Because of the interrelationship of some of these variables conclusions with respect to their effects on the transverse strength of a wall are not well defined. Some of the definite trends of the test results are as follows:

(a) The transverse strength of masonry walls increases with an increase in the tensile strength of the mortar. An increase in the tensile strength of mortar is also associated with an increase in the mortar compressive strength.

(b) The transverse strength of a masonry wall varies inversely with the thickness of the mortar joint.

(c) A decrease in the width of a mortar joint decreases the transverse strength of a masonry wall. This decrease in strength is attributed to the more rapid drying of the narrower bed and is more pronounced in hollow units because of the even more rapid drying created by the internal chimney effect of the hollow units.

(d) Initial rates of absorption of masonry units below 5 and above 30 grams per min. per 30 sq. in. decrease the transverse strength of masonry walls.

(e) The effect of the compressive strength of the masonry unit is not clear. Investigations in this area have led to the conclusion that other variables, such as surface roughness, may be more important.

(f) The quality of workmanship affects the width and thickness of the mortar joint, the quality of the mortar and the initial rate of absorption of the masonry unit. Each of these variables affects the transverse strength of a masonry wall and consequently the overall effect of quality of workmanship is difficult to quantify.

Several theoretical approaches have been used to correlate calculated and test flexural strengths of masonry walls. The moment magnifier method used by Yokel on unreinforced walls produced reasonable correlation with test results. The most promising method used for reinforced walls with no vertical load is similar to that used for determining the ultimate capacity of a reinforced concrete beam.

From the work that has been performed to date it is clear that additional information is required in the following areas:

(a) The cyclic behavior of transversely loaded masonry walls.

(b) The effect of reinforcement including correlation with methods for predicting the strength of the tested walls.

(c) The degree of fixity provided by typical wall-slab and wall-footing connections.

(d) An adequate small-scale test method to predict the flexural strength of full-scale masonry walls.

REFERENCES

1. Mayes, R. L. and Clough, R. W., "A Literature Survey - Compressive, Tensile, Bond and Shear Strength of Masonry," University of California, Berkeley, EERC Report No. 75-15, June 1975.

2. Mayes, R. L. and Clough, R. W., "State-of-the-Art in Seismic Shear Strength of Masonry - An Evaluation and Review," University of California, Berkeley, EERC Report No. 75-21, October 1975.

3. Mayes, R. L., Omote, Y. and Clough, R. W., "Cyclic Shear Tests of Masonry Piers, Volume 1 - Test Results," University of California, Berkeley, EERC Report No. 76-8, May 1976.

4. "ASTM Standard Method of Conducting Strength Tests of Panels for Building Construction" E72-61 (1961).

5. Fa :al, S. G. and Cattaneo, L. E., "Structural Performance of Masonry Walls Under Compression and Flexure," NBS Building Science Series

6. Yokel, F. Y., Mathey, R. G. and Dikkers, R. D., "Strength of Masonry Walls Under Compressive and Transverse Loads," National Bureau of Standards, Building Science Series 34, March 1971.

7. "ASTM Standard Method of Test for Bond Strength of Mortar to Masonry Unit," ASTM Designation E149-66 (1966).

8. Cox, F. W. and Ennega, J. L., "Transverse Strength of Concrete Block Walls," Journal of the American Concrete Institute, May 1968.

9. Stang, A. H., Parsons, D. E. and Foster, H. D., "Compressive and Transverse Strength of Hollow-Tile Walls," Technologic Papers of the Bureau of Standards, No. 311, Vol. 20, February 1926.

10. Richart, F. E., Moorman, R. B. B. and Woodworth, P. M., "Strength and Stability of Concrete Masonry Walls," University of Illinois, Engineering Experiment Station Bulletin No. 251.

11. Willoughby, A. B., Wilton, C., Gabrielsen, B. L. and Zaccor, J. V., "A Study of Loading Structural Response, and Debris Characteristics of Wall Panels," URS 680-5, Urs Research Company, July 1969.

12. Wilton, C., Gabrielsen, B., Edmunds, J. and Bechtel, S., "Loading and Structural Response of Wall Panels," URS 709-4, Urs Research Company, November 1969.

13. Wilton, C. and Gabrielsen, B., "Shock Tunnel Tests of Preloaded and Arched Wall Panels," URS 7030-10, Urs Research Company, June 1973.

14. Urs Research Company, "Structural Response and Loading of Wall Panels," URS 709-11.

15. Gabrielsen, B., Wilton, C. and Kaplan, K., "Response of Arching Walls and Debris From Interior Walls Caused by Blast Loading," URS 7030-23, Urs Research Company, February 1975.

16. Gabrielsen, B. L., "Response of Wall Panels Subjected to Blast Loading," ASCE National Structural Engineering Meeting Baltimore, Maryland, April 1971.

17. McKee, K. E. and Sevin, E., "Design of Masonry Walls For Blast Loading," Proceedings of the American Society of Civil Engineers, S.D., January 1958.

18. Morton, J. and Hendry, A. W., "An Experimental Investigation of the Lateral Strength of Brickwork Panels with Precompression Under Dynamic and Static Loading," Proceedings of Third International Brick Masonry Conference, ESSEN, 1973.

19. "Compressive, Transverse and Racking Strength Tests of Four-Inch Brick Walls," Research Report No. 9, Structural Clay Products Research Foundation, Geneva, Illinois, August 1965.

20. "Compressive, Transverse and Shear Strength Tests of Six and Eight-Inch Single-Wythe Walls Built with Solid and Heavy-Duty Hollow Clay Masonry Units," Research Report No. 16, Structural Clay Products Institute, September 1969.

21. Francis, A. J., Horman, C. B. and Jerrems, L. E., "The Effect of Joint Thickness and Other Factors on the Compressive Strength of Brickwork," Proceedings of the Second International Brick Masonry Conference held in Stoke-on-Trent, England, April 1970, pp. 31-37.

22. Whittemore, H. L., Stang, A. H. and Parsons, D. E., "Structural Properties of Six Masonry Wall Constructions," National Bureau of Standards Report BMS-5, November 1938.

23. Portland Cement Association, "Load Tests of Patterned Concrete Masonry Walls," Trowel Talk an aid to the Masonry Industry, 1963.

24. Scrivener, J. C., "Reinforced Masonry - Seismic Behavior and Design," Bulletin of New Zealand Society for Earthquake Engineering, Vol. 5, No. 4, December 1972.

25. Dickey, W. L. and Mackintosh, A., "Results of Variation of "b" or Effective Width in Flexure in Concrete Blocks Panels," Masonry Institute of America, 1971.

26. American National Standards Institute, American Standard Building Code Requirements for Masonry (National Bureau of Standards, 1953).

27. Scrivener, J. C., "Face Load Tests on Reinforced Hollow Brick Non-Load-Bearing Walls," New Zealand Engineering, July 1969.

28. "Compressive, Transverse and Racking Strength Tests of Four-Inch Structural Clay Facing Tile Walls," Research Report No. 11, Structural Clay Products Research Foundation, Geneva, Illinois, February 1967.

29. Johnson, F. B. and Matthys, J. H. "Structural Strength of Hollow Clay Tile Assemblages," Journal of the Structural Division, Proceedings of ASCE, Vol. 99, No. ST2, February 1973.

30. Yokel, F. Y. and Dikkers, R. D., "Strength of Load Bearing Masonry Walls," Journal of the Structural Division, Proceedings of ASCE, No. ST5, May 1971.

31. Yokel, F. Y., Robert, G. M. and Robert, D. D., "Compressive Strength of Slender Concrete Masonry Walls," Building Science Series 33,National Bureau of Standards, December 1970.

32. Meinheit, D. F. and Springfield, J., Discussion about "Strength of Load - Bearing Masonry Walls," Journal of the Structural Division, Proceedings of ASCE, No. ST2, February 1972.

33. MacGregor, J. G., Breen, J. E. and Pfrang, E. O., "Design of Slender Concrete Columns," Journal of the American Concrete Institute, Vol. 67, No. 1, January 1970.

34. Structural Clay Products Institute, Building Code Requirements for Engineered Brick Masonry (August 1969).

35. National Concrete Masonry Association, Specification for the Design and Construction of Load - Bearing Concrete Masonry (1968).

36. American Concrete Institute, Committee 531, "Concrete Masonry Structures - Design and Construction," Journal of the American Concrete Institute, Vol. 67, No. 5, May 1970 and Vol. 67, No. 6, June 1970.

37. Amrhein, J. E., "Reinforced Masonry Engineering Handbook. Clay and Concrete Masonry," second edition, Los Angeles, Masonry Institute of America, 1972, 1973.

38. Uniform Building Code, 1973 Edition Published by the International Conference of Building Officials, Whittier, California, 1973.

39. Culter, J. F., Plewes, W. G. and Mikluchin, P. T., "The Development of the Canadian Building Code for Masonry," Proceedings of the Second International Brick Masonry, Stoke-on-Trent, England, April 1970.

40. Monk, C. B., "SCR Brick Wall Tests," Research Report No. 1 of the Structural Clay Products Research Foundation, January 1965.

41. Cajdert, A. and Losberg, A., "Laterally Loaded Light Expanded Clay Block Masonry. The Effect of Reinforcement in Horizontal Joints," The 3rd International Brick-Masonry Conference, ESSEN, April 1973.

42. Haseltine, B. A. and Hodgkinson, H. R., "Wind Effects on Brick Panel Walls - Design Considerations," The 3rd International Brick-Masonry Conference, ESSEN, April 1973.

43. Baker, L. R., "Flexural Strength of Brickwork Panels," The 3rd International Brick-Masonry Conference, ESSEN, April 1973.

44. "1964 Masonry Design Code" Architectural Institute of Japan (In Japanese).

45. "Compressive and Transverse Tests of Five-Inch Brick Walls," Research Report No. 8,Structural Clay Products Research Foundation, May 1965.

46. Monk, C. B., "Structural Properties of Multiple Unit Six-inch Ceramic Glazed Structural Clay Facing Tile Walls," Research Report No. 6, Structural Clay Products Research Foundation, October 1956.

47. Satti, K. M. H. and Hendry, A. W., "The Modulus of Rupture of Brickwork," Third International Brick Masonry Conference, ESSEN, April 1973.

EARTHQUAKE ENGINEERING RESEARCH CENTER REPORTS

NOTE: Numbers in parenthesis are Accession Numbers assigned by the National Technical Information Service; these are followed by a price code. Copies of the reports may be ordered from the National Technical Information Service, 5285 Port Royal Road, Springfield, Virginia, 22161. Accession Numbers should be quoted on orders for reports (PB --- ---) and remittance must accompany each order. Reports without this information were not available at time of printing. Upon request, EERC will mail inquirers this information when it becomes available.

EERC 67-1 "Feasibility Study Large-Scale Earthquake Simulator Facility," by J. Penzien, J.G. Bouwkamp, R.W. Clough and D. Rea - 1967 (PB 187 905)A07

EERC 68-1 Unassigned

EERC 68-2 "Inelastic Behavior of Beam-to-Column Subassemblages Under Repeated Loading," by V.V. Bertero - 1968 (PB 184 888)A05

EERC 68-3 "A Graphical Method for Solving the Wave Reflection-Refraction Problem," by H.D. McNiven and Y. Mengi - 1968 (PB 187 943)A03

EERC 68-4 "Dynamic Properties of McKinley School Buildings," by D. Rea, J.G. Bouwkamp and R.W. Clough - 1968 (PB 187 902)A07

EERC 68-5 "Characteristics of Rock Motions During Earthquakes," by H.B. Seed, I.M. Idriss and F.W. Kiefer - 1968 (PB 188 338)A03

EERC 69-1 "Earthquake Engineering Research at Berkeley," - 1969 (PB 187 906)A11

EERC 69-2 "Nonlinear Seismic Response of Earth Structures," by M. Dibaj and J. Penzien - 1969 (PB 187 904)A08

EERC 69-3 "Probabilistic Study of the Behavior of Structures During Earthquakes," by R. Ruiz and J. Penzien - 1969 (PB 187 886)A06

EERC 69-4 "Numerical Solution of Boundary Value Problems in Structural Mechanics by Reduction to an Initial Value Formulation," by N. Distefano and J. Schujman - 1969 (PB 187 942)A02

EERC 69-5 "Dynamic Programming and the Solution of the Biharmonic Equation," by N. Distefano - 1969 (PB 187 941)A03

EERC 69-6 "Stochastic Analysis of Offshore Tower Structures," by A.K. Malhotra and J. Penzien - 1969 (PB 187 903)A09

EERC 69-7 "Rock Motion Accelerograms for High Magnitude Earthquakes," by H.B. Seed and I.M. Idriss - 1969 (PB 187 940)A02

EERC 69-8 "Structural Dynamics Testing Facilities at the University of California, Berkeley," by R.M. Stephen, J.G. Bouwkamp, R.W. Clough and J. Penzien - 1969 (PB 189 111)A04

EERC 69-9 "Seismic Response of Soil Deposits Underlain by Sloping Rock Boundaries," by H. Dezfulian and H.B. Seed 1969 (PB 189 114)A03

EERC 69-10 "Dynamic Stress Analysis of Axisymmetric Structures Under Arbitrary Loading," by S. Ghosh and E.L. Wilson 1969 (PB 189 026)A10

EERC 69-11 "Seismic Behavior of Multistory Frames Designed by Different Philosophies," by J.C. Anderson and V. V. Bertero - 1969 (PB 190 662)A10

EERC 69-12 "Stiffness Degradation of Reinforcing Concrete Members Subjected to Cyclic Flexural Moments," by V.V. Bertero, B. Bresler and H. Ming Liao - 1969 (PB 202 942)A07

EERC 69-13 "Response of Non-Uniform Soil Deposits to Travelling Seismic Waves," by H. Dezfulian and H.B. Seed - 1969 (PB 191 023)A03

EERC 69-14 "Damping Capacity of a Model Steel Structure," by D. Rea, R.W. Clough and J.G. Bouwkamp - 1969 (PB 190 663)A06

EERC 69-15 "Influence of Local Soil Conditions on Building Damage Potential during Earthquakes," by H.B. Seed and I.M. Idriss - 1969 (PB 191 036)A03

EERC 69-16 "The Behavior of Sands Under Seismic Loading Conditions," by M.L. Silver and H.B. Seed - 1969 (AD 714 982)A07

EERC 70-1 "Earthquake Response of Gravity Dams," by A.K. Chopra - 1970 (AD 709 640)A03

EERC 70-2 "Relationships between Soil Conditions and Building Damage in the Caracas Earthquake of July 29, 1967," by H.B. Seed, I.M. Idriss and H. Dezfulian - 1970 (PB 195 762)A05

EERC 70-3 "Cyclic Loading of Full Size Steel Connections," by E.P. Popov and R.M. Stephen - 1970 (PB 213 545)A04

EERC 70-4 "Seismic Analysis of the Charaima Building, Caraballeda, Venezuela," by Subcommittee of the SEAONC Research Committee: V.V. Bertero, P.F. Fratessa, S.A. Mahin, J.H. Sexton, A.C. Scordelis, E.L. Wilson, L.A. Wyllie, H.B. Seed and J. Penzien, Chairman - 1970 (PB 201 455)A06

EERC 70-5 "A Computer Program for Earthquake Analysis of Dams," by A.K. Chopra and P. Chakrabarti - 1970 (AD 723 994)A05

EERC 70-6 "The Propagation of Love Waves Across Non-Horizontally Layered Structures," by J. Lysmer and L.A. Drake 1970 (PB 197 896)A03

EERC 70-7 "Influence of Base Rock Characteristics on Ground Response," by J. Lysmer, H.B. Seed and P.B. Schnabel 1970 (PB 197 897)A03

EERC 70-8 "Applicability of Laboratory Test Procedures for Measuring Soil Liquefaction Characteristics under Cyclic Loading," by H.B. Seed and W.H. Peacock - 1970 (PB 198 016)A03

EERC 70-9 "A Simplified Procedure for Evaluating Soil Liquefaction Potential," by H.B. Seed and I.M. Idriss - 1970 (PB 198 009)A03

EERC 70-10 "Soil Moduli and Damping Factors for Dynamic Response Analysis," by H.B. Seed and I.M. Idriss - 1970 (PB 197 869)A03

EERC 71-1 "Koyna Earthquake of December 11, 1967 and the Performance of Koyna Dam," by A.K. Chopra and P. Chakrabarti 1971 (AD 731 496)A06

EERC 71-2 "Preliminary In-Situ Measurements of Anelastic Absorption in Soils Using a Prototype Earthquake Simulator," by R.D. Borcherdt and P.W. Rodgers - 1971 (PB 201 454)A03

EERC 71-3 "Static and Dynamic Analysis of Inelastic Frame Structures," by F.L. Porter and G.H. Powell - 1971 (PB 210 135)A06

EERC 71-4 "Research Needs in Limit Design of Reinforced Concrete Structures," by V.V. Bertero - 1971 (PB 202 943)A04

EERC 71-5 "Dynamic Behavior of a High-Rise Diagonally Braced Steel Building," by D. Rea, A.A. Shah and J.G. Bouwkamp 1971 (PB 203 584)A06

EERC 71-6 "Dynamic Stress Analysis of Porous Elastic Solids Saturated with Compressible Fluids," by J. Ghaboussi and E. L. Wilson - 1971 (PB 211 396)A06

EERC 71-7 "Inelastic Behavior of Steel Beam-to-Column Subassemblages," by H. Krawinkler, V.V. Bertero and E.P. Popov 1971 (PB 211 335)A14

EERC 71-8 "Modification of Seismograph Records for Effects of Local Soil Conditions," by P. Schnabel, H.B. Seed and J. Lysmer - 1971 (PB 214 450)A03

EERC 72-1 "Static and Earthquake Analysis of Three Dimensional Frame and Shear Wall Buildings," by E.L. Wilson and H.H. Dovey - 1972 (PB 212 904)A05

EERC 72-2 "Accelerations in Rock for Earthquakes in the Western United States," by P.B. Schnabel and H.B. Seed - 1972 (PB 213 100)A03

EERC 72-3 "Elastic-Plastic Earthquake Response of Soil-Building Systems," by T. Minami - 1972 (PB 214 868)A08

EERC 72-4 "Stochastic Inelastic Response of Offshore Towers to Strong Motion Earthquakes," by M.K. Kaul - 1972 (PB 215 713)A05

EERC 72-5 "Cyclic Behavior of Three Reinforced Concrete Flexural Members with High Shear," by E.P. Popov, V.V. Bertero and H. Krawinkler - 1972 (PB 214 555)A05

EERC 72-6 "Earthquake Response of Gravity Dams Including Reservoir Interaction Effects," by P. Chakrabarti and A.K. Chopra - 1972 (AD 762 330)A08

EERC 72-7 "Dynamic Properties of Pine Flat Dam," by D. Rea, C.Y. Liaw and A.K. Chopra - 1972 (AD 763 928)A05

EERC 72-8 "Three Dimensional Analysis of Building Systems," by E.L. Wilson and H.H. Dovey - 1972 (PB 222 438)A06

EERC 72-9 "Rate of Loading Effects on Uncracked and Repaired Reinforced Concrete Members," by S. Mahin, V.V. Bertero, D. Rea and M. Atalay - 1972 (PB 224 520)A08

EERC 72-10 "Computer Program for Static and Dynamic Analysis of Linear Structural Systems," by E.L. Wilson, K.-J. Bathe, J.E. Peterson and H.H.Dovey - 1972 (PB 220 437)A04

EERC 72-11 "Literature Survey - Seismic Effects on Highway Bridges," by T. Iwasaki, J. Penzien and R.W. Clough - 1972 (PB 215 613)A19

EERC 72-12 "SHAKE-A Computer Program for Earthquake Response Analysis of Horizontally Layered Sites," by P.B. Schnabel and J. Lysmer - 1972 (PB 220 207)A06

EERC 73-1 "Optimal Seismic Design of Multistory Frames," by V.V. Bertero and H. Kamil - 1973

EERC 73-2 "Analysis of the Slides in the San Fernando Dams During the Earthquake of February 9, 1971," by H.B. Seed, K.L. Lee, I.M. Idriss and F. Makdisi - 1973 (PB 223 402)A14

EERC 73-3 "Computer Aided Ultimate Load Design of Unbraced Multistory Steel Frames," by M.B. El-Hafez and G.H. Powell 1973 (PB 248 315)A09

EERC 73-4 "Experimental Investigation into the Seismic Behavior of Critical Regions of Reinforced Concrete Components as Influenced by Moment and Shear," by M. Celebi and J. Penzien - 1973 (PB 215 884)A09

EERC 73-5 "Hysteretic Behavior of Epoxy-Repaired Reinforced Concrete Beams," by M. Celebi and J. Penzien - 1973 (PB 239 568)A03

EERC 73-6 "General Purpose Computer Program for Inelastic Dynamic Response of Plane Structures," by A. Kanaan and G.H. Powell - 1973 (PB 221 260)A08

EERC 73-7 "A Computer Program for Earthquake Analysis of Gravity Dams Including Reservoir Interaction," by P. Chakrabarti and A.K. Chopra - 1973 (AD 766 271)A04

EERC 73-8 "Behavior of Reinforced Concrete Deep Beam-Column Subassemblages Under Cyclic Loads," by O. Küstü and J.G. Bouwkamp - 1973 (PB 246 117)A12

EERC 73-9 "Earthquake Analysis of Structure-Foundation Systems," by A.K. Vaish and A.K. Chopra - 1973 (AD 766 272)A07

EERC 73-10 "Deconvolution of Seismic Response for Linear Systems," by R.B. Reimer - 1973 (PB 227 179)A08

EERC 73-11 "SAP IV: A Structural Analysis Program for Static and Dynamic Response of Linear Systems," by K.-J. Bathe, E.L. Wilson and F.E. Peterson - 1973 (PB 221 967)A09

EERC 73-12 "Analytical Investigations of the Seismic Response of Long, Multiple Span Highway Bridges," by W.S. Tseng and J. Penzien - 1973 (PB 227 816)A10

EERC 73-13 "Earthquake Analysis of Multi-Story Buildings Including Foundation Interaction," by A.K. Chopra and J.A. Gutierrez - 1973 (PB 222 970)A03

EERC 73-14 "ADAP: A Computer Program for Static and Dynamic Analysis of Arch Dams," by R.W. Clough, J.M. Raphael and S. Mojtahedi - 1973 (PB 223 763)A09

EERC 73-15 "Cyclic Plastic Analysis of Structural Steel Joints," by R.B. Pinkney and R.W. Clough - 1973 (PB 226 843)A08

EERC 73-16 "QUAD-4: A Computer Program for Evaluating the Seismic Response of Soil Structures by Variable Damping Finite Element Procedures," by I.M. Idriss, J. Lysmer, R. Hwang and H.B. Seed - 1973 (PB 229 424)A05

EERC 73-17 "Dynamic Behavior of a Multi-Story Pyramid Shaped Building," by R.M. Stephen, J.P. Hollings and J.G. Bouwkamp - 1973 (PB 240 718)A06

EERC 73-18 "Effect of Different Types of Reinforcing on Seismic Behavior of Short Concrete Columns," by V.V. Bertero, J. Hollings, O. Küstü, R.M. Stephen and J.G. Bouwkamp - 1973

EERC 73-19 "Olive View Medical Center Materials Studies, Phase I," by B. Bresler and V.V. Bertero - 1973 (PB 235 986)A06

EERC 73-20 "Linear and Nonlinear Seismic Analysis Computer Programs for Long Multiple-Span Highway Bridges," by W.S. Tseng and J. Penzien - 1973

EERC 73-21 "Constitutive Models for Cyclic Plastic Deformation of Engineering Materials," by J.M. Kelly and P.P. Gillis 1973 (PB 226 024)A03

EERC 73-22 "DRAIN - 2D User's Guide," by G.H. Powell - 1973 (PB 227 016)A05

EERC 73-23 "Earthquake Engineering at Berkeley - 1973," (PB 226 033)A11

EERC 73-24 Unassigned

EERC 73-25 "Earthquake Response of Axisymmetric Tower Structures Surrounded by Water," by C.Y. Liaw and A.K. Chopra 1973 (AD 773 052)A09

EERC 73-26 "Investigation of the Failures of the Olive View Stairtowers During the San Fernando Earthquake and Their Implications on Seismic Design," by V.V. Bertero and R.G. Collins - 1973 (PB 235 106)A13

EERC 73-27 "Further Studies on Seismic Behavior of Steel Beam-Column Subassemblages," by V.V. Bertero, H. Krawinkler and E.P. Popov - 1973 (PB 234 172)A06

EERC 74-1 "Seismic Risk Analysis," by C.S. Oliveira - 1974 (PB 235 920)A06

EERC 74-2 "Settlement and Liquefaction of Sands Under Multi-Directional Shaking," by R. Pyke, C.K. Chan and H.B. Seed 1974

EERC 74-3 "Optimum Design of Earthquake Resistant Shear Buildings," by D. Ray, K.S. Pister and A.K. Chopra - 1974 (PB 231 172)A06

EERC 74-4 "LUSH - A Computer Program for Complex Response Analysis of Soil-Structure Systems," by J. Lysmer, T. Udaka, H.B. Seed and R. Hwang - 1974 (PB 236 796)A05

EERC 74-5 "Sensitivity Analysis for Hysteretic Dynamic Systems: Applications to Earthquake Engineering," by D. Ray 1974 (PB 233 213)A06

EERC 74-6 "Soil Structure Interaction Analyses for Evaluating Seismic Response," by H.B. Seed, J. Lysmer and R. Hwang 1974 (PB 236 519)A04

EERC 74-7 Unassigned

EERC 74-8 "Shaking Table Tests of a Steel Frame - A Progress Report," by R.W. Clough and D. Tang - 1974 (PB 240 869)A03

EERC 74-9 "Hysteretic Behavior of Reinforced Concrete Flexural Members with Special Web Reinforcement," by V.V. Bertero, E.P. Popov and T.Y. Wang - 1974 (PB 236 797)A07

EERC 74-10 "Applications of Reliability-Based, Global Cost Optimization to Design of Earthquake Resistant Structures," by E. Vitiello and K.S. Pister - 1974 (PB 237 231)A06

EERC 74-11 "Liquefaction of Gravelly Soils Under Cyclic Loading Conditions," by R.T. Wong, H.B. Seed and C.K. Chan 1974 (PB 242 042)A03

EERC 74-12 "Site-Dependent Spectra for Earthquake-Resistant Design," by H.B. Seed, C. Ugas and J. Lysmer - 1974 (PB 240 953)A03

EERC 74-13 "Earthquake Simulator Study of a Reinforced Concrete Frame," by P. Hidalgo and R.W. Clough - 1974 (PB 241 944)A13

EERC 74-14 "Nonlinear Earthquake Response of Concrete Gravity Dams," by N. Pal - 1974 (AD/A 006 583)A06

EERC 74-15 "Modeling and Identification in Nonlinear Structural Dynamics - I. One Degree of Freedom Models," by N. Distefano and A. Rath - 1974 (PB 241 548)A06

EERC 75-1 "Determination of Seismic Design Criteria for the Dumbarton Bridge Replacement Structure, Vol. I: Description, Theory and Analytical Modeling of Bridge and Parameters," by F. Baron and S.-H. Pang - 1975 (PB 259 407)A15

EERC 75-2 "Determination of Seismic Design Criteria for the Dumbarton Bridge Replacement Structure, Vol. II: Numerical Studies and Establishment of Seismic Design Criteria," by F. Baron and S.-H. Pang - 1975 (PB 259 408)A11 (For set of EERC 75-1 and 75-2 (PB 259 406))

EERC 75-3 "Seismic Risk Analysis for a Site and a Metropolitan Area," by C.S. Oliveira - 1975 (PB 248 134)A09

EERC 75-4 "Analytical Investigations of Seismic Response of Short, Single or Multiple-Span Highway Bridges," by M.-C. Chen and J. Penzien - 1975 (PB 241 454)A09

EERC 75-5 "An Evaluation of Some Methods for Predicting Seismic Behavior of Reinforced Concrete Buildings," by S.A. Mahin and V.V. Bertero - 1975 (PB 246 306)A16

EERC 75-6 "Earthquake Simulator Study of a Steel Frame Structure, Vol. I: Experimental Results," by R.W. Clough and D.T. Tang - 1975 (PB 243 981)A13

EERC 75-7 "Dynamic Properties of San Bernardino Intake Tower," by D. Rea, C.-Y. Liaw and A.K. Chopra - 1975 (AD/A008 406) A05

EERC 75-8 "Seismic Studies of the Articulation for the Dumbarton Bridge Replacement Structure, Vol. I: Description, Theory and Analytical Modeling of Bridge Components," by F. Baron and R.E. Hamati - 1975 (PB 251 539)A07

EERC 75-9 "Seismic Studies of the Articulation for the Dumbarton Bridge Replacement Structure, Vol. 2: Numerical Studies of Steel and Concrete Girder Alternates," by F. Baron and R.E. Hamati - 1975 (PB 251 540)A10

EERC 75-10 "Static and Dynamic Analysis of Nonlinear Structures," by D.P. Mondkar and G.H. Powell - 1975 (PB 242 434)A08

EERC 75-11 "Hysteretic Behavior of Steel Columns," by E.P. Popov, V.V. Bertero and S. Chandramouli - 1975 (PB 252 365)A11

EERC 75-12 "Earthquake Engineering Research Center Library Printed Catalog," - 1975 (PB 243 711)A26

EERC 75-13 "Three Dimensional Analysis of Building Systems (Extended Version)," by E.L. Wilson, J.P. Hollings and H.H. Dovey - 1975 (PB 243 989)A07

EERC 75-14 "Determination of Soil Liquefaction Characteristics by Large-Scale Laboratory Tests," by P. De Alba, C.K. Chan and H.B. Seed - 1975 (NUREG 0027)A08

EERC 75-15 "A Literature Survey - Compressive, Tensile, Bond and Shear Strength of Masonry," by R.L. Mayes and R.W. Clough - 1975 (PB 246 292)A10

EERC 75-16 "Hysteretic Behavior of Ductile Moment Resisting Reinforced Concrete Frame Components," by V.V. Bertero and E.P. Popov - 1975 (PB 246 388)A05

EERC 75-17 "Relationships Between Maximum Acceleration, Maximum Velocity, Distance from Source, Local Site Conditions for Moderately Strong Earthquakes," by H.B. Seed, R. Murarka, J. Lysmer and I.M. Idriss - 1975 (PB 248 172)A03

EERC 75-18 "The Effects of Method of Sample Preparation on the Cyclic Stress-Strain Behavior of Sands," by J. Mulilis, C.K. Chan and H.B. Seed - 1975 (Summarized in EERC 75-28)

EERC 75-19 "The Seismic Behavior of Critical Regions of Reinforced Concrete Components as Influenced by Moment, Shear and Axial Force," by M.B. Atalay and J. Penzien - 1975 (PB 258 842)A11

EERC 75-20 "Dynamic Properties of an Eleven Story Masonry Building," by R.M. Stephen, J.P. Hollings, J.G. Bouwkamp and D. Jurukovski - 1975 (PB 246 945)A04

EERC 75-21 "State-of-the-Art in Seismic Strength of Masonry - An Evaluation and Review," by R.L. Mayes and R.W. Clough 1975 (PB 249 040)A07

EERC 75-22 "Frequency Dependent Stiffness Matrices for Viscoelastic Half-Plane Foundations," by A.K. Chopra, P. Chakrabarti and G. Dasgupta - 1975 (PB 248 121)A07

EERC 75-23 "Hysteretic Behavior of Reinforced Concrete Framed Walls," by T.Y. Wong, V.V. Bertero and E.P. Popov - 1975

EERC 75-24 "Testing Facility for Subassemblages of Frame-Wall Structural Systems," by V.V. Bertero, E.P. Popov and T. Endo - 1975

EERC 75-25 "Influence of Seismic History on the Liquefaction Characteristics of Sands," by H.B. Seed, K. Mori and C.K. Chan - 1975 (Summarized in EERC 75-28)

EERC 75-26 "The Generation and Dissipation of Pore Water Pressures during Soil Liquefaction," by H.B. Seed, P.P. Martin and J. Lysmer - 1975 (PB 252 648)A03

EERC 75-27 "Identification of Research Needs for Improving Aseismic Design of Building Structures," by V.V. Bertero 1975 (PB 248 136)A05

EERC 75-28 "Evaluation of Soil Liquefaction Potential during Earthquakes," by H.B. Seed, I. Arango and C.K. Chan - 1975 (NUREG 0026)A13

EERC 75-29 "Representation of Irregular Stress Time Histories by Equivalent Uniform Stress Series in Liquefaction Analyses," by H.B. Seed, I.M. Idriss, F. Makdisi and N. Banerjee - 1975 (PB 252 635)A03

EERC 75-30 "FLUSH - A Computer Program for Approximate 3-D Analysis of Soil-Structure Interaction Problems," by J. Lysmer, T. Udaka, C.-F. Tsai and H.B. Seed - 1975 (PB 259 332)A07

EERC 75-31 "ALUSH - A Computer Program for Seismic Response Analysis of Axisymmetric Soil-Structure Systems," by E. Berger, J. Lysmer and H.B. Seed - 1975

EERC 75-32 "TRIP and TRAVEL - Computer Programs for Soil-Structure Interaction Analysis with Horizontally Travelling Waves," by T. Udaka, J. Lysmer and H.B. Seed - 1975

EERC 75-33 "Predicting the Performance of Structures in Regions of High Seismicity," by J. Penzien - 1975 (PB 248 130)A03

EERC 75-34 "Efficient Finite Element Analysis of Seismic Structure - Soil - Direction," by J. Lysmer, H.B. Seed, T. Udaka, R.N. Hwang and C.-F. Tsai - 1975 (PB 253 570)A03

EERC 75-35 "The Dynamic Behavior of a First Story Girder of a Three-Story Steel Frame Subjected to Earthquake Loading," by R.W. Clough and L.-Y. Li - 1975 (PB 248 841)A05

EERC 75-36 "Earthquake Simulator Study of a Steel Frame Structure, Volume II - Analytical Results," by D.T. Tang - 1975 (PB 252 926)A10

EERC 75-37 "ANSR-I General Purpose Computer Program for Analysis of Non-Linear Structural Response," by D.P. Mondkar and G.H. Powell - 1975 (PB 252 386)A08

EERC 75-38 "Nonlinear Response Spectra for Probabilistic Seismic Design and Damage Assessment of Reinforced Concrete Structures," by M. Murakami and J. Penzien - 1975 (PB 259 530)A05

EERC 75-39 "Study of a Method of Feasible Directions for Optimal Elastic Design of Frame Structures Subjected to Earthquake Loading," by N.D. Walker and K.S. Pister - 1975 (PB 257 781)A06

EERC 75-40 "An Alternative Representation of the Elastic-Viscoelastic Analogy," by G. Dasgupta and J.L. Sackman - 1975 (PB 252 173)A03

EERC 75-41 "Effect of Multi-Directional Shaking on Liquefaction of Sands," by H.B. Seed, R. Pyke and G.R. Martin - 1975 (PB 258 781)A03

EERC 76-1 "Strength and Ductility Evaluation of Existing Low-Rise Reinforced Concrete Buildings - Screening Method," by T. Okada and B. Bresler - 1976 (PB 257 906)A11

EERC 76-2 "Experimental and Analytical Studies on the Hysteretic Behavior of Reinforced Concrete Rectangular and T-Beams," by S.-Y.M. Ma, E.P. Popov and V.V. Bertero - 1976 (PB 260 843)A12

EERC 76-3 "Dynamic Behavior of a Multistory Triangular-Shaped Building," by J. Petrovski, R.M. Stephen, E. Gartenbaum and J.G. Bouwkamp - 1976

EERC 76-4 "Earthquake Induced Deformations of Earth Dams," by N. Serff and H.B. Seed - 1976

EERC 76-5 "Analysis and Design of Tube-Type Tall Building Structures," by H. de Clercq and G.H. Powell - 1976 (PB 252 220) A10

EERC 76-6 "Time and Frequency Domain Analysis of Three-Dimensional Ground Motions, San Fernando Earthquake," by T. Kubo and J. Penzien (PB 260 556)A11

EERC 76-7 "Expected Performance of Uniform Building Code Design Masonry Structures," by R.L. Mayes, Y. Omote, S.W. Chen and R.W. Clough - 1976

EERC 76-8 "Cyclic Shear Tests on Concrete Masonry Piers," Part I - Test Results," by R.L. Mayes, Y. Omote and R.W. Clough - 1976 (PB 264 424)A06

EERC 76-9 "A Substructure Method for Earthquake Analysis of Structure - Soil Interaction," by J.A. Gutierrez and A.K. Chopra - 1976 (PB 257 783)A08

EERC 76-10 "Stabilization of Potentially Liquefiable Sand Deposits using Gravel Drain Systems," by H.B. Seed and J.R. Booker - 1976 (PB 258 820)A04

EERC 76-11 "Influence of Design and Analysis Assumptions on Computed Inelastic Response of Moderately Tall Frames," by G.H. Powell and D.G. Row - 1976

EERC 76-12 "Sensitivity Analysis for Hysteretic Dynamic Systems: Theory and Applications," by D. Ray, K.S. Pister and E. Polak - 1976 (PB 262 859)A04

EERC 76-13 "Coupled Lateral Torsional Response of Buildings to Ground Shaking," by C.L. Kan and A.K. Chopra - 1976 (PB 257 907)A09

EERC 76-14 "Seismic Analyses of the Banco de America," by V.V. Bertero, S.A. Mahin and J.A. Hollings - 1976

EERC 76-15 "Reinforced Concrete Frame 2: Seismic Testing and Analytical Correlation," by R.W. Clough and J. Gidwani - 1976 (PB 261 323)A08

EERC 76-16 "Cyclic Shear Tests on Masonry Piers, Part II - Analysis of Test Results," by R.L. Mayes, Y. Omote and R.W. Clough - 1976

EERC 76-17 "Structural Steel Bracing Systems: Behavior Under Cyclic Loading," by E.P. Popov, K. Takanashi and C.W. Roeder - 1976 (PB 260 715)A05

EERC 76-18 "Experimental Model Studies on Seismic Response of High Curved Overcrossings," by D. Williams and W.G. Godden - 1976

EERC 76-19 "Effects of Non-Uniform Seismic Disturbances on the Dumbarton Bridge Replacement Structure," by F. Baron and R.E. Hamati - 1976

EERC 76-20 "Investigation of the Inelastic Characteristics of a Single Story Steel Structure Using System Identification and Shaking Table Experiments," by V.C. Matzen and H.D. McNiven - 1976 (PB 258 453)A07

EERC 76-21 "Capacity of Columns with Splice Imperfections," by E.P. Popov, R.M. Stephen and R. Philbrick - 1976 (PB 260 378)A04

EERC 76-22 "Response of the Olive View Hospital Main Building during the San Fernando Earthquake," by S. A. Mahin, R. Collins, A.K. Chopra and V.V. Bertero - 1976

EERC 76-23 "A Study on the Major Factors Influencing the Strength of Masonry Prisms," by N.M. Mostaghel, R.L. Mayes, R. W. Clough and S.W. Chen - 1976

EERC 76-24 "GADFLEA - A Computer Program for the Analysis of Pore Pressure Generation and Dissipation during Cyclic or Earthquake Loading," by J.R. Booker, M.S. Rahman and H.B. Seed - 1976 (PB 263 947)A04

EERC 76-25 "Rehabilitation of an Existing Building: A Case Study," by B. Bresler and J. Axley - 1976

EERC 76-26 "Correlative Investigations on Theoretical and Experimental Dynamic Behavior of a Model Bridge Structure," by K. Kawashima and J. Penzien - 1976 (PB 263 388)A11

EERC 76-27 "Earthquake Response of Coupled Shear Wall Buildings," by T. Srichatrapimuk - 1976 (PB 265 157)A07

EERC 76-28 "Tensile Capacity of Partial Penetration Welds," by E.P. Popov and R.M. Stephen - 1976 (PB 262 899)A03

EERC 76-29 "Analysis and Design of Numerical Integration Methods in Structural Dynamics," by H.M. Hilber - 1976 (PB 264 410)A06

EERC 76-30 "Contribution of a Floor System to the Dynamic Characteristics of Reinforced Concrete Buildings," by L.J. Edgar and V.V. Bertero - 1976

EERC 76-31 "The Effects of Seismic Disturbances on the Golden Gate Bridge," by F. Baron, M. Arikan and R.E. Hamati - 1976

EERC 76-32 "Infilled Frames in Earthquake Resistant Construction," by R.E. Klingner and V.V. Bertero - 1976 (PB 265 892)A13

UCB/EERC-77/01 "PLUSH - A Computer Program for Probabilistic Finite Element Analysis of Seismic Soil-Structure Interaction," by M.P. Romo Orga .sta, J. Lysmer and H.B. Seed - 1977

UCB/EERC-77/02 "Soil-Structure Interaction Effects at the Humboldt Bay Power Plant in the Ferndale Earthquake of June 7, 1975," by J.F. Valera, H.B. Seed, C.F. Tsai and J. Lysmer - 1977 (PB 265 795)A04

UCB/EERC-77/03 "Influence of Sample Disturbance on Sand Response to Cyclic Loading," by K. Mori, H.B. Seed and C.K. Chan - 1977 (PB 267 352)A04

UCB/EERC-77/04 "Seismological Studies of Strong Motion Records," by J. Shoja-Taheri - 1977 (PB 269 655)A10

UCB/EERC-77/05 "Testing Facility for Coupled-Shear Walls," by L. Li-Hyung, V.V. Bertero and E.P. Popov - 1977

UCB/EERC-77/06 "Developing Methodologies for Evaluating the Earthquake Safety of Existing Buildings," by No. 1 - B. Bresler; No. 2 - B. Bresler, T. Okada and D. Zisling; No. 3 - T. Okada and B. Bresler; No. 4 - V.V. Bertero and B. Bresler - 1977 (PB 267 354)A08

UCB/EERC-77/07 "A Literature Survey - Transverse Strength of Masonry Walls," by Y. Omote, R.L. Mayes, S.W. Chen and R.W. Clough - 1977